

Design and development of an off-grid e-learning centre for rural communities



Vusimuzi Edgar Selaule

20145250

A dissertation submitted in fulfilment of the requirements for the
Magister Technologiae: Engineering: Electrical

Department: Electronic Engineering

Faculty of Engineering and Technology

Vaal University of Technology

Vanderbijlpark

Supervisor: Mr RM Schoeman

Co- Supervisor: Prof H.C.vZ. Pienaar

Declaration

I, Vusimuzi Edgar Selaule, declare that this project is my own, unaided work. It is being submitted for the requirements for the Magister Technologiae: Engineering: Electrical to the Department: Electronic Engineering at the Vaal University of Technology, Vanderbijlpark. It has not been submitted before to any academic institution.

A handwritten signature in black ink, appearing to be 'V. Selaule' with a stylized flourish at the end.

Vusimuzi Edgar Selaule

Date: 23 January 2015

Acknowledgements

I hereby wish to express my gratitude to the following individuals who enabled this document to be completed successfully:

- Mr RM Schoeman for your mentorship, encouragement and guidance for the timeous completion of this research.
- Dr JF Janse van Rensburg for encouragement to do my Magister Technologiae: Engineering: Electrical degree and for mentorship.
- Prof HCvZ Pienaar guidance and support throughout this study.
- Telkom Centre of Excellence for the study bursary.
- Vaal University of Technology Centre of Alternative Energy and sponsor (Telkom, TFMC, M-Tech and THRIP) for funding.
- Staff and fellow post-graduate students from the Department of Electronic Engineering for guidance and motivation.
- Family and friends for support and encouragement throughout this study.

Dedication

I dedicate this dissertation to my parents Vuyelwa Petra and Wilson Phephelaphi Selaule.

Thank you for giving me the courage to chase my dreams and the endurance to reach for the stars. Words cannot express my gratitude for the blessing you are to me.

Abstract

The lack of electricity in off-grid rural communities in South Africa (SA) and Africa as well as the budget constraints on these communities restrict these communities from connecting to any online resources (internet and e-books) for educational purposes, thus creating a major contributor to the global digital divide.

Renewable energy sources such as solar energy, wind energy and biomass were presented as potential alternatives to grid-connected electricity for remote rural locations. Solar energy was identified as the amply available alternative energy resource in SA. Solar radiation was converted by photovoltaic technology to electricity. National power grid isolation (off-grid) was achieved by using a stand-alone photovoltaic system. Photovoltaic technology classification, material categorisation and system sizing for an e-learning centre was presented. Practical set-ups were utilised to determine the most cost-effective equipment mix of power utilization, power management/storage and ICT equipment to build a pilot e-learning centre.

It was established that one photovoltaic panel can be employed to fully recharge a battery of a pilot e-learning centre with an operational period of 7 hours using the available sunlight hours. Owing to the susceptibility of the Vaal Triangle region to thunderstorms causing overcast conditions for days, a ratio of back-up battery capacity (Ah) to number of days (seven hours per day) without sunlight was determined. An algorithm was also derived for sizing the pilot e-learning centre for full scale implementation.

Future research recommendations based on this study for a reduced system costs of an off-grid e-learning for rural communities powered by a renewable energy resource were presented. This will increase access to basic education in SA and reduce the global digital divide.

Table of contents

Declaration	i
Acknowledgements	ii
Dedication	iii
Abstract	iv
List of figures	vii
List of tables	xi
List of abbreviations and definitions	i
Chapter 1 Introduction and overview	1
1.1 Background	1
1.2 Problem statement	2
1.3 Research objectives	2
1.4 Research methodology	3
1.5 Delimitations	3
1.6 Importance of this research	3
1.7 Overview of the dissertation	4
1.8 Summary	4
Chapter 2 Renewable energy resources	5
2.1 Introduction	5
2.2 Renewable energy resources in SA	5
2.3 Photovoltaic technology classification	12
2.4 Photovoltaic technology cost analysis	16
2.5 Photovoltaic technology life cycle cost analysis	17
2.6 Photovoltaic system sizing	18
2.6.1 Estimated electric load (E-learning ICT equipment)	19
2.6.2 E-learning centre lighting	23
2.6.3 Photovoltaic module operation and sizing	27
2.6.4 Photovoltaic system inverter and wire specification	29

2.6.5	Energy storage devices	34
2.6.6	Battery types and sizing for photovoltaic system	34
2.6.7	Electronic converters in photovoltaic system	45
2.7	E-learning and the global digital divide	47
2.8	Summary	48
Chapter 3 Research design, set-up and results		49
3.1	Introduction	49
3.2	Photovoltaic panels power-efficiency evaluation	49
3.3	ICT equipment (laptops) power-efficiency evaluation	54
3.4	Light intensity and power-efficiency evaluation of light sources	59
3.5	Power-efficiency evaluation of DC-DC converters	65
3.6	Power-efficiency evaluation of charge controllers	71
3.7	Summary	76
Chapter 4 Research data analysis		77
4.1	Introduction	77
4.2	Data analysis to determine the most power-efficient photovoltaic panel	77
4.3	Data analysis to determine the most power-efficient ICT equipment (laptops)	80
4.4	Data analysis to determine the most power-efficient light sources	81
4.5	Data analysis to determine the most power-efficient DC-DC converters	86
4.6	Charge controller power-efficiency data analysis	87
4.7	Pilot e-learning centre	87
4.8	Pilot e-learning centre sizing for full scale implementation	99
4.9	Summary	103

Chapter 5	Conclusion and recommendations	104
5.1	Introduction	104
5.2	Conclusions	104
5.3	Future research recommendations based on this study	105
References		107
Annexure A	Photovoltaic panels manufacturers' parameters	125
Annexure B	Jitbit macro program	128
Annexure C	Charge controller (Microcare 12/24 10A MPPT)	130
Annexure D	DC-DC converter (Motormate IPC 1210)	132
Annexure E	Lights [MR16**(PAR16)	133
Annexure F	Lead acid battery (20Ah)	134
Annexure G	Lead acid battery (100Ah)	136
Annexure H	Laptops purchase invoice	138
Annexure I	Turnitin originality report	139
Annexure J	NRF nexus title search	140

List of figures

Figure 1	Availability and access to ICT in villages	1
Figure 2	Potential wind power in SA	6
Figure 3	Biomass potential in SA	7
Figure 4	Annual rainfall (mm/year) in SA	8
Figure 5	Micro hydro potential in SA	9
Figure 6	Annual solar radiation in SA	11
Figure 7	Photovoltaic material categorisation	13
Figure 8	Solar photovoltaic global capacity, 1995-2012	16
Figure 9	Photovoltaic system types	20
Figure 10	Energy consumption of commercial buildings' lighting globally	23
Figure 11	Electromagnetic spectrum visible portion highlighted	24
Figure 12	The recommended luminaire cut off-angle for uninterrupted and accessional use of the VDU	25
Figure 13	Main groups of light sources	26
Figure 14	LED viewing angle	27
Figure 15	Inverter total efficiency and photovoltaic DC voltage as a function of loading	29
Figure 16	Summary of inverter sizing considering significant factors	30
Figure 17	American wire gauge wire sizes	32
Figure 18	Battery life cycles vs. DOD	36
Figure 19	Typical battery discharge characteristics	37
Figure 20	Battery discharge characteristics and equivalent scaled battery discharge characteristics	38
Figure 21	Li – ion discharge reserve time as function of residual capacity	39

Figure 22	Possible battery characteristics as a function of time for a 15 Ah battery assuming 100% DOD	41
Figure 23	Photovoltaic battery systems with a charge controller	42
Figure 24	Various types of rechargeable batteries [a-lead acid, b-(NiCd), c-(NiMH), d-(LI-ion), e-(Li-ion polymer)]	43
Figure 25	Configuration of a two stage photovoltaic PCS	45
Figure 26	Basic DC-DC converter circuits	46
Figure 27	Set-up block diagram used to evaluate the power output of photovoltaic panels	50
Figure 28	Laboratory set-up used to evaluate the power output of photovoltaic panels	50
Figure 29	Measured voltage for all three photovoltaic panels (24 hour cycle)	52
Figure 30	Measured current for all three photovoltaic panels (24 hour cycle)	52
Figure 31	Determined power output for each photovoltaic panel (24 hour cycle)	52
Figure 32	PV1 measured watt/Rand percentage	53
Figure 33	PV2 measured watt/Rand percentage	53
Figure 34	PV3 measured watt/Rand percentage	53
Figure 35	Set-up block diagram used to evaluate and verify the most energy-efficient laptop	54
Figure 36	Laboratory set-up used to evaluate and verify the most energy-efficient laptop	55
Figure 37	Laptop average power consumption without battery pack	56
Figure 38	Measured laptops input current with test procedure action steps	58
Figure 39	Measured laptops input voltage with test procedure action step	58

Figure 40	Light intensity evaluation set-up	59
Figure 41	Evaluated LED-based SSL technology interior light sources	60
Figure 42	Set-up used to determine the power-efficiency of SSL technologies based on LEDs	64
Figure 43	Set-up block diagram used to evaluate DC-DC converters	66
Figure 44	Laboratory set-up used to evaluate DC-DC converter	66
Figure 45	Measured input voltage range of a Kerio Technologies DC-DC converter (DD70)	67
Figure 46	Measured input and output voltage (Motormate (IPC-1210) DC-DC converter)	69
Figure 47	Measured input and output current (Motormate (IPC-1210) DC-DC converter)	69
Figure 48	Input and output power (Motormate (IPC-1210) DC-DC converter)	70
Figure 49	Power-efficiency (Motormate IPC-1210 DC-DC converter)	70
Figure 50	Set-up block diagram used to evaluate charge controllers	73
Figure 51	Laboratory set-up used to evaluate charge controllers	73
Figure 52	Microcare 12/24 10AMP MPPT charge controller measured voltage and current	74
Figure 53	Photovoltaic panel daily average power	79
Figure 54	Average Illuminance efficiency (lx/W)	82
Figure 55	Set-up used to determine the required number of MR16**(PAR16) LED	83
Figure 56	Set-up block diagram of a pilot e-learning centre with system measuring devices marked in red	88
Figure 57	Pilot e-learning centre set to 24 hour operational periods with a 100Ah battery	94

Figure 58	Pilot e-learning centre set to 17 hour operational periods with a 100Ah battery	95
Figure 59	Pilot e-learning centre set to 7 hour operational periods with a 100Ah battery using two photovoltaic panels (PV2)	97
Figure 60	Pilot e-learning centre set to 7 hour operational periods with a 100Ah battery using one photovoltaic panel (PV2)	98

List of tables

Table 1	Historical developments in photovoltaic solar conversion	12
Table 2	List of compliant Energy Star 5.0 desktop Computers with power specifications	21
Table 3	List of compliant Energy Star 5.0 notebook Computers with power specifications	22
Table 4	Recommended minimum illuminance for educational buildings	25
Table 5	Tilt angle and latitude (\varnothing) relationship	28
Table 6	Wire type and ampacity	31
Table 7	One way length for various AWG wire sizes at 5% voltage drop	32
Table 8	SOC of a sealed 12 V lead acid battery based on measured battery voltage	36
Table 9	Recommended battery cut-off voltage	37
Table 10	Manufacturer acceptable battery DOD	39
Table 11	Comparison of characteristics for commonly used rechargeable battery	44
Table 12	Converter output voltage equations	47
Table 13	Laptop power consumption test procedure with battery packs connected	57
Table 14	Manufacture electrical parameters of evaluated LED-based SSL technology	60
Table 15	Light intensity at selected height above test surface	61
Table 16	Measured test surface centre illuminance	63
Table 17	Viewing angle of each LED-based SSL technology interior light source	63
Table 18	Manufactures and measured power rating	64

Table 19	DC-DC converter manufacturers' electrical parameters	65
Table 20	Measured input voltage range for all evaluated DC-DC converters	68
Table 21	Average efficiency for all evaluated DC-DC converters	71
Table 22	Charge controller manufacturers' electrical parameters	72
Table 23	Photovoltaic panel voltage to establish RCV, LRV, LVD and HVD of each charge controller	75
Table 24	Efficiency of evaluated charge controllers	75
Table 25	Hypothesis (P-value) testing results for evaluated PV panels	78
Table 26	Conditions for accepting or rejecting a null hypothesis	78
Table 27	Photovoltaic panel total average power	79
Table 28	Hypothesis (P-value) testing results for power consumption of evaluated laptops	80
Table 29	Laptop peak charge current, charge and discharge time summarised	81
Table 30	Scenario (A) measured light intensity for multiple MR16**(PAR16) LEDs to maintain illuminance of 500lx	85
Table 31	Scenario (B) measured light intensity for multiple MR16**(PAR16) LEDs to maintain illuminance of 500 lx	85
Table 32	Variation in power-efficiency of DC-DC converters from the same manufacturer	86
Table 32	Summary of a battery's voltages and DOD levels for a 12V lead acid battery	89

Table 33	Summary of a battery's voltages and DOD levels for a 12V lead acid battery	89
Table 34	Pilot e-learning centre's equipment list (including quantity used)	99
Table 35	Measured current of listed equipment in Table 34	100
Table 36	Cable specifications for the annealed copper cable used for wiring the pilot e-learning centre devices	101
Table 37	Conclusions reached to meet the objectives of this study	105

List of abbreviations and definitions

A		LRV	Load reconnect voltage
AC	Alternating current		
AGM	Absorbed glass mat	LVD	Low voltage disconnect
Ah	Amp-hour		
AWG	American wire gauge		
C		MPPT	Maximum power point tracker
CB	Circuit breaker		
CdS	Cadmium sulphide		
CdTe	Cadmium telluride		
CIGS	Copper indium gallium selenide	NEC	National electric code
CIS	Copper indium selenide		
D		RET	Renewable energy technology
D.A.I.C	Data acquisition interface circuit	RCV	Photovoltaic array reconnect voltage
DC	Direct current		
DOD	Depth of discharge	SA	South Africa
E		SABS	South African bureau of standards
E-learning	Technology based education	SOC	State of charge
		SSL	Solid state lighting
I			
ICT	Information and communication technology	VDU	Visual display unit
L		V.I.C	Voltage interface circuit
LCC	Life cycle cost analysis	VLA	Vented lead acid
LED	Light emitting diode	VRLA	Valve regulated lead acid
		VUT	Vaal University of Technology

Chapter 1 Introduction and overview

1.1 Background

Electricity has a major influence on a nation's development and it is globally a pivotal economic progress indicator. Characterised by ease of conveyance, instant availability and convertibility to other forms of energy, electricity is the main source of energy for both industrial and domestic use (Rahman & de Castro 1995:307). Figure 1 illustrates that electricity is the driving force to access the available ICT infrastructure (Sumbwanyambe, Nel & Clarke 2011:2).

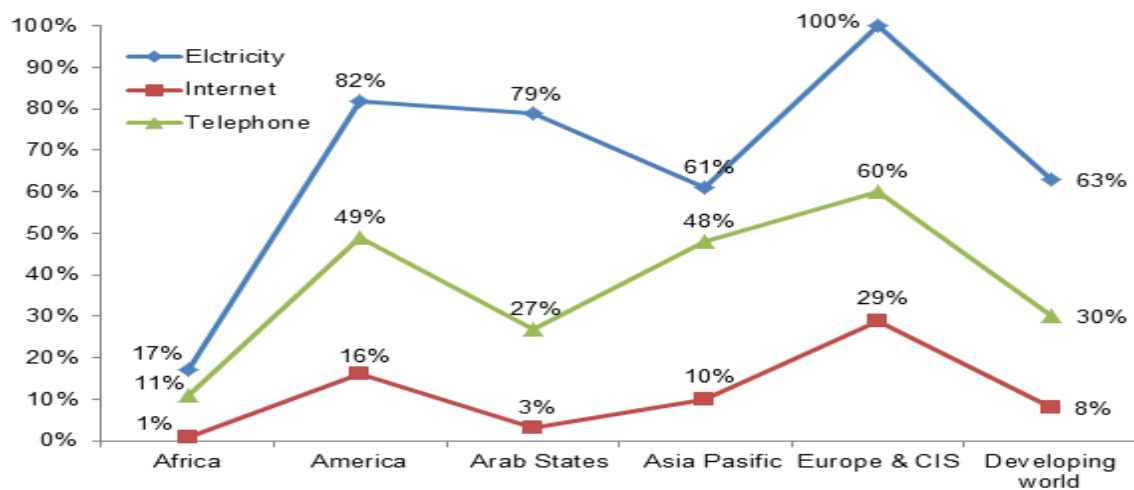


Figure 1 Availability and access to ICT in Villages (Sumbwanyambe *et al.* 2011:2)

When electricity is produced from the combustion of coal it causes substantial pollution (Williams 1993:8). The use of renewable energy resources decreases reliance on fossil fuels. Using fossil fuels and the resultant depletion of fossil fuels has a negative impact on nature (Baños, Manzano-Agugliaro, Montoya, Gil, Alcayde & Gómez 2011:1754). Biomass, hydropower, geothermal, solar, wind as well as marine energies are identified and defined by Manzano-Agugliaro, Alcayde, Montoya, Zapata-Sierra and Gil (2013:135) as renewable

energy resources which are cost-effective, sustainable and applicable without any negative effects.

Technology-based learning (e-learning) can contribute to reducing the barrier to basic education (Gebremichael & Jackson 2006:269). The ineffective application of appropriate technology (such as technology which converts renewable energy to electricity) and lack thereof in Africa negatively impacts on education in remote areas (Keats & Beebe 2004:954).

1.2 Problem statement

The lack of electricity in off-grid rural communities in South Africa (SA) and Africa as well as the budget constraints on these communities restrict these communities to connect to any online resources (internet and e-books) for educational purposes, thus creating a major contributor to the global digital divide.

1.3 Research objectives

The objectives of this research are to:

- Determine an appropriately available renewable energy resource for powering a rural e-learning centre.
- Determine the most cost-effective equipment mix of power utilisation, power management/storage and ICT equipment.
- Design and build a pilot e-learning centre using the most cost-effective equipment mix.
- Provide guidelines for the full scale implementation of an off grid e-learning centre for rural communities.

1.4 Research methodology

In this research, an available renewable energy resource will be utilised to develop a cost-effective, off-grid power plant for rural e-learning centres. A comprehensive literature study of an amply available renewable energy resource in SA is presented. Cost and efficiency analysis of the identified renewable energy technology (RET), power storage device as well as information and communication technology (ICT) equipment will be done to establish the most cost-effective equipment mix.

Regression analysis will be undertaken on empirical data recorded by the data logger to determine optimised methods for electrical distribution and control. Based on the results of the data analysis full scale implementation guidelines of an off-grid e-learning centre will be provided.

1.5 Delimitations

This research does not include optimising internet connection of the off-grid rural e-learning centre, optimising software requirements for e-learning as well as actual full scale implementation (construction) of the pilot power plant.

1.6 Importance of this research

This research will be beneficial to off-grid rural communities in SA and Africa because it will increase access to basic education via e-learning powered by a renewable energy resource. This research will also have a positive impact in reducing reliance on fossil fuel-produced electricity as well as decreasing the digital divide.

1.7 Overview of this dissertation

This dissertation accounts for the research done to design and develop an off-grid e-learning centre for rural communities

Chapter 2 comprises a literature review undertaken to identify the optimum alternative energy resource available in SA. The principal technology types and system sizing of the identified renewable energy resource is presented.

Chapter 3 covers the practical set-ups used to determine the most cost-effective equipment mix for power utilisation, ICT equipment selection and lighting.

Chapter 4 presents discussions based on data analysis of results obtained in the previous chapter to determine the most cost-efficient and cost-effective equipment mix. A pilot e-learning centre set-up and evaluation is also outlined in this chapter using a determined cost-effective equipment mix.

Chapter 5 covers the conclusions and provides recommendations for future research from this study.

1.8 Summary

Providing e-learning to rural off-grid communities is pivotal in bridging the digital divide suffered by previously disadvantaged communities. Using renewable energy resources to meet the power requirements of the e-learning centre in a cost-effective manner as well as providing a full scale implementation guideline makes it a viable solution to accessing basic education.

Chapter 2 Renewable energy resources

2.1 Introduction

Globally the power requirements of remote areas cannot be met by extending grid-connected electricity as this can cost up to seven times the normal supply cost (Liming 2009:1097). Sin Giap, Chong Eng and Thangaveloo (2011:18) accounts that the low return of investment and high infrastructure investment makes grid-connected electricity extension not a viable solution to supply very small populations mostly in remote rural areas. In SA the state-owned electricity utility, Eskom also highlights high cost requirements to extend grid-connected electricity to remote areas as a major hurdle (Sitshinga 2012:118).

Renewable energy source such as solar, wind and biomass are potential alternatives to grid-connected electricity for remote rural locations (Alvarenga, Costa & Lobo 1996:1152). RETs can be used for small stand-alone power stations producing electricity from locally available material in an environmentally sound manner (Liming 2009:1097).

2.2 Renewable energy resources in SA

In South Africa (SA), less than 1% of the total electricity used is produced by RETs (RSA Department of Minerals and Energy 2002:4). The advantage of using RETs for small stand-alone power stations is that they can be situated near the region to be supplied thus eliminating transmission costs (Nguyen 2007:2579). Kaundinya, Balachandra and Ravindranath (2009:2043) confirm that adoption of an RET stand-alone power station has the advantage of accessibility but economic feasibility and load factors are still prohibiting factors for its application.

Photovoltaic systems contrary to other RETs are favourable as stand-alone systems in isolated regions internationally, this is due to their current and focused increasing cost competitiveness when utilised independent of grid-connect electricity (Kaundinya *et al.* 2009:2042). Bugaje (2006:604) lists solar energy (photovoltaic and thermal), wind energy as well as biomass as amply available renewable energy sources on the African continent. Diab (as quoted by the Department of Minerals and Energy (2002:6) generalises the map of wind in SA as shown in Figure 2.



Figure 2 Potential wind power in SA (RSA Department of Minerals and Energy 2002:6)

Consistent with Kimemia and Annegarn (2011:382) biomass is generally used in non-electrified rural areas in SA. Dasappa (2011:204) points out that biomass is essentially an organic biological material comprising of wood chips, tree stumps, dead trees and agricultural residue. Sriram and Shahidehpour (2005:614) generalise major bio-power technologies for extracting biomass energy as

fermentation, direct combustion, pyrolysis, co-firing, gasification and anaerobic RSA digestion. The RSA Department of Minerals and Energy (2002:4) depicted the total biomass potential in SA as shown in Figure 3 using information from the SA Energy Resource Database.

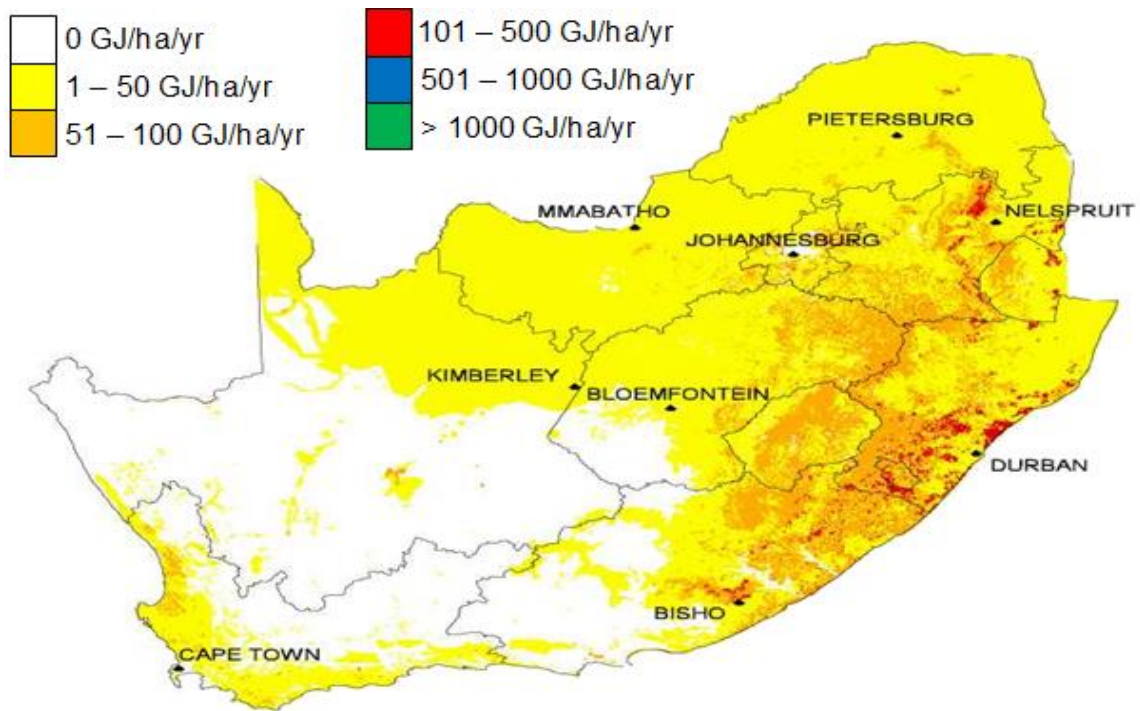


Figure 3 Biomass potential in SA (RSA Department of Minerals and Energy 2002:7)

Unlike biomass, hydropower, in accordance with Darmawi, Sipahutar, Bernas and Imanuddin (2013:215) uses the velocity of water streams from rivers and oceans, to harness hydro-energy. Using a hydrodynamic process hydro-energy is kinetic energy converted to electricity. Yüksel (2010:462) highlight that a hydropower project can be designed to meet the requirements of a specific location. However, other types of hydropower utilize vast land space which change the terrestrial ecosystem to an aquatic ecosystem raising environmental concerns (Frey & Linke 2002:1264).

The Department of Minerals and Energy (2002:10) states that SA has a low potential for hydropower due to the low rain fall experienced in the country. Figure 4 illustrates the average annual rainfall (mm/year) in SA according to the RSA Department of Development, Environment, Conservation and Tourism (2012:37).

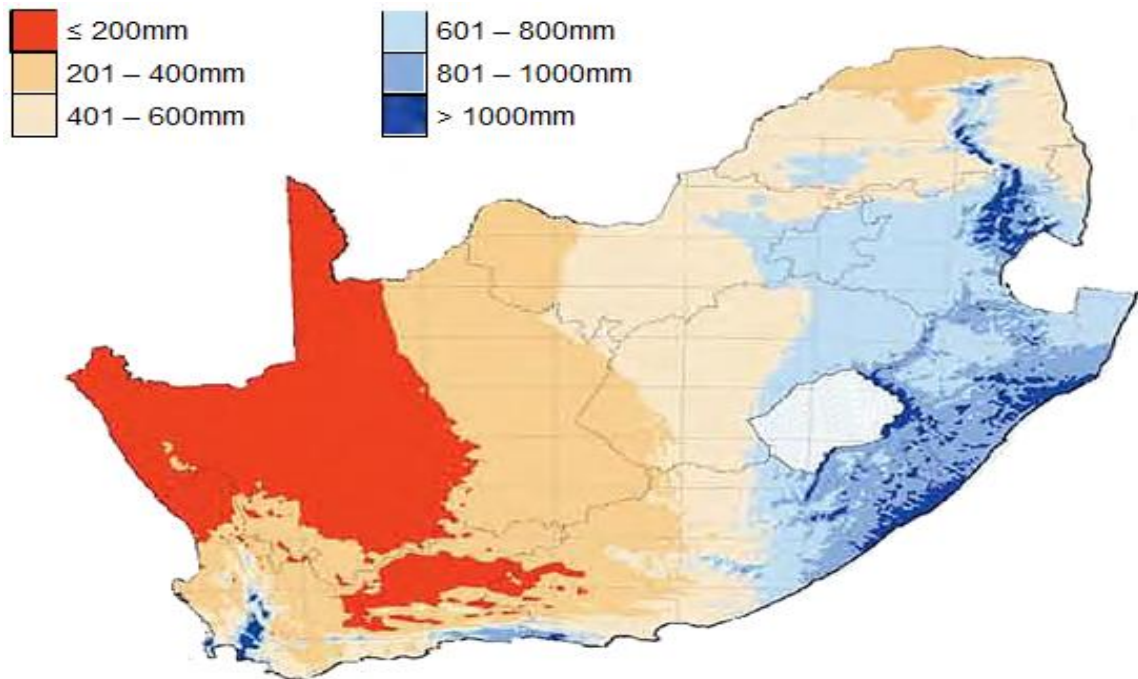


Figure 4 Annual rainfall (mm/year) in SA (RSA Department of Development, Environment, Conservation and Tourism 2012:37)

Hydropower can be categorised as small hydropower, mini-hydropower, micro-hydropower and pico-hydropower with power output limits not universally agreed upon (Kaunda 2013:10). Unlike large hydropower systems, small hydropower installations according to Winkler (2005:29) do not need huge dams to operate. The main advantage of small hydropower is technology robustness, high efficiency, slow rate of change as well as high level of predictability owing to annual rainfall patterns (Taele, Mokhutšoane & Hapazari 2012:449).

Micro-hydro plants are preferred as small stand-alone power sources principally when there are small rivers and waterfalls. Synchronous or induction generators are employed for micro hydro scheme because they are simple to construct, cost less and are robust (Zobaa & Bansal 2011:478).

In SA there are three small hydropower plants in operation. These three facilities are First falls, Second falls and Ncora all owned by Eskom. Hydro-capacity in SA totals 668 MW with small hydro-electrical installations contributing approximately 10% of the total capacity. Figure 5 shows areas with the potential of exploiting small hydropower (RSA Department of Minerals and Energy 2002:10).

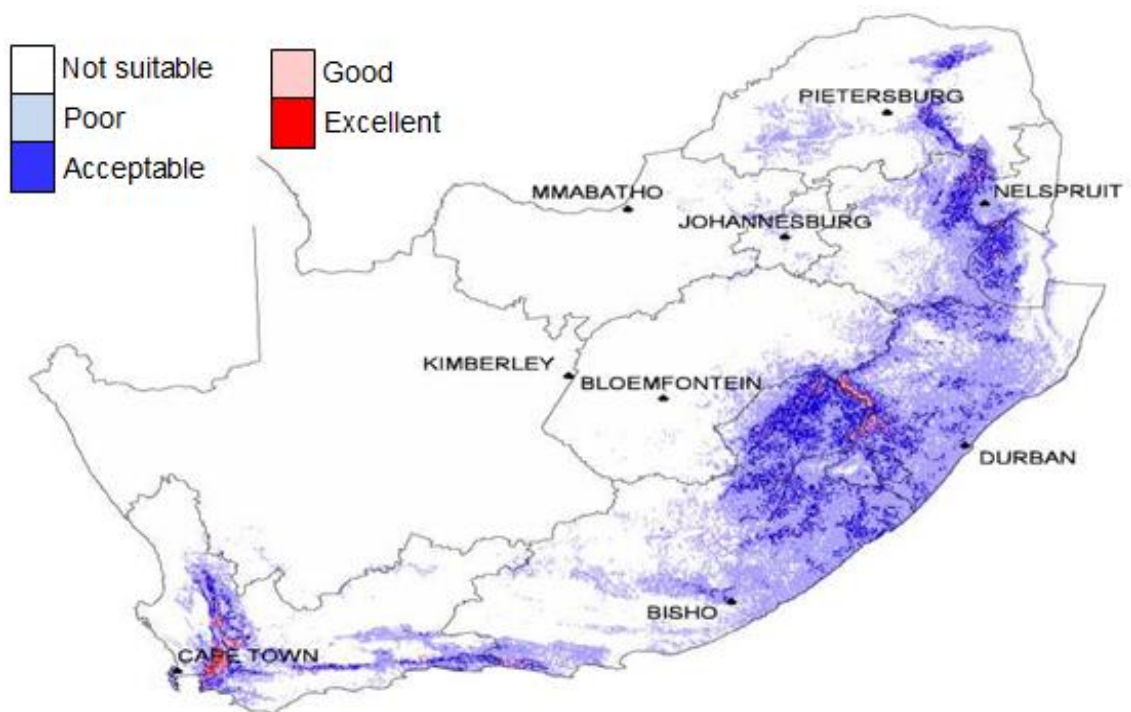


Figure 5 Micro hydro potential in SA (RSA Department of Minerals and Energy 2002:10)

Solar energy is a renewable energy resource with the most potential in SA (Pegels 2010:4948). Solar energy may be utilised for growing crops, space

heating and producing electricity (Taylor 1983:249). Electricity is produced from solar energy by using photovoltaic effect which employs photons passing through a semiconductor material (Zobaa & Bansal 2011:207).

In SA electricity generated from photovoltaic technology has a high potential because of the abundantly present natural resource (sunlight) (Munzhedzi & Sebitosi 2009:165). Photovoltaic systems are designed to convert solar radiation into electricity either as a stand-alone system or grid-connected systems (Sharma, Colangelo & Spagna 1995:162).

In Africa due to the difficult and distant terrain of scattered homesteads photovoltaic stand-alone system application is appropriate because continued innovation in the technology is leading to minimum required qualified maintenance (Karekezi & Ranja 1997:2). In SA photovoltaic systems are extensively employed for supplying power cellular telecommunications network (RSA Department of Minerals and Energy 2002:12).

The major obstacle of the technology remains its initial cost, preventing its full potential to be realised (Winkler 2005:30). Photovoltaic systems are the most favourable as an energy technology for the future, when comparing renewable energy projects currently in progress (Sharma *et al.* 1995:161).

According to Phuangpornpitak and Kumar (2007:1531) the photovoltaic market increased as a result of reduced costs followed by photovoltaic systems being utilised in remote areas where grid expansion is uneconomical. Dengyuan, Jingfeng, Zhiyan, Gaofei, Hongfang, Haijiao, Bo, Grenko, Borden, Sauer, Roessler, Jianhua, Haitao, Bultman, Vlooswijk and Venema (2012:3004) state that industry analysts concur that low cost per watt of electricity generated from

photovoltaic system is attained in many electrical markets and the goal of the photovoltaic industry is to attain grid parity through mass production.

In areas remote from grid-connected electricity, photovoltaic systems are used as stand-alone electricity sources in SA. The Department of Minerals and Energy (2002:11) states that SA receives high solar radiation as illustrated in Figure 6.

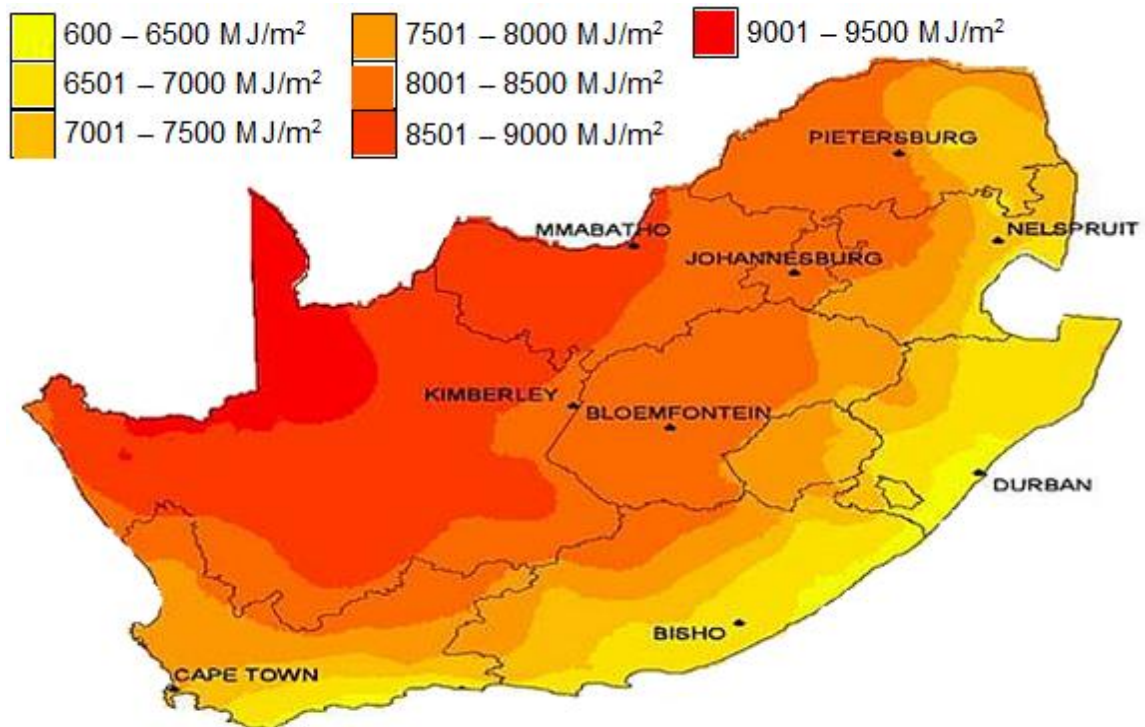


Figure 6 Annual solar radiation in SA (RSA Department of Minerals and Energy 2002:7)

Liming (2009:1097) concludes that as an alternative to grid-connected electricity extension for supplying electricity to rural (remote) areas, local renewable sources can be used as a solution to the problem. This solution is an environmentally friendly way to produce energy using renewable energy sources.

2.3 Photovoltaic technology classification

Photovoltaic history dates back to 1839 when Edmond Becquerel observed that a small voltage and current is generated when metal plates (platinum or silver) soaked in a suitable solution are exposed to light, that is the photovoltaic effect (Kazmerski 1997:73).

Photovoltaic effect is the conversion of photons from the sun into electricity in semiconductors such as solar cells (Hamakawa 1994:275). Bell Laboratories initiated the development of a practical device in the early 1950s (Markvart 1988:3/1). El Chaar, Lamont and El Zein (2011:2167) tabulates the historic developments in photovoltaic solar energy conversion as shown in Table 1.

Table 1 Historical developments in photovoltaic solar conversion (El Chaar *et al.* 2011:2167)

Scientist and innovation	Year
Becquerel discovers the photovoltaic effect	1839
Adams and Day notice photovoltaic effect in selenium	1876
Planck claims the quantum nature of light	1900
Wilson proposes Quantum theory of solids	1930
Mott and Schottky develop the theory of solid-state rectifier (diode)	1940
Barddeen, Brattain and Shockley invent the transistor	1949
Charpin, Fuller and Pearson announce 6% efficiency silicon solar cell	1954
Reynolds et al. highlights solar cell based on cadmium sulphide	1954
First use of solar cells on an orbiting satellite Vanguard 1	1958

Silicon is a prominent raw material in photovoltaic solar cell manufacturing. This is attributed to the material's abundance and high-efficiency potential (McCann, R. Catchpole, J. Weber & W. Blakers 2001:135). However the high material cost of silicon prompted research into thin film technology, reducing material

consumption and decreasing the input energy in the fabrication process thus lessening the cost of photovoltaic solar cell application (Razykov, Ferekides, Morel, Stefanakos, Ullal & Upadhyaya 2011:1581).

Material properties such as a band-gap between 1.1 and 1.7 eV, direct band structure, non-toxicity, long-term stability and a high photovoltaic conversion efficiency are prerequisites for an ideal photovoltaic solar cell material (Goetzberger & Hebling 2000:3). Tyagi, Rahim, Rahim and Selvaraj (2013) categorises photovoltaic material as shown in Figure 7.

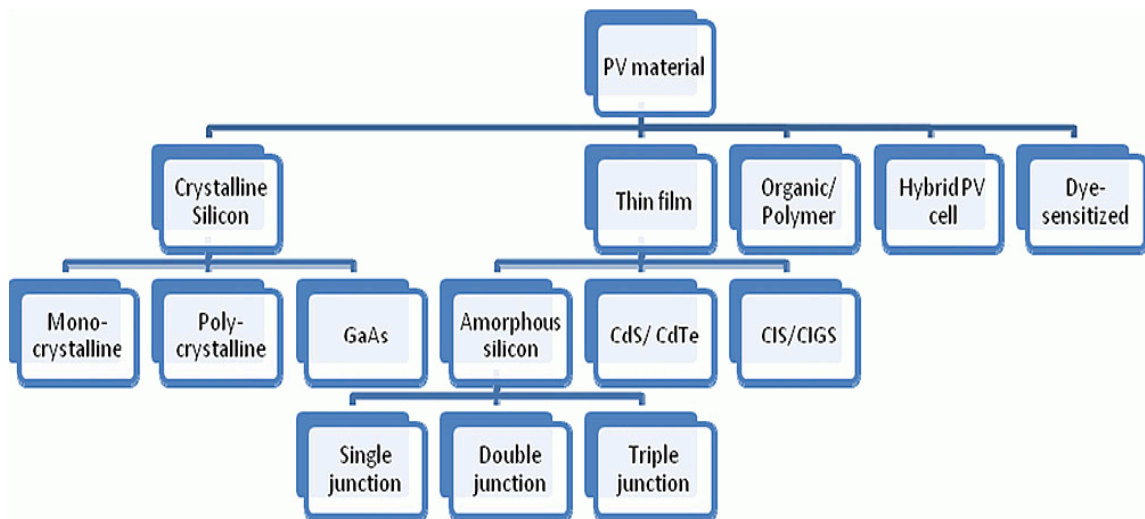


Figure 7 Photovoltaic material categorisation (Tyagi *et al.* 2013:446)

High conversion efficiency, low material cost and stability are essential factors governing commercial viability of photovoltaic solar cells. Three types of thin film technology which reduce material cost are cadmium telluride (CdTe), copper indium selenide (CIS) and amorphous silicon alloy (Guha 1998:190).

Non-crystallised silicon (amorphous silicon) has single, double and triple junction designs that absorb sunlight efficiently (Guha & Yang 2006:1917) and are susceptible to degradation (Parida, Iniyan & Goic 2011:1627). The width of an

amorphous solar cell is about 300 nm because of its direct band gap which is approximately 1.7 eV. This makes solar absorption of an amorphous solar cell 100 time greater than that of crystalline silicon solar cell (van Swaaij, Smets & Zeman 2012:2). Contrary to their high solar absorption, amorphous silicon solar cells have low conversion efficiency ranging between 5 - 7%, 8 - 10% for double- and triple-junction technologies (Parida *et al.* 2011:1627).

Unlike amorphous silicon solar cells, cadmium sulphide (CdS)/cadmium telluride (CdTe) solar cells have long-term stability (Böer 2011:426). Temperature variations and moisture sensitivity are a couple of the hindrances associated with CdS solar cells application (Spakowski 1967:21). The major limitations of cadmium is that it is a toxic metal and tellurium supply globally is minimal (Böer 2011:429). Similar to the amorphous silicon solar cell the copper indium gallium selenide (CIGS)/copper indium selenide (CIS) solar cell is also susceptible to degradation yielding a short operational lifespan (Radue, van Dyk & Macabebe 2009:2385).

Although organic solar cells have low conversion efficiency, future research in technology's mechanical properties may improve the reliability of the solar cell (Xing, Simin, Zhang, Shengzhi, Zhicheng, Hao & Sheng 2012:2132). Low material cost of organic solar cells propels research into optimising the technology to compete with mono- and poly-crystalline silicon which dominate the photovoltaic market (Ratcliff, Zacher, Steirer, Gantz, MacDonald, Macech, Tadytin, Ou & Armstrong 2011:3472).

The combination of organic and inorganic materials produces hybrid solar cells. The intent of the combination is to establish a mutual relationship between both material groups to better exploit the advantages of both materials (Wright & Uddin 2012:88). Organic material provides a high solar absorption coefficient

(Zhokhavets, Erb, Gobsch, Al-Ibrahim & Ambacher 2006:349) and environmental stability is provided by the inorganic material (Wright & Uddin 2012:88). The technology is still in its infancy stage yielding low conversion efficiency with much research being undertaken (Dong, Yunfang, Xiao, Fute, Tao & Baoquan 2013:347). Wu, Tian and Jiang (2005:645) conducted research into the technology that produced a higher ratio of performance to cost by tracking the maximum power point.

Crystalline silicon solar cells (mono-crystalline, poly-crystalline and gallium arsenide (GaAs)) dominate the photovoltaic market owing to their high efficiency when compared to other solar cell materials (Tyagi *et al.* 2013:445). Although wafer silicon has a high efficiency a substantial amount of material thickness (300 μm) (Munzer, Holdermann, Schlosser & Sterk 1999:2055) is required owing its low light absorption characteristic (Solanki, Bilyalov, Beaucarne & Poortmans 2003:1320). Cost reduction of wafer silicon solar cells can thus be achieved by reducing the material thickness which contributes 50-60% of the total cost of the silicon solar cell (Munzer *et al.* 1999:2055).

Thus thin crystalline solar cells have the benefit of low material cost similar to other thin film technology (cadmium telluride (CdTe), copper indium selenide (CIS) and amorphous silicon) but maintains the advantages of crystalline silicon (Blakers 1998:385). Thin crystalline silicon solar cells are narrower (10-50 μm) than wafer silicon solar cells (200-300 μm) which increases the degree of electrical active defect state on the cell (Kunz, Gazuz, Hessmann, Gawehns, Burkert & Brabec 2011:2454).

The compulsion to substitute fossil-fuel based energy resources with renewable energy resources is directly proportional to the photovoltaic industry growth (Liang, Chen, Liang, Yang, Shen & Shi 2010:2297). Solar photovoltaic

technology is the potential solution for future energy demands owing to the substantial research in the technology and milestones achieved to improve its performance (Parida *et al.* 2011:1633). Future research and development of thin film crystalline solar cells are inspired by its potential advantages of cost reduction, high-efficiency potential, raw material abundance and research liaison with integrated circuit industry (McCann *et al.* 2001:135).

2.4 Photovoltaic technology cost analysis

The major contributors to photovoltaic module cost are raw material cost and manufacturing cost (Applasamy 2011:214). Global photovoltaic application peaked at 100 GW in 2012 as shown in Figure 8 (Renewable energy policy network for the 21st century (REN21) 2013:40). The escalation in photovoltaic application globally can be attributed to reduction in manufacturing costs and an increase in government incentive for both consumer and producer (Branker, Pathak & Pearce 2011:4471).

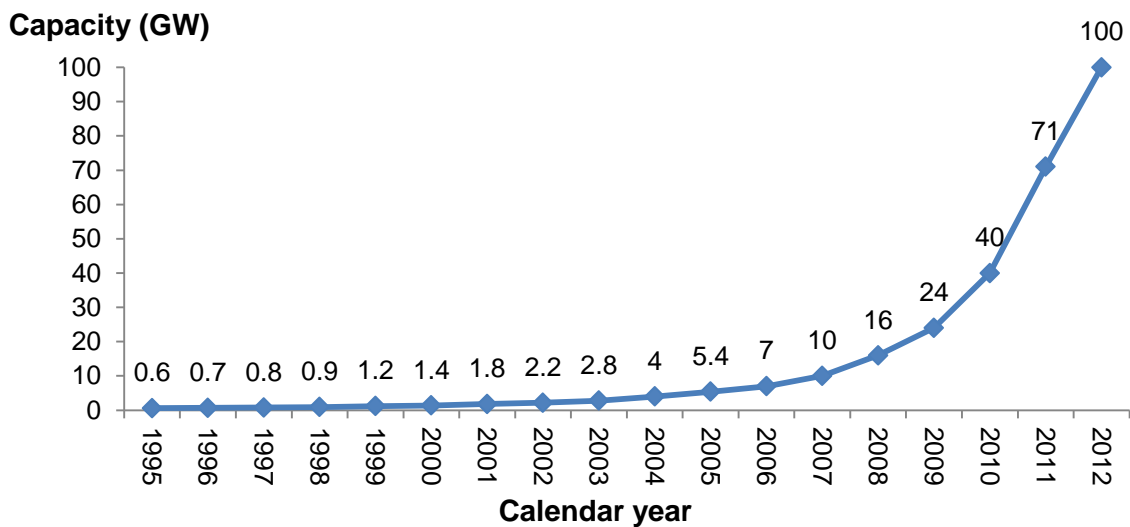


Figure 8 Solar photovoltaic global capacity, 1995-2012 (Renewable energy policy network for the 21st century (REN21) 2013:40)

The total cost of a photovoltaic system is determined by the cost of the photovoltaic module (array) size, storage device size and other required components for a particular application. Thus accurate design of the photovoltaic system is fundamental to cost analysis of the system (Chel, Tiwari & Chandra 2009:1172).

2.5 Photovoltaic technology life cycle cost analysis

Currently low published photovoltaic costs are based only on large scale grid-connected photovoltaics requiring no power storage, excluding other cost-contributing factors (Erickson & Chapman 1995:1131). Life cycle cost (LCC) analysis on the other hand is the total cost of energy delivered by a system during its lifespan in today's money value considering future inflation (Kalogirou 2009:665).

In Malaysia Applasamy (2011:218) conducted life cycle cost analysis of stand-alone photovoltaic systems for household application over a period of 25 years using various photovoltaic modules, concluding that the cost of supplying electricity using photovoltaics was five times more than conventional methods of supplying electricity.

Contrary to Applasamy (2011:218), Shen (2008:702) establishes that stand-alone photovoltaic system cost can be minimised in Malaysia by employing life cycle costing including non-technical factors as photovoltaic panel tilt angle, the maximum battery depth discharge, inflation and interest rate of the system. Photovoltaic systems remain the most cost-effective for various applications because of their low life cycle unit cost (Koner, Dutta & Chopra 2000:321).

Life cycle cost assessment can be utilised to compare various photovoltaic systems with each other, with other systems (Notton, Muselli & Poggi 1998:305) and determine the most cost-effective system design, employing equation 1 (Foster, Ghasseme & Cota 2010:236).

$$LCC = C + M_{pw} + E_{pw} + R_{pw} - S_{pw} \quad \dots(1)$$

Where,

$LCC \equiv$ life cycle cost.

$C \equiv$ Initial investment cost.

$M_{pw} \equiv$ sum of annual operation and maintenance costs.

$E_{pw} \equiv$ energy cost (annual sum of fuel cost).

$R_{pw} \equiv$ sum of annual replacement cost.

$S_{pw} \equiv$ salvage value (net worth at end of final year).

$pw \equiv$ present worth.

2.6 Photovoltaic system sizing

Photovoltaic system sizing is aimed at meeting the energy requirements of an application utilising available solar radiation (Chapman 1990:965). When applying a photovoltaic system, the energy supply should exceed the application's energy demand (Skunpong & Plangklang 2011:121). Energy requirements for various photovoltaic system applications determine the photovoltaic panel size and energy storage capacity (Haifeng, Liqin & Asgarpour 2008:2). When sizing a stand-alone photovoltaic system the load and storage systems are designed initially (Hontoria, Aguilera & Zufiria 2003:2423).

Accurate photovoltaic system sizing reduces the system's life cycle cost which include acquisition costs, maintenance costs and operations costs (Kaye 1994:1192). Optimum solar energy utilisation is realised when a photovoltaic

system is sized in consideration of the irradiation, the load and required power storage (Eiichi & Kurokawa 1994:1196).

Under- and over-sizing of a photovoltaic system decreases supply reliability and increases power generation costs (Markvart 2000:110). Development and innovation in off-grid photovoltaic components which are the photovoltaic module, battery bank and power conditioning unit (Nikhil & Subhakar 2012:1136) resulted in increased reliability and reduced system life cycle costs (Kaye 1994:1192).

Photovoltaic system sizing methods can be classified into three groups according to their simplicity: intuitive method, numerical method and analytical method (Posadillo & López Luque 2008:1039). The last sizing method has an advantage of a combination of accuracy and simplicity (Hontoria *et al.* 2003:2423).

The analytical method is more useful when considering stand-alone photovoltaic systems as it incorporates many suitable variables including solar radiation, clearness index, latitude, efficiency of photovoltaic module, loss of load probability, unit cost of the photovoltaic module as well as the battery (Jakhrani, Othman, Rigit, Samo & Kamboh 2012:681).

2.6.1 Estimated electric load (E-learning ICT equipment)

The load-based photovoltaic sizing method is usually used to determine stand-alone photovoltaic system parameters (Rizzo, Piegari, Tricoli, Munteanu & Topa 2009:1). Stand-alone photovoltaic system can be classified into three subdivisions: direct connected systems (photovoltaic to load without storage), hybrid system (photovoltaic with other non-renewable resources) and stand-alone

system (photovoltaic with storage) as shown in Figure 9 (IEEE 1998). Stand-alone systems are usually utilised in off-grid applications (Campoccia, Favuzza, Sanseverino & Zizzo 2010:158).

The electric load of a stand-alone off-grid photovoltaic system can be estimated by listing the various loads (AC and DC), power requirement for each load, load operational hours per day and the number of operational days per week (McCarney, Olson & Weiss 1987:26).

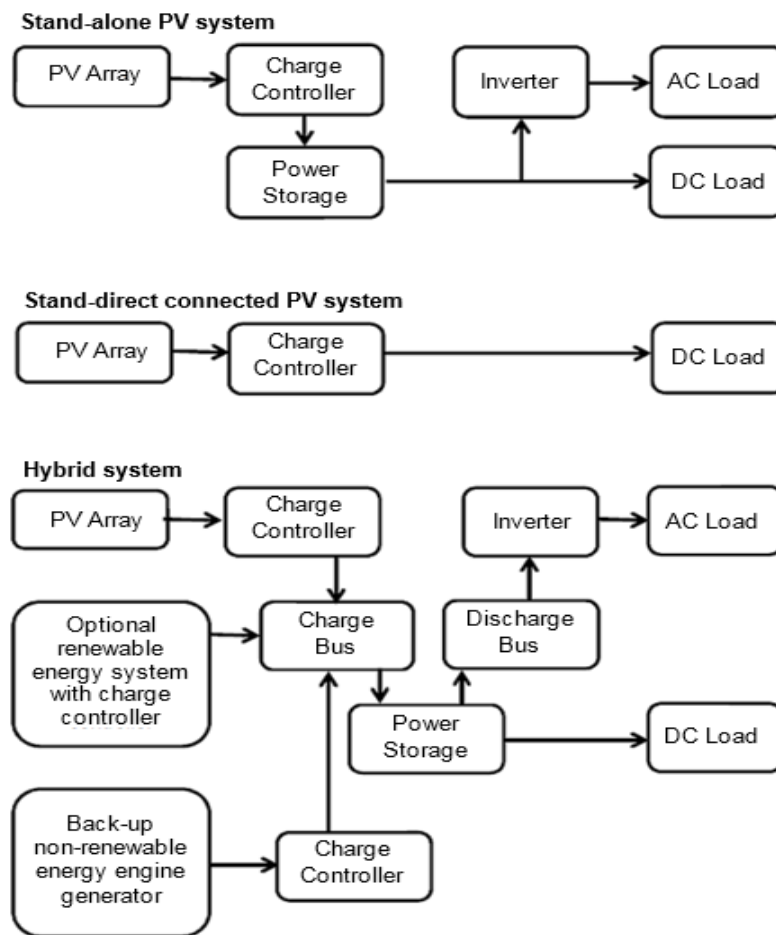


Figure 9 Photovoltaic system types (IEEE Guide for Terrestrial Photovoltaic Power System Safety 1998:3)

In brief, the electric load of a system (stand-alone off-grid photovoltaic system) are appliances and equipment to be powered by the system. The electric load of a system can be tabulated or illustrated on a graph (IEEE Std 1013 2007:4).

The electric power requirements of a load can be reduced by using DC loads (eliminating inverter power losses) and performing tasks during the day maximising battery efficiency (McCarney *et al.* 1987:22). The stand-alone off-grid photovoltaic system will be utilised to power an e-learning centre thus the significant load of the system will be computers and other ICT infrastructure (Education Dynamics 2012). Table 2 lists Energy Star 5.0 power specifications for qualified desktop computers (EU Energy Star 2012b).

Table 2 List of compliant Energy Star 5.0 desktop computers with power specifications (EU Energy Star 2012b)

Manufacturer (Brand)	Idle mode (W)	Standby (off mode) (W)	Sleep mode (W)	Total Energy Consumption (kWh)
Acer	12,8 – 82,1	0,2 – 0,8	1,9 – 4,0	43,1 – 880,0
ASUS	10,4 – 147,3	0,1 – 1,9	1,0 – 4,4	41,0 – 175,0
Compaq	12,9 – 49,5	0,3 – 1,0	1,1 – 4,6	47,7 – 178,8
Dell	10,2 – 145,3	0,2 – 2,1	1,3 – 3,9	31,0 – 290,1
Fujitsu	10,8 – 71,5	0,3 – 0,8	1,3 – 3,5	40,1 – 260,2
HP	5,0 – 204,0	0,3 – 1,7	0,6 – 5,2	16,3 – 387,4
Lenovo	9,0 – 71,3	0,6 – 2,5	0,6 – 3,7	29,0 – 250,2
LG	26,8 – 30,0	0,4 – 0,5	0,8 – 1,0	96,0 – 105,5
MSI	7,7 – 49,7	0,3 – 1,7	0,6 – 6,8	23,6 – 138,6
Samsung	7,7 – 30,4	0,4 – 1,7	0,7 – 3,0	29,9 – 103,5
Sony	31,7 – 56,0	0,3 – 1,8	0,3 – 2,6	113,6 – 200,4
Toshiba	6,6 – 24,9	0,3 – 1,7	0,7 – 1,2	20,1 – 91,7

The energy efficiency of laptops is 50%-80% higher than desktop computers; this is attributed to critical power management design of laptops (EU Energy Star 2012a). Table 3 lists Energy Star 5.0 power specifications for qualified notebook computers.

Table 3: List of compliant Energy Star 5.0 notebook computers with power specifications (EU Energy Star 2012b)

Manufacturer (Brand)	Idle mode (W)	Standby (off mode) (W)	Sleep mode (W)	Average Annual Energy Consumption (kWh)
LG	6.5 – 17.0	0.3 – 0.9	0,4 – 1,1	28.05
Lenovo	1.2 – 18.7	0.2 – 1.4	0,5 – 1,8	30.7
Toshiba	5.2 – 19.1	0.2 – 1.9	0,6 – 2,8	31.6
Acer	4.7 – 18.9	0,1 – 1,2	0,3 – 1,6	33.85
Compaq	7.3 – 17.4	0,4 – 0,8	0,7 – 1,3	36
MSI	5.8 – 16.9	0.3 – 0.7	0,6 – 1,9	36.85
HP	5.1 – 24.8	0.3 – 1,1	0,6 – 1,6	43.65
Sony	5.1 – 19.8	0.2 – 0.9	0,7 – 1,7	44.5
Samsung	5.2 – 15.8	0.2 – 0.8	0,5 – 1,9	47.05
ASUS	4.5 – 26.8	0,1 – 1,0	0,4 – 2,8	49.3
Dell	6.3 – 25.6	0,2 – 1,9	0,6 – 3,2	51.5
Fujitsu	6.5 – 30.6	0,2 – 1,7	0,6 – 2,4	54.15

The minimum stipulated software requirement for e-learning computers is Microsoft Windows XP and Microsoft Windows 7 operating systems (SAP 2011; Adobe Reader 2013; iBwave 2013). The e-learning centre minimum computer performance requirements will be derived from the minimum prerequisites for Microsoft Windows 7 instead of Microsoft windows XP because technical support for the latter ends in April 8, 2014 (Microsoft Windows 2013).

2.6.2 E-learning centre lighting

Electrical lighting is a major load on a building's power supply. Electricity consumed globally in most commercial buildings by lighting was estimated to be 1133 TWh in 2005. Figure 10 shows the energy consumption of commercial buildings' lighting globally (Internal Energy Agency 2006:210)

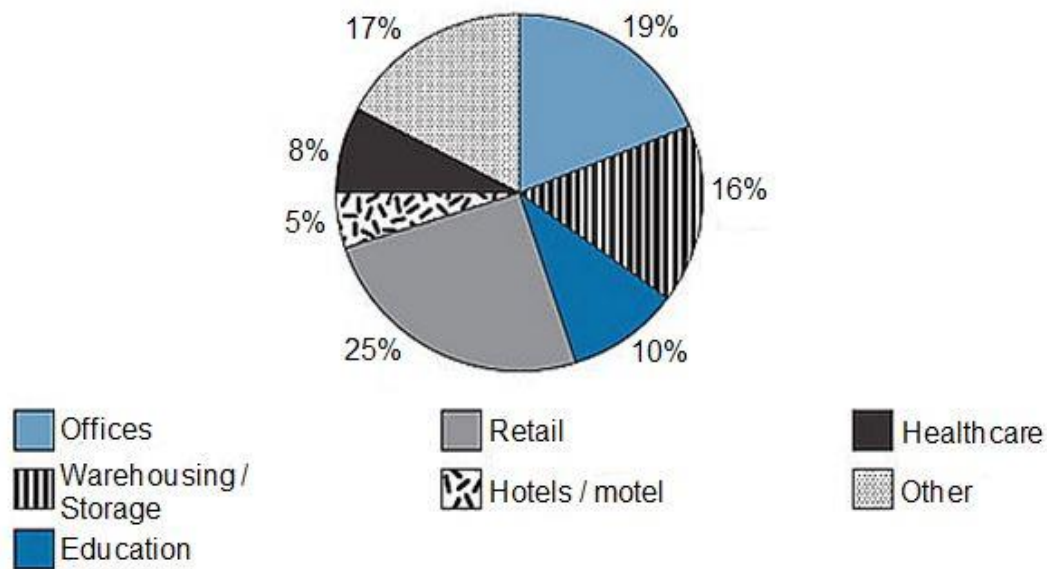


Figure 10 Energy consumption of commercial building's lighting globally (Internal Energy Agency 2006)

Currently the most important factors concerning lighting are quality of light, cost, energy efficiency and daylight use. Lighting quality can be evaluated based on the level of visual comfort and task light requirements (Halonen, Tetri & Bhusal 2010:13). A general acceptable definition of lighting quality is that the client's and designer's objectives and constraint are met by the light installation. One of the objectives to achieve lighting quality is to create a visually comfortable luminous environment (Boyce 2003). Visual discomfort results from glare (discomfort glare or disability glare).

Discomfort glare occurs when the task to be carried out or the task background is too bright (Fischer 1986:128). Disability glare is caused by bright light sources resulting in difficulty in seeing the task being done (Pritchard 1995:12).

Seeing or vision can be defined as a process in which electromagnetic radiation stimulates the retina of an eye creating sensation of sight or light (Pritchard 1995:1). The eye distinguishes between different wavelengths in the visible portion of the electromagnetic spectrum which ranges from 380 nm to 780 nm. The different wavelengths in the visual spectrum give a sensation of colour (Coaton & Marsden 1997:3). Figure 11 highlights the visible portion of the electromagnetic spectrum.

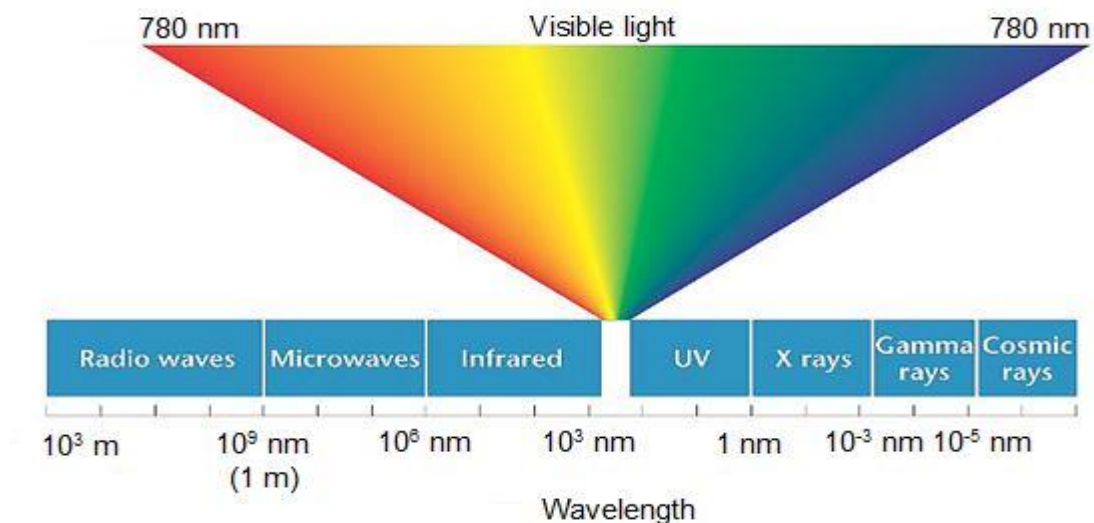


Figure 11 Electromagnetic spectrum visible portion highlighted (Elmasry & Sun 2010:15)

The South African Bureau of Standards (SABS) provides guidelines and references for interior lighting (average luminance over a surface) for the formation of good viewing conditions, ensuring a comfortable visual environment using artificial lighting for various rooms and activities as shown in Table 4 (South African National Standards 2005:18).

Table 4 Recommended minimum illuminance for educational buildings (South African National Standards 2005:18)

Type of interior	Minimum illuminance (lx)
Classrooms and tutorial rooms	300
Classroom for viewing classes	500
Lecture Hall	500
Classroom for adult education	500
Chalk board (vertical illuminance)	500
Technical drawing rooms	750
Practical rooms and laboratories	500
Computer practice rooms	500
Student common rooms and assembly halls	200
Library shelves, stacks	300
Reading tables	400

An illuminance of 500 lx should be maintained in rooms where all work stations utilise a visual display unit (VDU). The recommended luminaire cut-off angle 50 and 60 for continuous and occasional use of the VDU respectively is shown in Figure 12 (South African National Standards 2005).

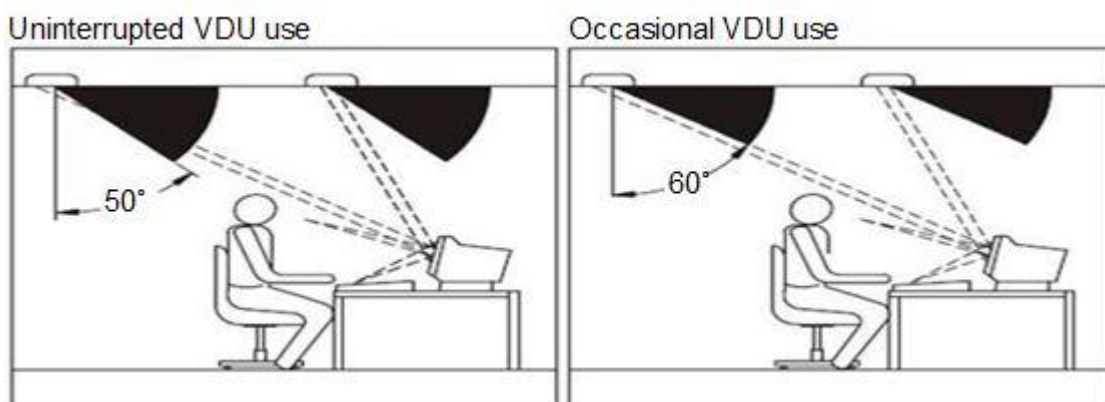


Figure 12 The recommended luminaire cut-off angle for uninterrupted and occasional use of the VDU (South African National Standards 2005:52)

Since 1879 when Thomas Alva Edison invented the incandescent lamp, various light sources have currently been developed with significantly improved lighting quality, efficiency, energy consumption and lifespan. Figure 13 illustrates the for main groups of light sources (Zumtobel 2013).

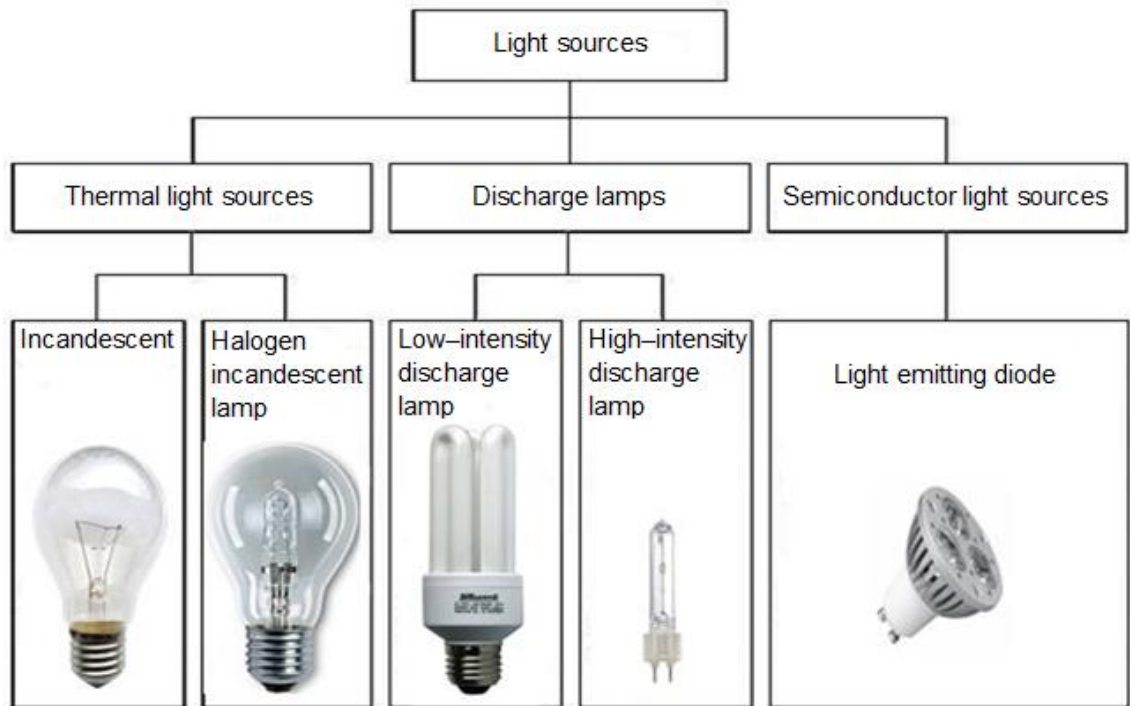


Figure 13 Main groups of light sources (Zumtobel 2013:81)

The semiconductor lighting source or solid state lighting (SSL) technology based on light emitting diodes (LEDs) is developing rapidly with future focused energy efficiency that surpasses thermal light sources and discharge lamps. Notable operational advantages of LED technology when compared to other lighting sources are: high energy efficiency, low power utilisation, long lifespan (25 000 - 50 000 hours), less heat emitted, no ultra violet or infrared radiation and high luminous efficacy.

The viewing angle of an LED influences its luminous intensity. Therefore if two LEDs have the same luminous intensity value but varying viewing angles, the LED with the smaller viewing angle will have the lower total light output (Held 2008:42). Mazda (1981:41) defines the LED viewing angle as the point at which luminous intensity is half the value observed at zero degrees (viewed head on) as shown in Figure 14.

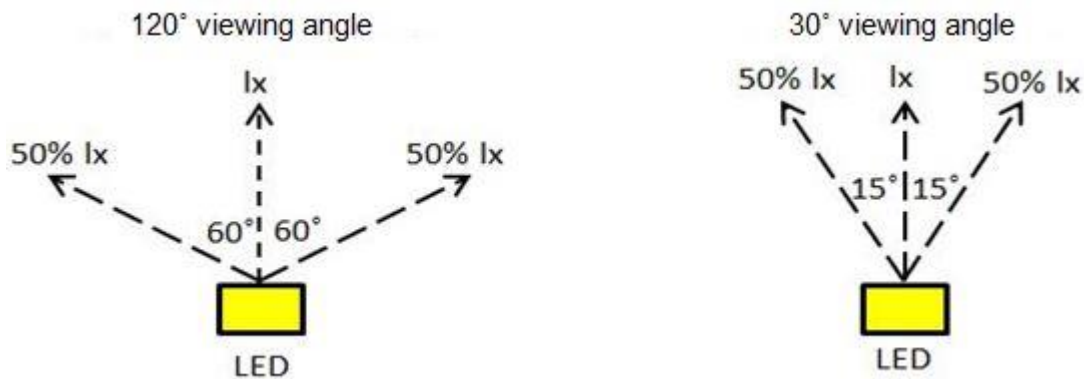


Figure 14 LED viewing angle (Arrow North American Components 2014)

The selection of luminaires to be employed is established based on the following: type of activity to be executed in the room, the room occupancy and illuminance requirements for tasks (Fischer 1986:132). Halonen *et al.* (2010:13) conclude that the significant factors influencing artificial light source selection are: illuminance intensity, individual control of luminaries, energy efficiency and total cost.

2.6.3 Photovoltaic module operation and sizing

The amount of solar irradiance captured by a photovoltaic panel is related to the panel's orientation and tilt angle which affects the panel's power output (Jafarkazemi & Saadabadi 2013:44). Conventional orientation of photovoltaic

panels is towards the equator. In the northern hemisphere photovoltaic panels face south and in the southern hemisphere photovoltaic panels face north. The optimum tilt angle of photovoltaic panels is installation site dependant since solar radiation varies for every location daily (Yadav & Chandel 2013:503).

Numerous factors including the latitude of a location influence a photovoltaic panel's tilt angle. Several studies have been undertaken to establish the relationship between photovoltaic installation location latitude and optimum tilt angle (Gharakhani Siraki & Pillay 2012:1920). Table 5 lists generally used relationships between latitude (ϕ) and tilt angles as determined by several authors (Yadav & Chandel 2013:507).

Table 5 Tilt angle and latitude (ϕ) relationship (Yadav & Chandel 2013:507)

Reference	Tilt Angle	Remarks
Duffie and Beckman	$(\phi + 15^\circ) \pm 15^\circ$	For all the equations the minus sign is used for summer months and positive sign for winter months.
Heywood	$(\phi - 10^\circ)$	
Lunde	$(\phi \pm 15^\circ)$	
Chinnery	$(\phi + 10^\circ)$	
Löf and Tybout	$\phi + (10^\circ \rightarrow 30^\circ)$	
Garg	$(\phi \pm 15^\circ), 0.9\phi$	
Hottel	$(\phi + 20^\circ)$	
Kern and Harris	$(\phi + 10^\circ)$	
Yellot	$(\phi + 20^\circ)$	
Elminir	$(\phi + 15^\circ) \pm 15^\circ$	

Cheng, Sanchez Jimenez and Lee (2009:1650) obtained an average of 98.6% photovoltaic system operation using the location's latitude for the photovoltaic panel's tilt angle. The highest average solar irradiance will fall on the collector with a tilt angle equal to the latitude of the location of installation (McCarney *et al.* 1987:123).

2.6.4 Photovoltaic system inverter and wire specification

AC loads cannot be powered directly from photovoltaic panels because DC electricity is generated by photovoltaic panels (Elma & Selamogullari 2011:1-318). An essential link between the energy produced by the photovoltaic panel and the AC load is provided by an inverter which converts DC electricity to AC electricity (Bower & Whitaker 2002:1406).

Photovoltaic system sizing based on the rationale that the actual DC output of a photovoltaic system will always be below its standard test condition (STC) rating, justified undersizing photovoltaic system inverters to 30% less power output than that of the photovoltaic system (Keller & Affolter 1995:5). This sizing method resulted in substantial energy loss owing to development in photovoltaic technology as well as improved inverter efficiency at 95%-97% with slightly reduced efficiency at full load. Thus undersized inverters operate below their maximum performance levels depending on a location's irradiation (Burger & Rüther 2006:33). Figure 15 shows an inverter's total efficiency and photovoltaic DC voltage as a function of loading.

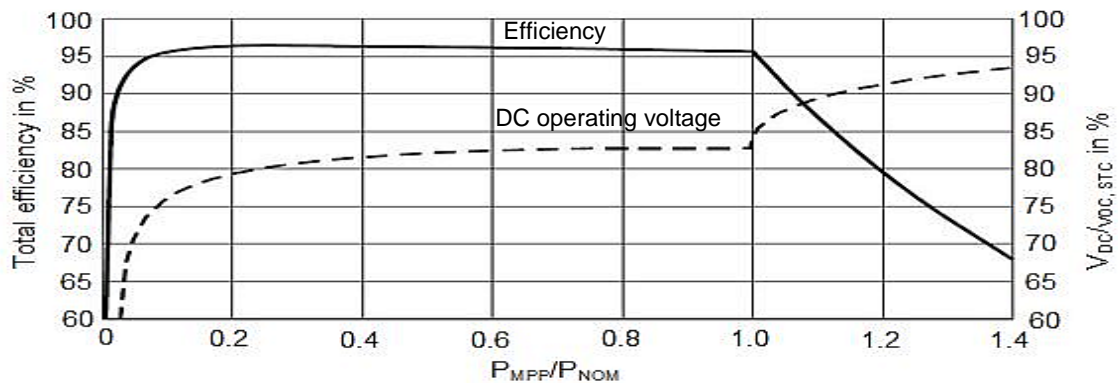


Figure 15 Inverter total efficiency and photovoltaic DC voltage as a function of loading (Burger & Rüther 2006:34)

Significant factors that influence inverter sizing are meteorological factors (irradiance and air temperature), economic factors (inverter initial cost, electricity rate, feed-in tariffs and return on investment) and inverter's innate characteristics (protection scheme and efficiency curve) (Chen, Li, Brady & Lehman 2013:97). Figure 16 illustrates a summary of inverter sizing considering significant factors.

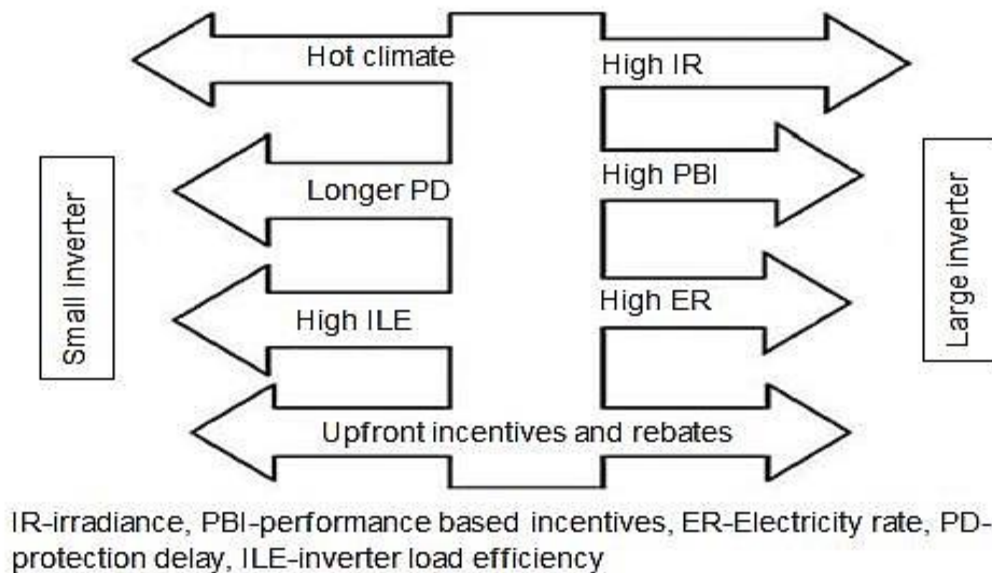


Figure 16 Summary of inverter sizing considering significant factors (Chen *et al.* 2013:97)

The input and output power of a photovoltaic system inverter is transmitted from the solar panel to the load via a network of transmission wires (Yuventi 2012:2997). Over-current protection and system grounding are essential safety features when wiring a photovoltaic system. Over-current protection can be obtained by considering the current carrying ability (ampacity) of a cable before using it to wire a photovoltaic system (McCarney *et al.* 1987:150). The national electric code (NEC) recommends various cable sizes, conducting material and the wire current carrying (ampacity) limit (Yuventi 2012:2996). Table 6 lists wire types and their ampacity. Observation and application of the NEC standards

reduce dangers associated with photovoltaic system electrical installation (John 2001:4).

Table 6 Wire type and ampacity (John 2001:4)

Temperature rating of conductor						
AWG size	Copper			Aluminium		
	60 °C	75 °C	90 °C	60 °C	75 °C	90 °C
	Type					
	TW, UF	RHW, THW, THHW	RHW, THW, THHW	TW, UF	RHW, THW, THHW	RHW, THW, THHW
	Ampacity (A)					
18	-	-	14	-	-	-
16	-	-	18	-	-	-
14	20	20	25	-	-	-
12	25	25	30	20	20	25
10	30	35	40	25	30	35
8	40	50	55	30	40	45
6	55	65	75	40	50	60
4	70	85	95	55	65	75
3	85	100	110	65	75	85
2	95	115	130	75	90	100
1	110	130	150	85	100	115

H - heat resistance; T - thermoplastic insulated; W - Approved for damp and wet conditions; U – underground; F – Feeder

The wire size is given according to the American wire gauge (AWG) where the size of the wire is directly proportional to the current ampacity and inversely proportional to the AWG number (McCarney *et al.* 1987:150). Figure 17 shows American wire gauge wire sizes.

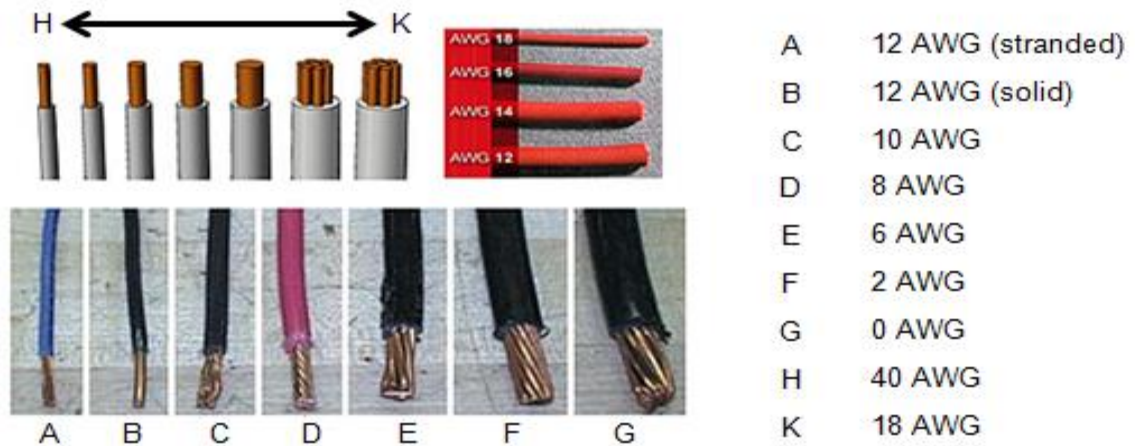


Figure 17 American wire gauge wire sizes (McCarney *et al.* 1987:150)

The length of a wire, current flow in a wire and AWG size of a wire are a function of a cable's voltage drop (line losses) which influences optimum sizing of photovoltaic wire requirements (McCarney *et al.* 1987:151). Table 7 lists the suggested one-way length for various AWG wire sizes (5% voltage drop), grey area indicating exceeded ampacity.

Table 7 One way length for various AWG wire sizes at 5% voltage drop (Northern Arizona Wind and Sun Company 2012:81)

Current (A)	Power (W)	AWG sizes									
		14	12	10	8	6	4	2	1/0	2/0	3/0
120V _{AC/DC}		Maximum length one-way (m)									
2	240	129	200								
4	480	57	100	157							
6	720	43	69	100	171						
8	960	31	48	83	129	203					
10	1200	26	40	66	103	163					
15	1800	17	26	40	69	109	171				
20	2400		20	31	51	83	129	206			

Table 7 (Continued) One way length for various AWG wire sizes at 5% voltage drop (Northern Arizona Wind and Sun Company 2012:81)

Current (A)	Power (W)	AWG sizes													
		14	12	10	8	6	4	2	1/0	2/0	3/0				
120V _{AC/DC}		Maximum length one-way (m)													
25	3000			26	40	66	103	166							
30	3600			20	34	54	86	137				220			
40	4800				26	40	66	103				166	206		
50	6000				20	31	52	83				131	166	208	
24V _{DC}															
1	24	52	80	126	206										
2	48	26	40	63	103							162			
4	96	11	20	31	52							81			
6	144	9	14	20	34							54	86		
8	192	6	11	16	26	40	66								
10	240	5	8	13	20	33	52					82			
15	360	3	5	8	14	22	34					55	88		
20	480		4	6	11	16	26					41	66	82	105
25	600			5	8	13	20	33	52	66	84				
30	720			4	7	11	17	27	44	55	69				
40	960				5	8	13	20	33	41	52				
12V _{DC}															
1	12	26	40	63	103	162									
2	24	13	20	31	51	81						132	206		
4	48	5	10	16	26	40						66	103	166	206
6	72	4	7	10	17	27						43	69	110	137
8	96	3	5	8	13	20	33	51	83	103	130				
10	120	2	4	7	10	16	26	41	66	82	104				

Table 7 (Continued) One way length for various AWG wire sizes at 5% voltage drop (Northern Arizona Wind and Sun Company 2012:81)

Current (A)	Power (W)	AWG sizes									
		14	12	10	8	6	4	2	1/0	2/0	3/0
12V _{DC}		Maximum length one-way (m)									
15	180	1	3	4	7	10	17	27	44	55	69
20	240			3	5	8	13	20	33	41	52
25	300			2.4	4	7	10	16	26	33	42
30	360			2	3	5	9	14	22	27	35
40	480			2.4	4	6	10	16	20	26	

2.6.5 Energy storage devices

The electricity produced from renewable energy resources such as solar energy varies independently from load demand (Koeppel & Korpas 2006:2). The random nature of renewable energy resources prompted research into development of energy storage devices and methods (Ibrahim, Ilinca & Perron 2008:1223).

Available energy storage methods can be categorised into mechanical, chemical and thermal technologies. The leading energy storage technologies are battery storage, fuel cells and super-caps. The last are characterised by factors such as efficiency, storage capacity and discharge time (Zahedi 2011:869). There are various energy storage devices and methods, but only the battery as energy storage device will be discussed in this research.

2.6.6 Battery types and sizing for photovoltaic system

Rechargeable batteries are preferably used in photovoltaic systems with consideration of the following parameters: storage capacity, state of charge

(SOC), depth of discharge (DOD), number of useful charge-discharge cycles, operational lifespan, charging and discharging rate and battery efficiency (Salanki 2013:138).

The battery's storage capacity is the maximum electrical charge stored by chemical bonds within a battery's cells. The battery's storage capacity is a product of the discharge current (in amps) and the discharge time (in hours) (Marwali, Maricar & Shrestha 2000:540). The current that the battery can provide (discharge current) can be calculated if the duration of the current drawn is known (Salanki 2013:128). Then the current drawn is given by:

$$I = \frac{C}{t} \quad \dots(2)$$

Where

$C \equiv \text{Capacity of the battery (Ah)}$

$t \equiv \text{Discharge time (h)}$

$I \equiv \text{Discharge current (A)}$

The unit of measurement for battery storage capacity is amp-hours (Ah or mAh) where current is the prevalent function of available capacity and watt-hours (Wh or mWh) where voltage is the main function indicative of available capacity (Heacock & Freeman 1995:186).

The available percentage capacity of a battery can be measured using a battery's SOC (Marwali *et al.* 2000:540). Thus the percentage ratio of available capacity to rated capacity of a battery expresses the available SOC percentage of a battery (Deepti & Ramanarayanan 2006:89).

$$SOC (\%) = \left[\frac{\text{Available Capacity (Ah)}}{\text{Rated Capacity (Ah)}} \right] \times 100 \quad \dots(3)$$

SOC can be determined by fluid electrolyte (SOC being deduced from acid density) for unsealed batteries. Battery voltage is used to determine SOC for sealed batteries (Sonnenenergie 2008:306). Table 8 shows the SOC of a sealed 12 V lead acid battery based on measured battery voltage.

Table 8 SOC of a sealed 12 V lead acid battery based on measured battery voltage (Quaschnig 2005:162)

Voltage range (V)	SOC
> 14.4	Stop charging, battery is full
13.5 – 14.1	Normal voltage range during charging without load
12.0 – 14.1	Normal voltage range during charging with load
11.5 – 12.7	Normal voltage range during discharge
11.4	Disconnect load, start charging

When a battery is utilised, the DOD of a battery increases in proportional to the decrease in SOC of the battery (Salanki 2013:132). The battery's depth of discharge is inversely proportional to the number of useful charge-discharge cycles as illustrated in Figure 18 (Shen 2008:704).

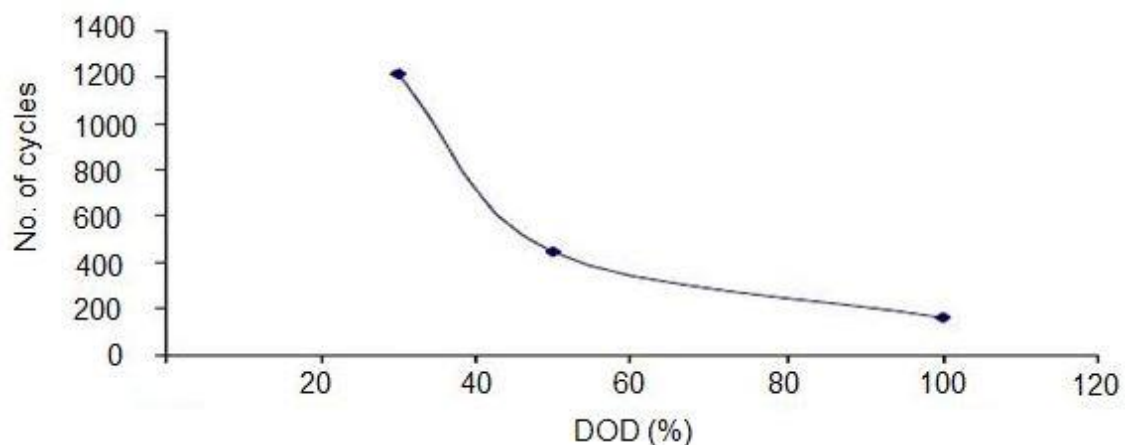


Figure 18 Battery life cycles vs. DOD (Shen 2008:704)

The DOD is a manufacturer specification which indicates how much the battery can be discharged in one cycle before recharging (Hankins 2010:52). The DOD is controlled by the battery's cut-off voltage and discharge rate. The cut-off voltage of a battery is the voltage at which battery discharging should be terminated. Table 9 shows recommended cut-off voltages for various battery types (Battery University 2003).

Table 9 Recommended battery cut-off voltage (Battery University 2003)

Battery type	Li-manganese	Li-phosphate	Lead acid	NiCd/NiMH
Voltage (V)	3.00	2.7	1.75	1.00

One of the fundamental parameters of a battery is the discharge reserve time. The discharge reserve time of a battery is the duration a battery will be able to supply power to the load before reaching its cut-off voltage (Pascoe & Anbuky 2000:589). The discharge reserve time of a lead acid battery (VRLA) can be calculated utilising a unified discharge approach for the entire discharge period. The advantage of this approach is that it is independent of battery conditions and variation in battery operating conditions. Figure 19 shows the typical discharge battery characteristics (Crompton, T.R. 2000:5)

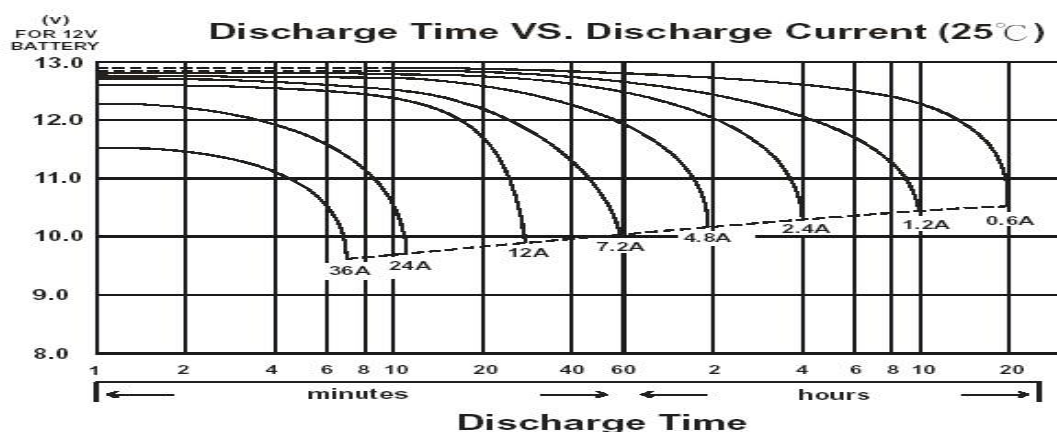


Figure 19 Typical battery discharge characteristics (Crompton, T.R. 2000:5)

The unified discharge approach employs a scaling method to combine the discharge voltage characteristic curve at various discharge rates as shown in Figure 20 (Pascoe & Anbuky 2004:297). A uniform voltage can be calculated using equation 4.

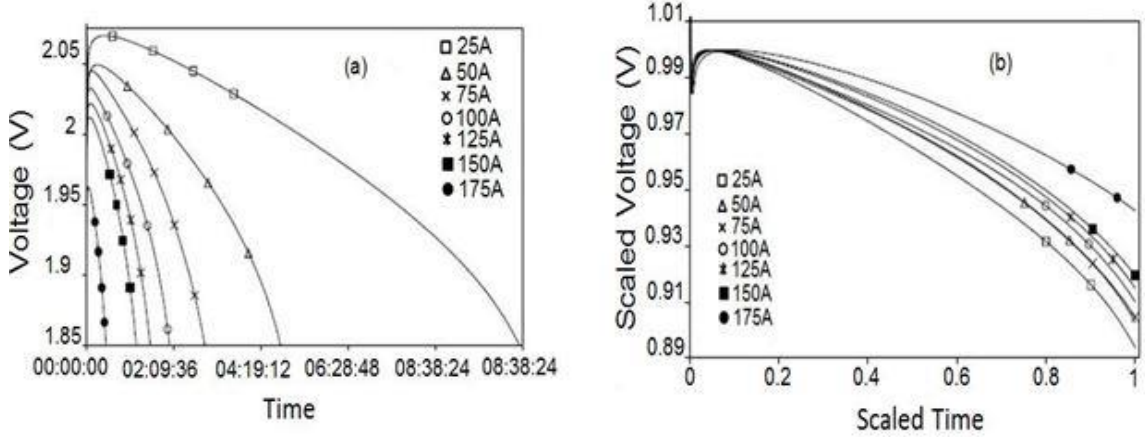


Figure 20 (a) Battery discharge characteristic and (b) equivalent scaled battery discharge characteristics (Pascoe & Anbuky 2004:297)

$$V_u(t) = \frac{(V(t) - V_e)}{V_p - V_e} \quad \dots(4)$$

Where

$V_u(t) \equiv$ Scaled discharge voltage at time (t)

$V(t) \equiv$ Discharge voltage at time (t)

$V_e \equiv$ Battery_{cut-off} voltage

$V_p \equiv$ Battery_{start} voltage

Che-Chi, Shao-Yu and Jih-Chien (2013:179) employ a simple model to determine the discharge reserve time of a Li – ion battery. The model uses the association between the battery's residual capacity and discharge current. Figure 21 illustrates Li – ion discharge reserve time as function of residual capacity (equation 5).

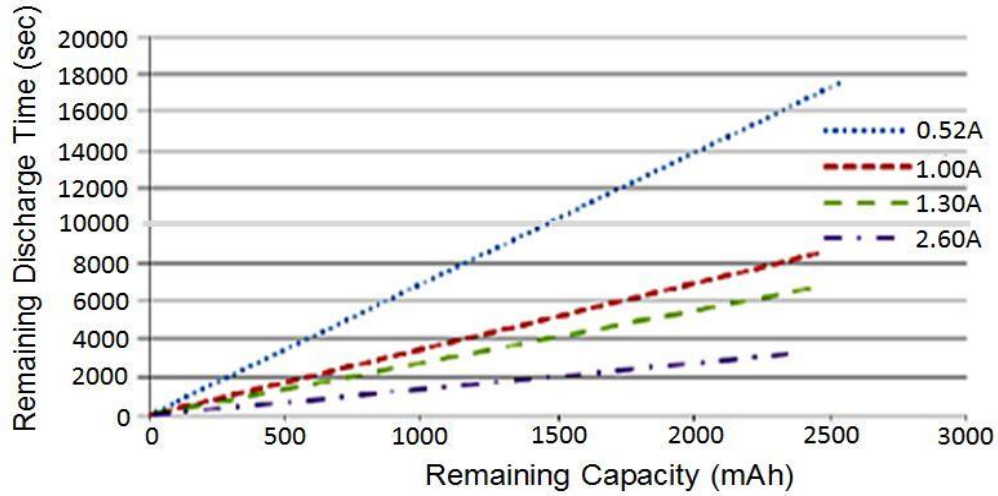


Figure 21 Li – ion discharge reserve time as function of residual capacity (Che-Chi et al. 2013:179)

$$T_r = \frac{C_r}{I_L} \times 3.6 \quad \dots(5)$$

Where

$T_r \equiv$ Discharge reserve time (in seconds)

$C_r \equiv$ Residual capacity (in mAh)

$I_L \equiv$ Discharge current (in Ampere)

The acceptable level of DOD for various rechargeable battery types is shown in Table 10. In practical application of the batteries DOD should be regarded at 50% of manufacturers DOD (Salanki 2013:130).

Table 10 Manufacturers acceptable battery DOD (Salanki 2013:130)

Battery type	Acceptable DOD (%)
Lead - acid	70 – 90
Nickel cadmium	70 – 90
Nickel metal hydride	60 – 70
Li – ion	80 – 90
Li polymer	90 – 98

Using the manufacturers specified battery DOD, the number of batteries (connected in parallel) required for optimum energy storage can be calculated using equation 6 (Balfour 2011:77).

$$\text{Number of Batteries} = \frac{N_c \times E_L}{DOD \times C} \quad \dots(6)$$

Where $N_c \equiv \text{Number of storage days}$

$E_L \equiv \text{Load energy (Wh)}$

$DOD \equiv \text{depth of discharge}$

$C \equiv \text{Capacity of the battery (Wh)}$

And $E_L = P_L \times H_D \times D_W \div 7 \quad \dots(7)$

Where $P_L \equiv \text{Load power consumption (W)}$

$H_D \equiv \text{Operational time per day (h)}$

$D_W \equiv \text{Operational days per week}$

The number of useful charge-discharge cycles (no. of cycles) is reached when the storage capacity is reduced and the battery can no longer supply power (end of operational lifespan). The operational lifespan of a battery is also influenced by other factors such the charge and discharge rate. This rate considerably reduces the operational lifespan of a battery if it higher than the manufacturer's specifications (Babazadeh, Wenzhong & Duncan 2012:3). Figure 22 shows the possible battery characteristics as a function of time for a 15 Ah battery assuming 100% DOD (Salanki 2013:132).

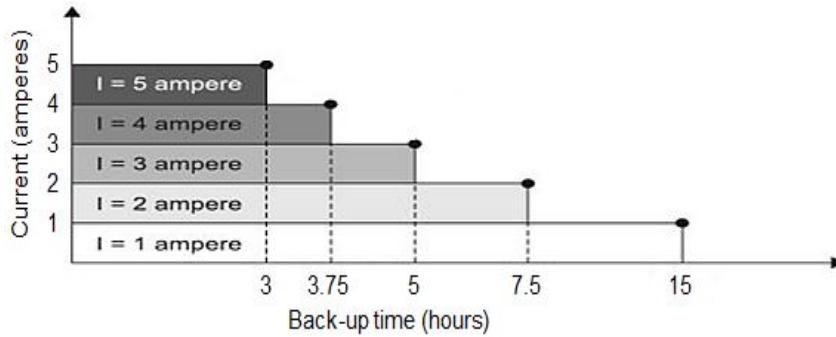


Figure 22 Possible battery characteristics as a function of time for a 15 Ah battery assuming 100% DOD (Salanki 2013:132)

A battery's discharge rate is expressed as the battery's C-rate (Sangwine 1994:52). The term C_x/t (where t is the discharge time in hour and x is the defined capacity discharge rate) is employed to express the c – rate (Dell, Rand & Chemistry 2001:19). Thus a battery with a C-rate of $C_5/10$ will be discharged at 10A an hour for ten hours, with a defined capacity of 100 Ah at a 5-h rate (Sangwine 1994:52). The charge rate of a battery is expressed as a function of the battery's defined capacity at a specific charge current. Therefore a 40h charge rate of a 10 Ah battery is equal to $C/40 = 10/40 = 0.25$ A (Crompton, T.P.J. 2000:Glossary 3).

The operational lifespan of a battery is also affected negatively by overcharging and deep discharge. Overcharging for instance occurs when a battery at 100 per cent SOC (zero per cent DOD) is directly coupled to a photovoltaic panel exposed to high insolation, resulting in excess current supply to the battery (Hankins 2010:54). Deep battery discharge means that the battery is operating at a minimum DOD of 80% (Bard, Inzelt & Scholz 2012:195) as a result of high load usage.

A charge controller is used to control the charging and discharging of a battery. Charge controller battery voltage regulation differs among controllers (Foster,

Ghassemi & Cota 2009:290). The four basic manufacturer specified parameters and characteristics being: photovoltaic array high voltage disconnect (HVD) – the voltage at which the charge controller stops charging the battery, photovoltaic array reconnect voltage (RCV) – voltage at which the charge controller restarts charging the battery, low voltage disconnect (LVD) – voltage at which charge controller disconnects the load from the battery (eliminate deep discharge), load reconnect voltage (LRV) – voltage at which the charge controller reconnects the load to the battery (Foster *et al.* 2009). Figure 23 show basic series and parallel configuration of a charge controller utilised in a photovoltaic battery system (Quaschnig 2005:168).

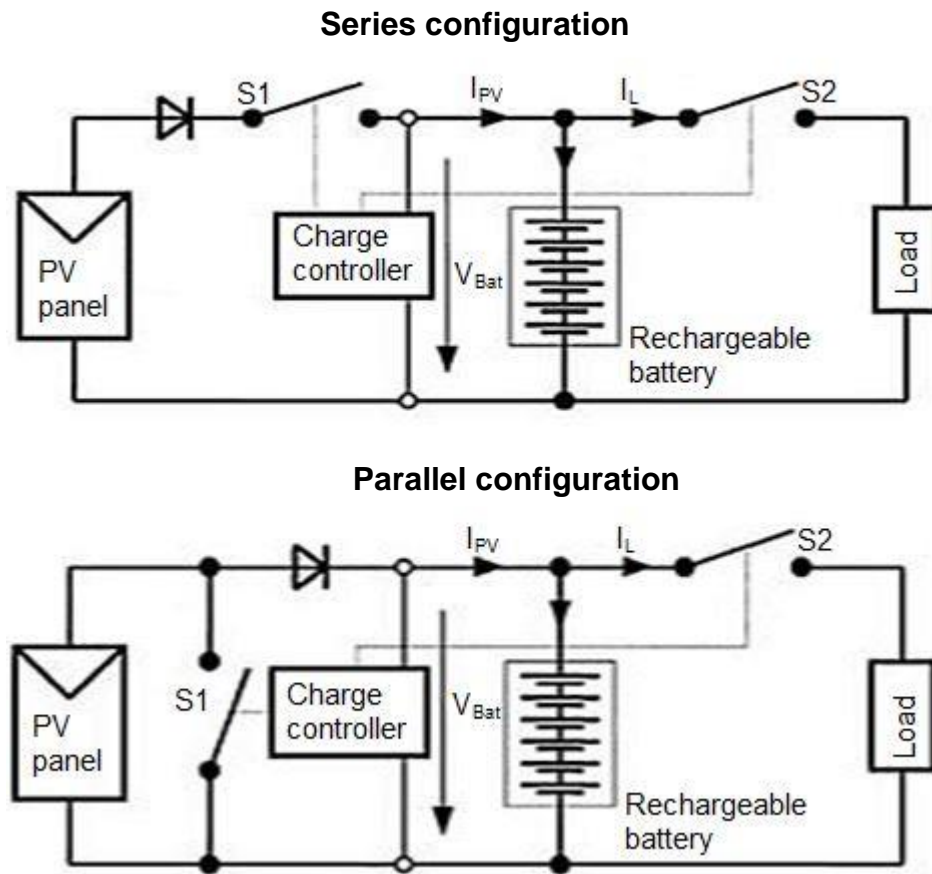


Figure 23 Photovoltaic battery systems with a charge controller (Quaschnig 2005:168)

The parallel configuration also known as shunt configuration requires a large heat sink. This is because it regulates battery voltage by redirecting or shunts the charging current from the batteries (Papadopoulou 2011:143). Foster *et al.* (2009:292) list parameters for the selection criteria of charge controllers as follows: regulator available charging steps, maximum array current, variability of set points and hysteresis, efficiency, spare parts availability, cost and warranty. Solar chargers without maximum power point tracking (MPPT) current rating can be calculated using equation 8 (Pode & Diouf 2011:180). Figure 24 shows the widely available rechargeable batteries

$$\text{Solar charge current rating} = I_{sc} \times 1.3 \quad \dots(8)$$

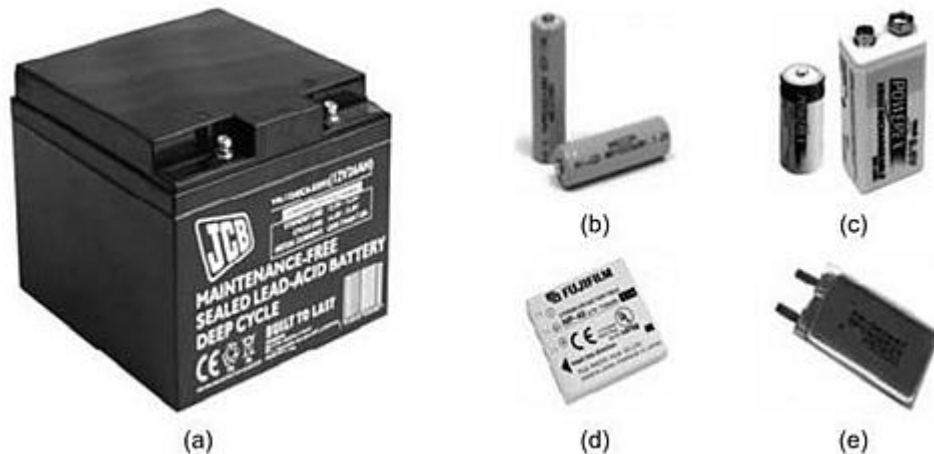


Figure 24 Various types of rechargeable batteries [a-lead acid, b-(NiCd), c-(NiMH), d-(Li-ion), e-(Li-ion polymer)] (Salanki 2013:124)

Lead acid batteries are preferred energy storage devices for optimum sized photovoltaic systems because they are inexpensive, have a high energy storage capacity and operational life cycle (Rizzo *et al.* 2009:3). Table 11 compares the characteristics of the six widely available rechargeable batteries. Lead acid batteries can be categorised into two classes which are the vented lead acid

(VLA) and sealed or valve regulated lead acid (VRLA) which is further sub-categorised into the absorbed glass mat (AGM) battery and the Gel battery (gel cell) (Salanki 2013:138).

Table 11 Comparison of characteristics for commonly used rechargeable battery (Battery University 2003)

	NiCd	NiMH	Lead Acid	LI-ion	Li-ion polymer
Internal Resistance (mΩ)	100–200	200–300	< 100	150–250	200–300
Package	6 V	6 V	12 V	7.2 V	7.2 V
Cycle Life (to 80% initial capacity)	1500	300–500	200–300	500–1000	300–500
Fast Charge Time	1h	2 – 4h	8–16h	2–4h	2–4h
Self-discharge/ Month	20%	30%	5%	10%	10%
Maintenance Requirement (days)	30–60	60–90	3–6	Not required	Not required
Cost per Cycle	\$0.04	\$0.12	\$0.10	\$0.14	\$0.29
Commercial Use since	1950	1990	1970	1991	1999

The main disadvantage of VLA batteries is that they require regular re-filling of water which is lost as a result of venting out the gas produced during the charging and discharging process.

Battery performance in circuit is determined by the electrical characteristics of the battery and its physical properties have a large influence on the size and weight of the load it will power (Texas Instruments 2011:3). Thus the long-term

operation of a optimally sized photovoltaic system has to consider the lifespan of the storage device (battery) (Nikhil & Subhakar 2013:776).

2.6.7 Electronic converters in the photovoltaic system

In off-grid photovoltaic systems, converters are normally used for load matching (Bansal, Saini & Joshi 2012:1). In grid-connected photovoltaic systems converters are usually used to match the required grid voltage level (Jianwu, Wei & Liyan 2012:3446). Figure 25 illustrates a commonly utilised two stage photovoltaic power conditioning system (PCS).

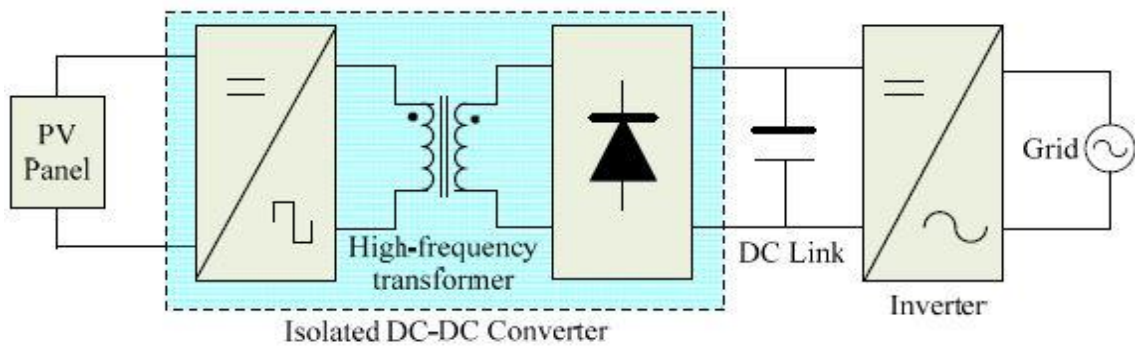


Figure 25 Configuration of a two stage photovoltaic PCS (Jianwu *et al.* 2012:3447)

In Figure 23, the output of the DC-DC converter is a regulated dc voltage from a higher or lower photovoltaic panel voltage. Generally topologies utilised for photovoltaic PCS DC-DC converter can be classified either as isolate converter topology or as non-isolated converter topology.

One of the key essential DC-DC converter prerequisite is high efficiency (Jong-Pil, Byung-Duk, Dong-Wook, Tae-Jin & Ji-Yoon 2007:3). According to Thumann and Franz (2009:376) efficiency is determined by the ratio of the output power to the input power. Figure 26 shows basic DC-DC converter circuits (Erickson

2001:5). A buck converter is a step down converter used for applications requiring not more than 85% of the converter's input voltage with a pulsating input current (Winder 2011:40). Contrary to a buck converter, the boost converter's voltage output is higher than its input voltage. The boost converter is also characterised by a pulsating output current.

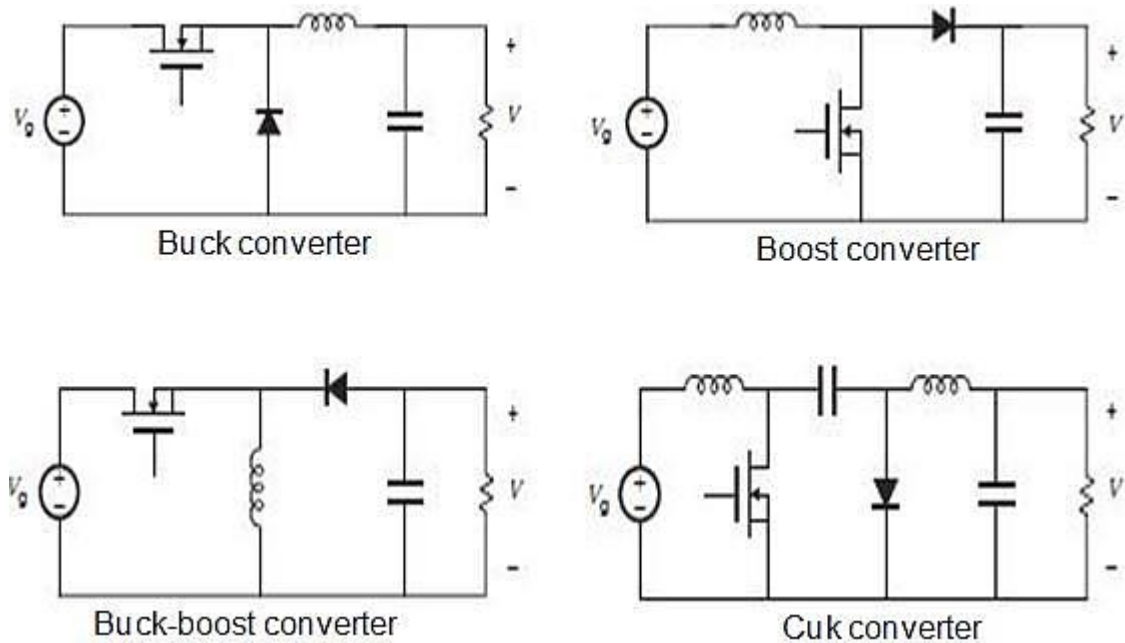


Figure 26 Basic DC-DC converter circuits (Erickson 2001:5)

The buck-boost converter combines characteristics of both buck converter and boost converter. The output of the buck-boost converter can either be higher or lower than its input voltage with a pulsating input and output current. A cuk converter has a notable advantage over the buck boost converter, which is namely a non-pulsating current input and output (Whitaker 2005:1083). Table 12 shows the equations for the output voltage of the different converter types.

Table 12 Converter output voltage equations (Whitaker 2005:1083)

Converter type	Equation
Buck	$V_o = DV_{in}$
Boost	$V_o = V_{in}/(1 - D)$
Buck-boost	$V_o = DV_{in}/(1 - D)$
Cuk	$V_o = DV_{in}/(1 - D)$

Where : $V_o \equiv DC$ output voltage; $D \equiv$ Duty cycle ratio ($D = t_{on}/T_s$); $V_{in} \equiv DC$ input voltage

2.7 E-learning and the global digital divide

Information and communication technology is one of the major contributors to global digital divide which creates a barrier to basic education (Gebremichael & Jackson 2006:269). The digital divide can be defined as the imbalanced access to and utilisation of technology (Fuchs & Horak 2008:99).

In Africa the digital divide hinders enhancing education owing to the lack and the ineffective application of technology (Keats & Beebe 2004:953). Technology innovation and development in the past decades led to the internet being used as an educational environment eliminating the communication time and distance limitation (Jianhua & Yingjian 2008:56). This can replace the traditional one location-based teaching technique with a technology-based academic method (Moscinska & Rutkowski 2011:460). In SA the official teacher's school day is seven hours long and is limited to weekdays only (OECD 2008:173).

The major obstacle to global digital inclusion is internet access with only 6% of the world population as having access, 1% of which is in developing countries (Rao 2005:362). The technology-based academic method (e-learning) is aimed at assisting scholars to use more web resources improving their computer literacy skills as well as decreasing the teacher student ratio (Nyarko & Ventura 2010:427). E-learning as a product of ICT (Nwokediuko 2012:1) is anticipated to

resolve a number of academic problems such as deficiency of quality material, instructor scarcity and combination of part-time and adult education students (Koponen, Tedre & Vesisenaho 2011:1).

In SA university distance education and in house tuition currently use e-learning as e-delivery, delivering existing study material converted to PDF via the internet; this can be attributed to low internet accessibility in SA (Hendrik & Serfontein 2004:947). Unlike in other Sub-Saharan countries where major ICT infrastructure improvement is required (Athanas, Jiang, Li & Chen 2008:270), high connection costs broaden the digital divide in the country (Fuchs & Horak 2008:110). Leading to student accessing the internet via university campuses and schools, which is not sufficient to realise the benefits of the world wide web (Oyedemi 2012:303)

2.8 Summary

In this chapter, solar energy is identified as the amply available alternative energy resource in SA. In areas remote to the grid such as rural communities solar energy technology (photovoltaic technology) can be used as a stand-alone electricity source. Photovoltaic technology classification, material categorisation and system sizing for e-learning was presented.

In Chapter 3, experimental practical set-up methods will be employed to evaluate and determine the most cost-effective equipment mix for power utilisation, storage and ICT equipment as system load.

Chapter 3 Research design, set-up and results

3.1 Introduction

This chapter introduces practical experimental set-ups used to determine the most cost-effective equipment mix for solar power utilisation, ICT equipment selection and lighting. This chapter also presents results from practical set-ups which were evaluated.

3.2 Photovoltaic panels power-efficiency evaluation

In Chapter 2 it was established that solar energy is a renewable energy resource with the most potential in SA when compared to other available renewable energy resources. The international photovoltaic technology market increased as a result of reduced costs which increased the technology's potential to be employed in rural communities.

The most cost-effective photovoltaic panel was determined from local available low-cost photovoltaic panels based on power efficiency. Three solar panels were chosen for evaluation from the same manufacturer.

The power output of the photovoltaic panels was evaluated using the set-up block diagram shown in Figure 27. The set-up was used to evaluate the power output of the panels at the actual environment of operation. It comprises three solar panels (PV1, PV2 and PV3). Photovoltaic panel one (PV1), model CHN75-36M is a mono-crystalline 75 watt panel. Photovoltaic panel two (PV2) model CHN75-72P, is a poly-crystalline 75 watt panel. Photovoltaic panel three (PV3) model M500P, is a poly-crystalline 55 watt panel. Annexure A illustrates the parameters of all three panels as specified by the manufacturers.

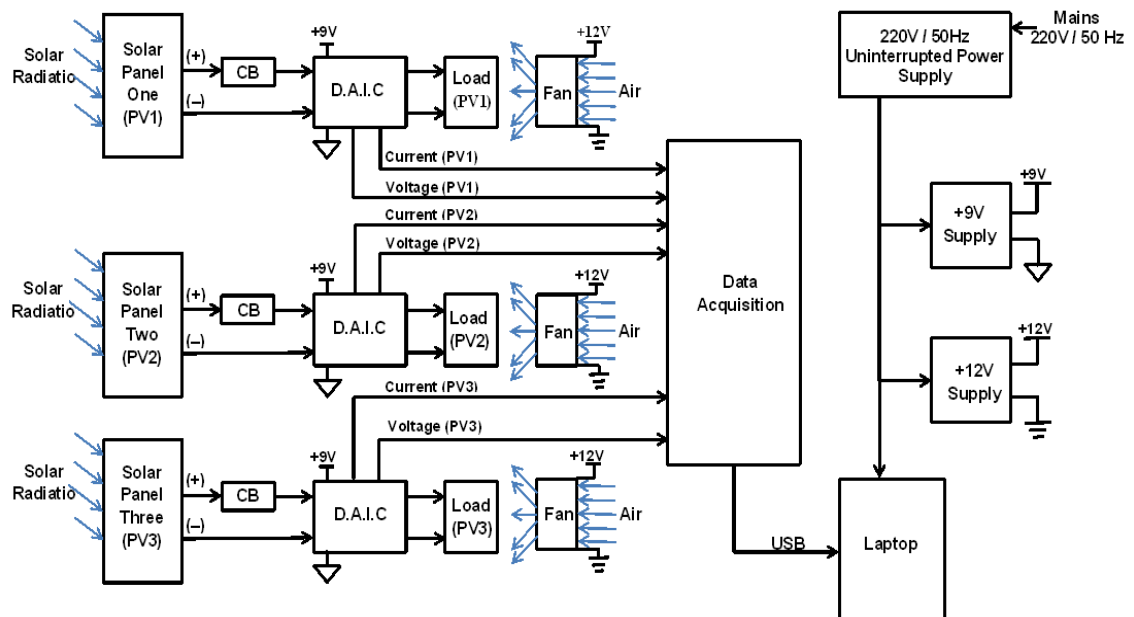


Figure 27 Set-up block diagram used to evaluate the power output of photovoltaic panels

Figure 28 shows the actual laboratory set-up used to evaluate the power output of photovoltaic panels (wired as the block diagram in Figure 27).

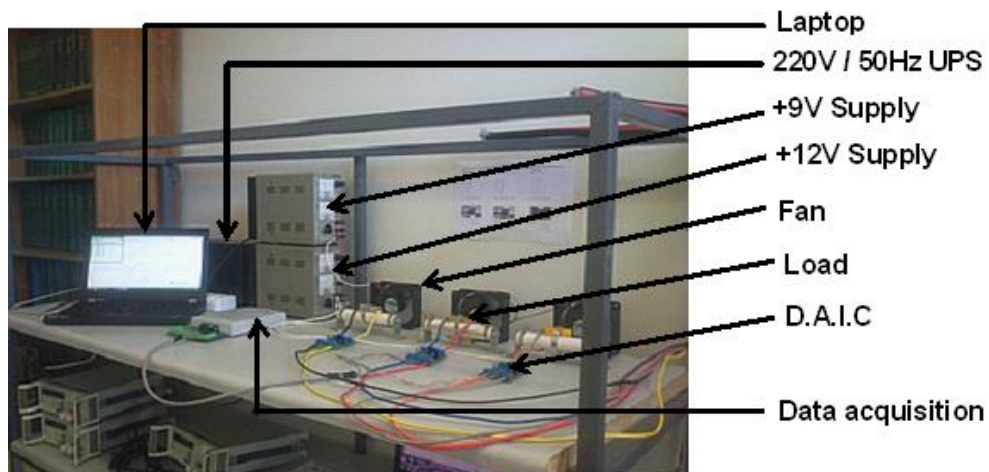


Figure 28 Laboratory set-up used to evaluate the power output of photovoltaic panels

All the photovoltaic panels were orientated due north at an optimised tilt angle of 26 degrees equal to the location's latitude in accordance with literature reviewed in Chapter 2. The panels were connected to a load via a 10A circuit breaker (CB) through a data acquisition interface circuit (D.A.I.C). The load was calculated to draw maximum power from the panel as shown.

$$\text{Load (PV1)} = \frac{V_{mp}}{I_{mp}} = \frac{17.16V}{4.37A} = 3.9\Omega \quad \dots(9)$$

$$\text{Load (PV2)} = \frac{V_{mp}}{I_{mp}} = \frac{17.6V}{4.26A} = 4.13\Omega \quad \dots(10)$$

$$\text{Load (PV3)} = \frac{V_{mp}}{I_{mp}} = \frac{18.4V}{2.98A} = 6.17\Omega \quad \dots(11)$$

Where: $V_{mp} \equiv$ Voltage at maximum power
 $I_{mp} \equiv$ Current at maximum power

A data acquisition unit was used to record the measured data from the D.A.I.C. The data acquisition device was connected to a laptop via a universal serial bus (USB) for real-time data capturing. Three 12V fans were used to dissipate the resistive load heat. Continuous data acquisition of voltage and current was maintained for 49 days for all evaluated panels.

All data recording was done on a 24 hour cycle at a sample rate of 6 samples per minute. Midday data when the sun is at its highest in the sky (11:00 to 13:00) was considered for analysis (720 samples), because solar noon does not occur exactly at clock noon (Messenger & Ventre 2005). The power output of each panel was determined from measured voltage and current as illustrated in Figures 29, 30 and 31.

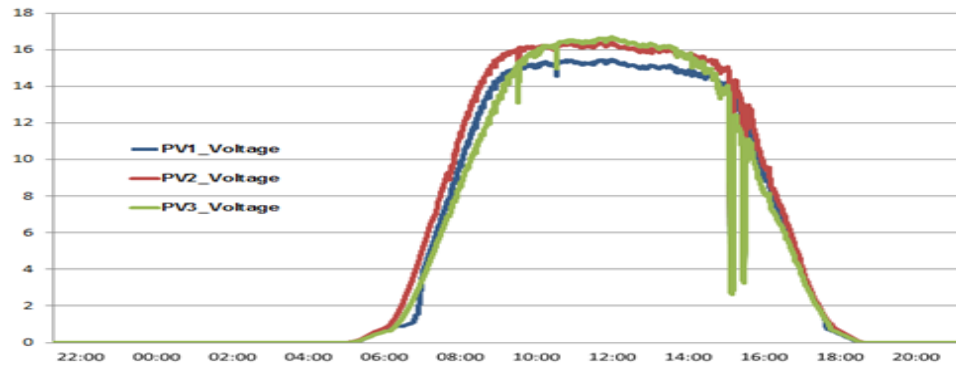


Figure 29 Measured voltage for all three photovoltaic panels (24 hour cycle)

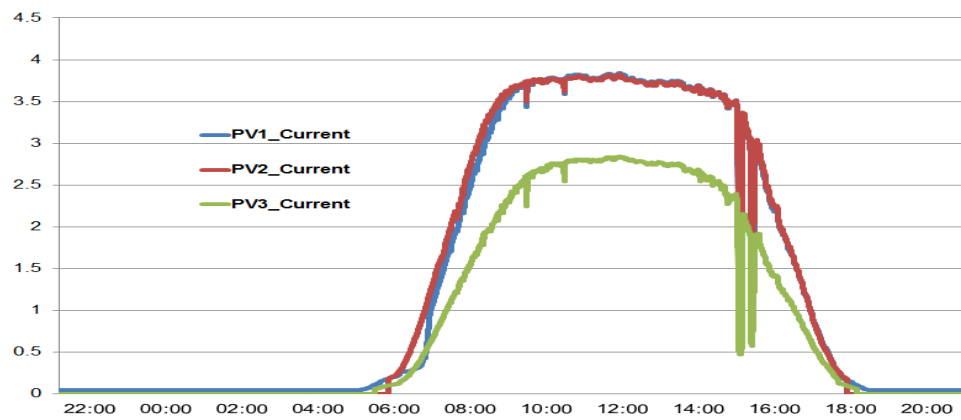


Figure 30 Measured current for all three photovoltaic panels (24 hour cycle)

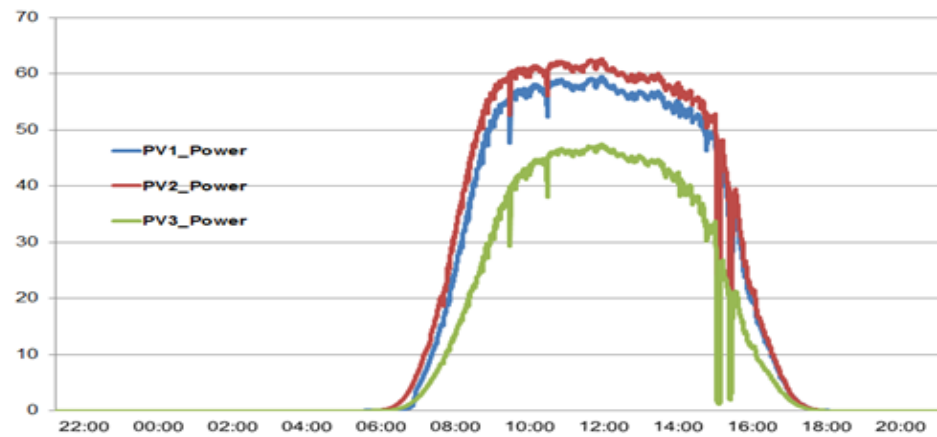


Figure 31 Determined power output for each photovoltaic panel (24 hour cycle)

Figures 32, 33 and 34 show the measured percentage watts per Rand produced by each panel.

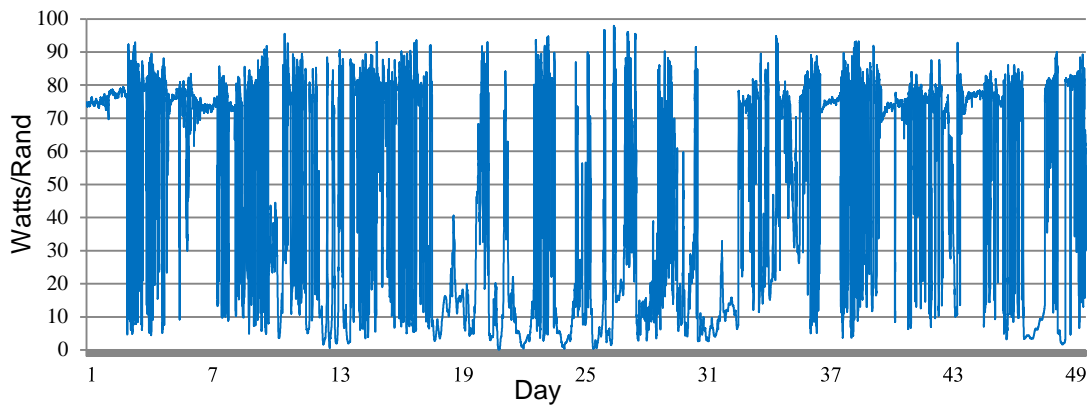


Figure 32 PV1 measured watt/Rand percentage

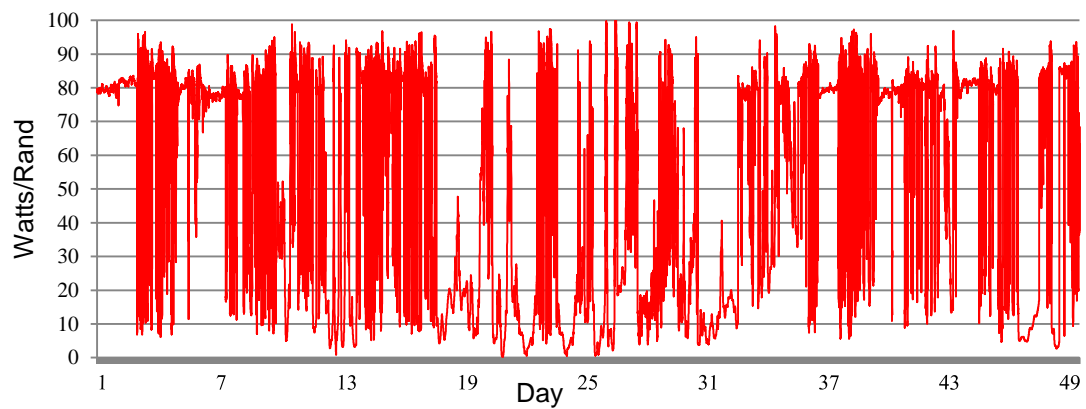


Figure 33 PV2 measured watt/Rand percentage

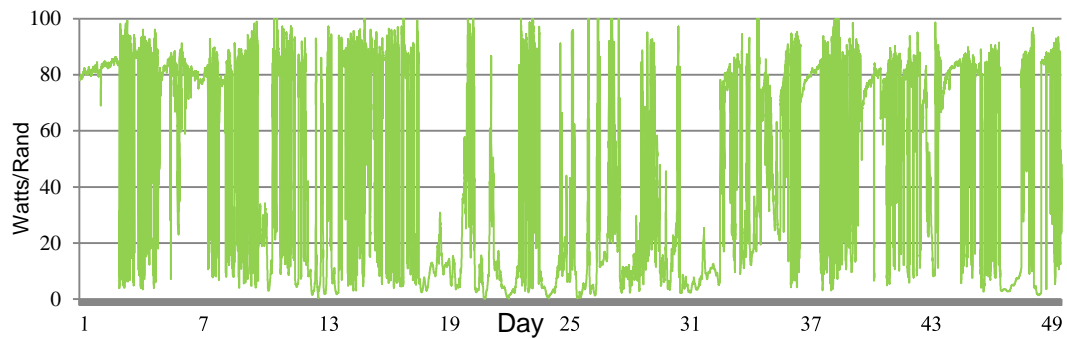


Figure 34 PV3 measured watt/Rand percentage

Figure 36 shows the actual laboratory set-up used to evaluate and verify the most energy efficient laptop (wired as the block diagram in Figure 35).

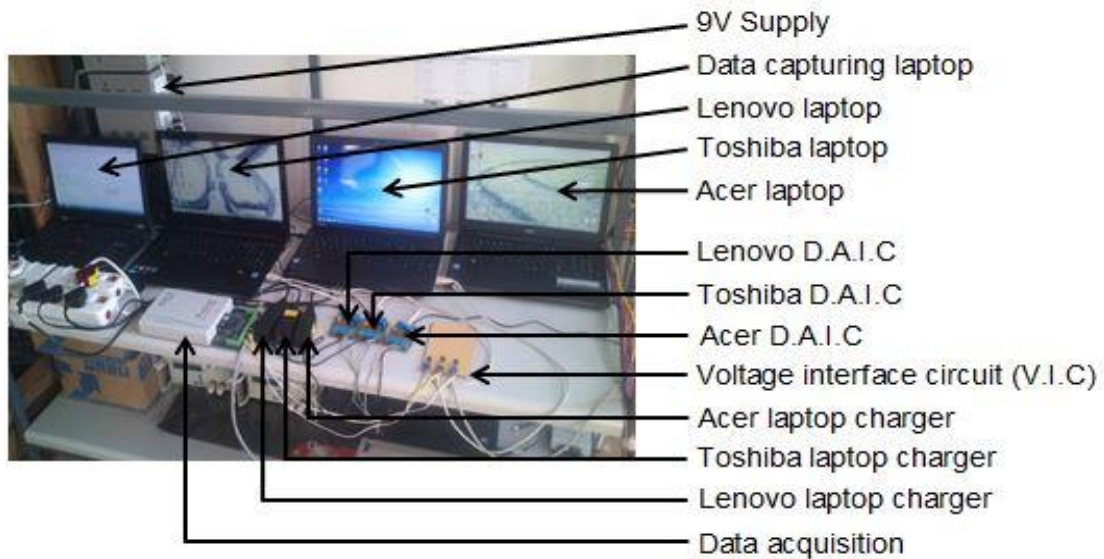


Figure 36 Laboratory set-up used to evaluate and verify the most energy efficient laptop

The top three laptops (entry level models) from Chapter 2, Table 3 (Lenovo, Acer as well as a Toshiba) were evaluated. The LG laptop (entry level model) was excluded in the experiment because it was unavailable from local market supplier. Each laptop brand had its own brand specified entry level system specifications (i.e. system processor, storage, memory, network communication display and graphics). All the laptops utilised Windows 8.1 single language as an operating system in line with reviewed literature in Chapter 2.

A macro program was written (Annexure B) using jitbit macro recorder software to simulate normal laptop user interface. Power consumption evaluation tests were conducted on all three laptops initially without their battery packs connected. The power consumption test was then repeated for all three laptops with their battery packs connected. The battery packs were fully discharged before they were used in the laptops.

A D.A.I.C circuit was developed and used to measure voltage and current from each laptop charger (Schoeman, Swart & Pienaar 2013). The D.A.I.C circuit was also used to interface the measured parameters (voltage and current) with the data acquisition device's (Pico Log ADC-24 data logger) input operational voltage and current input range. The Pico Log ADC-24 data logger was used because of the following specifications: 24-bit A/D converter, maintains a gain error of 0.1%, 16 input channels (8 differential and 8 single-ended) and USB powered as well as connectivity to laptop or PC.

The initial laptop power consumption test was done without the laptop battery packs being connected. The input power supply (220Vac) for all three laptop chargers were connected to the mains (220Vac) by a single switch multiple plug connector. This was done to synchronise their power input time. Three D.A.I.C circuits were connected to the output of the three laptop chargers. The voltage and current drawn from all three laptops was recorded over a period of 10 days. Figure 37 show the average power consumption of the three laptops without their battery packs.

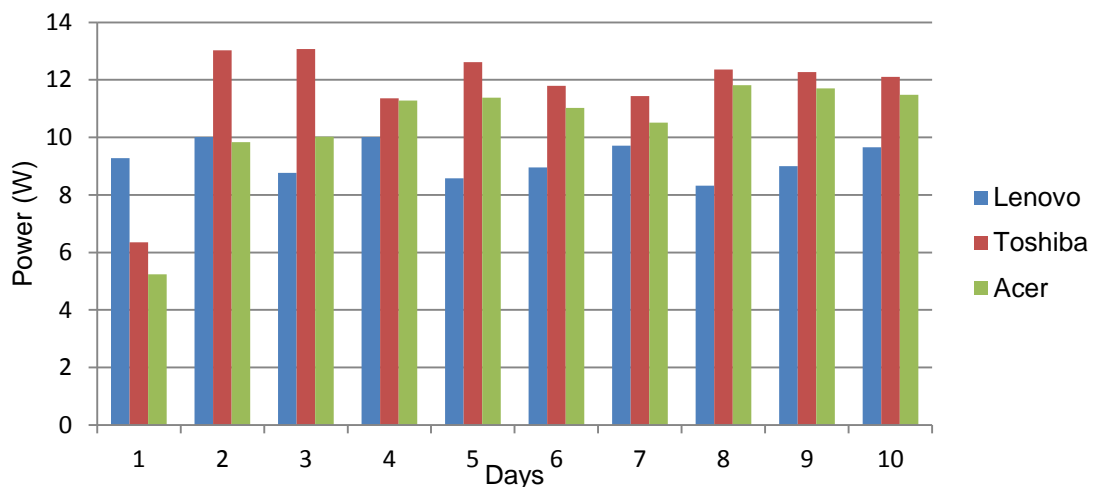


Figure 37 Laptop average power consumption without battery pack

The laptop power consumption test was repeated with the laptops-battery packs connected. This was done to evaluate the laptop batteries' charge, discharge parameters and laptops' power management. A written macro was used to simulate normal user operational conditions. A voltage interface circuit (V.I.C) was developed similar to D.A.I.C but without current sensor circuit. The V.I.C was used to measure voltage from USB ports of all three laptops under test. The V.I.C interfaced the measured USB voltage with the Pico Log ADC-24 data logger. The laptop power consumption test procedure with battery packs connected is shown in Table 13.

Table 13 Laptop power consumption test procedure with battery packs connected

Action steps	Status		Delay before next action step
	Laptop	Laptop charger	
1. Start data recording (Pico Log data acquisition software)	Off	Off	5 minutes
2. Switch on all laptop chargers	Off	On	20 minutes
3. Switch on all laptops and measure laptops' USB voltage	On	On	5 minutes
4. Run macro on all laptops	On	On	Laptop battery status indicator at 100%
5. Switch off charger for laptop battery status at 100% (repeat until all chargers are switched off)	On	Off	Battery fully discharged
6. All laptops automatically shut down (battery fully discharged)	Off	Off	Test complete

Figure 38 shows the graphical representation of the laptops' power consumption test with battery packs connected.

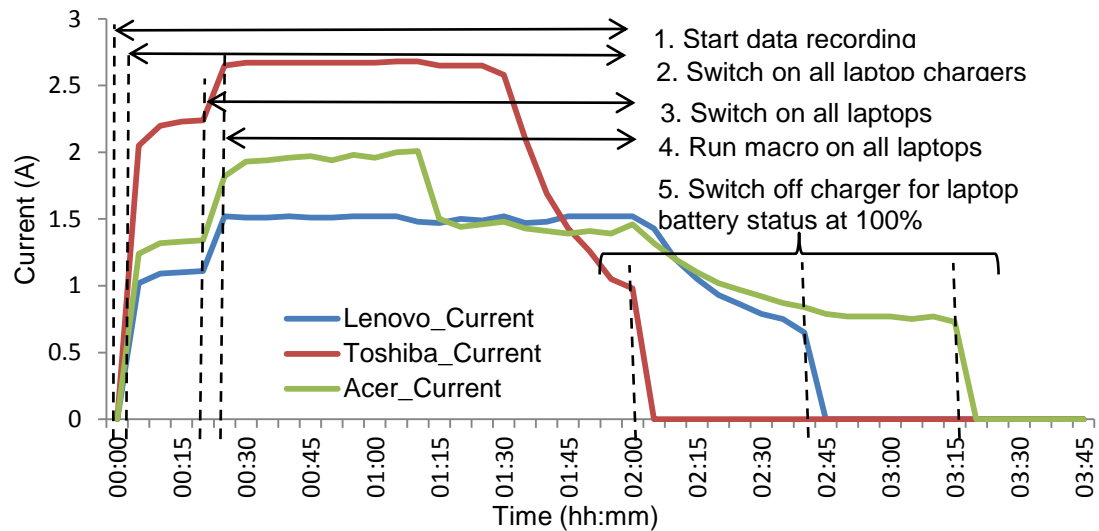


Figure 38 Measured laptops' input current with test procedure action steps

Figure 39 illustrates the measured laptops' input voltage with test procedure action step 3 and 6 described in Table 13.

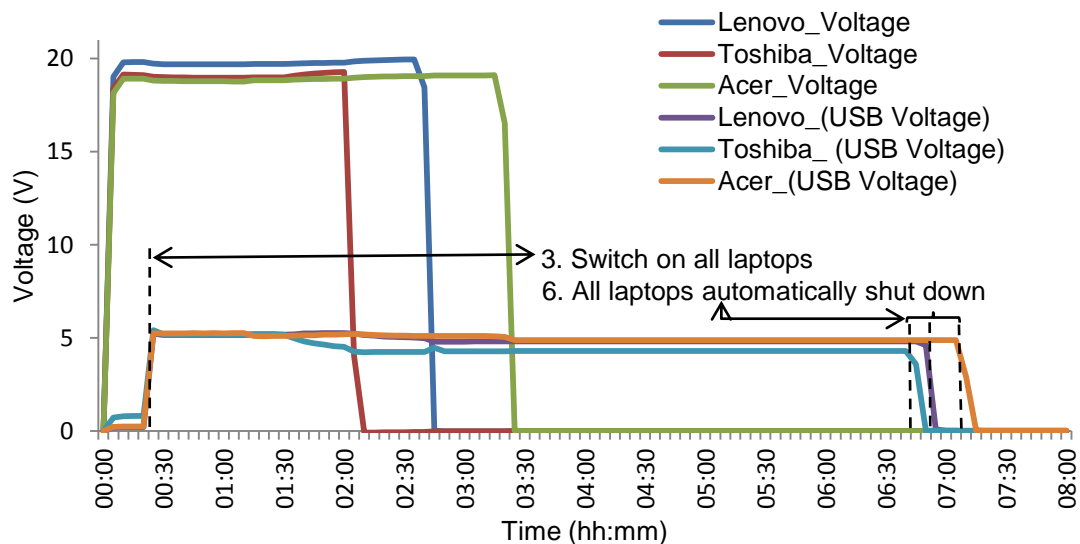


Figure 39 Measured laptops' input voltage with test procedure action steps

3.4 Light intensity and power-efficiency evaluation of light sources

In the previous chapter, literature reviewed indicated that SSL technologies based on LEDs have an operational advantage when compared to other lighting sources (thermal and discharge light sources). Figure 40 shows the set-up used to evaluate light intensity of various SSL technologies based on LEDs. It was also pointed out in the previous chapter that light source selection is based on the following criteria: illuminance intensity (South African National Standards 2005), individual control of luminaries, energy efficiency and cost. SSL technologies based on LEDs were evaluated to determine their energy efficiency based on their illuminance.

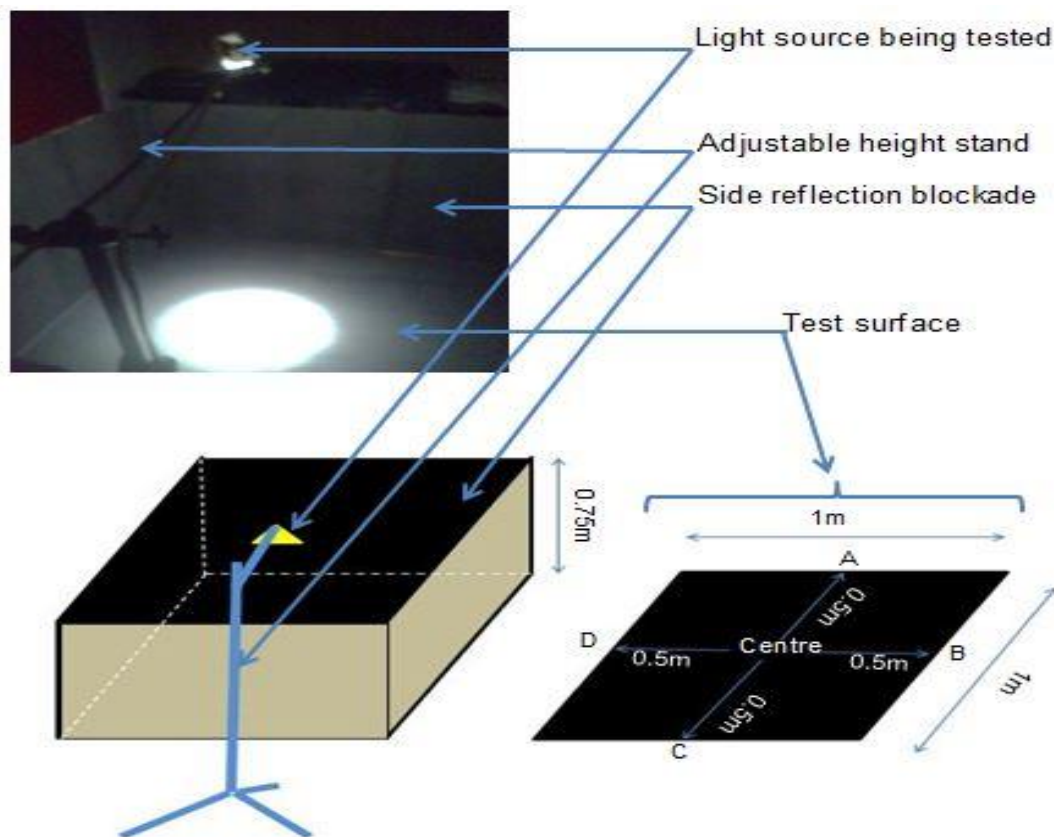


Figure 40 Light intensity evaluation set-up

Six locally available LEDs based SSL technology interior light sources were evaluated. Figure 41 shows the evaluated LED-based SSL technology interior light sources. Table 14 illustrates the manufacturers electrical parameters of evaluated LED-based SSL technology.



Figure 41 Evaluated LED-based SSL technology interior light sources

Table 14 Manufacture electrical parameters of evaluated LED-based SSL technology

Part number	Voltage (V_{DC})	Power (W)	Cost (ZAR)
MR16**(PAR16)	12	3	79.00
MR16W4P4W	12	4	99.00
MR16 60SMD	11-14	4	70.00
MR16 W6W	12	6	149.00
MR16/GU10/E27	12	3	79.00
G4-10 SMD	12	1.8	45.00

Light intensity evaluations were done in a dark room where minimum external light enters the room. The light evaluation set-up in Figure 40 consisted of a power supply, test surface, side reflection blockades, an adjustable height stand and a light source being tested.

A DC power supply (ATTEN instruments, TPR 3005 - 3C) was used to supply voltage as specified by the light source manufacturer. The test surface and the side reflection blockades were painted with deep black chalkboard paint to reduce light reflection. In telescope design deep black chalkboard paint is used to decrease light reflection (Neumann 2013). The adjustable height stand is used to place the light source being tested directly above the centre of the test surface at selected test heights of 1.0m, 1.5m, 2.0m and 2.5m.

Light intensity of all tested light sources was measured at points A, B, C and D on the test surface for all selected test heights. A Tenmars LED light meter (TM – 209M) was used to measure light intensity. Table 15 shows light intensity evaluation results at selected test heights of 1.0m, 1.5m, 2.0m and 2.5m.

Table 15 Light intensity at selected heights above test surface

Part number	Light intensity (lux) at 1.0m height above test surface			
	A	B	C	D
MR16**(PAR16)	9.340	8.660	9.450	10.700
MR16W4P4W	192.500	44.100	25.570	88.000
MR16 60SMD	52.900	55.000	57.500	61.300
MR16 W6W	81.900	84.600	94.600	108.800
MR16/GU10/E27	49.800	36.430	48.400	86.400
G4-10 SMD	31.220	33.940	35.970	31.670
	Light intensity (lux) at 1.5m height above test surface			
MR16**(PAR16)	14.060	14.150	17.700	20.810
MR16W4P4W	100.700	132.800	142.300	123.800
MR16 60SMD	19.000	19.810	19.680	20.140
MR16 W6W	78.100	75.800	105.700	111.100
MR16/GU10/E27	53.600	47.300	63.600	77.400
G4-10 SMD	19.890	18.570	19.260	19.680

Table 15 (continued) Light intensity at selected heights above test surface

Part number	Light intensity (lux) at 2.0m height above test surface			
	A	B	C	D
MR16**(PAR16)	16.000	13.980	24.430	35.290
MR16W4P4W	95.400	103.800	110.400	92.100
MR16 60SMD	20.090	30.770	30.320	32.350
MR16 W6W	68.300	61.100	75.800	85.300
MR16/GU10/E27	41.900	36.700	48.600	62.400
G4-10 SMD	11.850	11.980	11.450	11.770
	Light intensity (lux) at 2.5m height above test surface			
MR16**(PAR16)	22.170	27.600	37.780	32.350
MR16W4P4W	86.700	92.500	86.200	89.800
MR16 60SMD	11.640	12.280	12.320	11.890
MR16 W6W	48.600	45.000	55.900	61.800
MR16/GU10/E27	33.260	26.020	31.900	43.400
G4-10 SMD	7.470	7.640	7.680	7.550

Literature reviewed in Chapter 2 highlighted that the viewing angle of an LED affects its luminous intensity. The viewing angle of the six evaluated LED-based SSL technology interior light sources was determined using the light intensity evaluation set-up in Figure 40.

The viewing angle for each evaluated LED-based SSL technology interior light source was determined by measuring the centre illuminance and measuring the distance where it is at 50% in line with marked test surface points (i.e. A, B, C and D). Table 16 illustrates measured illuminance of LED-based SSL technology interior light sources.

Table 16 Measured test surface centre illuminance

Part Number	Height above test surface (m)	Test surface centre illuminance (lx)	Distance to 50% centre illuminance from test surface centre (m)			
			A	B	C	D
MR16**(PAR16)	0.5	505	0.145	0.135	0.14	0.145
MR16W4P4W	0.5	3162	0.15	0.16	0.14	0.14
MR16 60SMD	0.5	342.3	0.34	0.3	0.27	0.3
MR16 W6W	0.5	203.1	0.18	0.16	0.12	0.15
MR16/GU10/E27	0.5	1316	0.17	0.17	0.12	0.145
G4-10 SMD	0.5	188	0.35	0.35	0.29	0.28

Table 17 shows the viewing angle of each LED-based SSL technology interior light source.

Table 17 Viewing angle of each LED-based SSL technology interior light source

Part number	Viewing angle at point (°)				Average viewing angle (°)
	A	B	C	D	
MR16**(PAR16)	16.172	15.11	15.642	16.172	31.549
MR16W4P4W	16.699	17.745	15.642	15.642	32.872
MR16 60SMD	34.216	30.964	28.369	30.964	62.348
MR16 W6W	19.799	17.1745	13.496	16.699	33.923
MR16/GU10/E27	18.778	18.778	13.496	16.172	33.661
G4-10 SMD	34.216	34.992	30.114	29.249	64.421

Figure 42 shows a set-up used to determine the power-efficiency (power consumption) of SSL technologies based on LEDs. A DC power supply (ATTEN

instruments, TPR 3005 - 3C) was used to supply voltage as specified by the light source manufacturer.

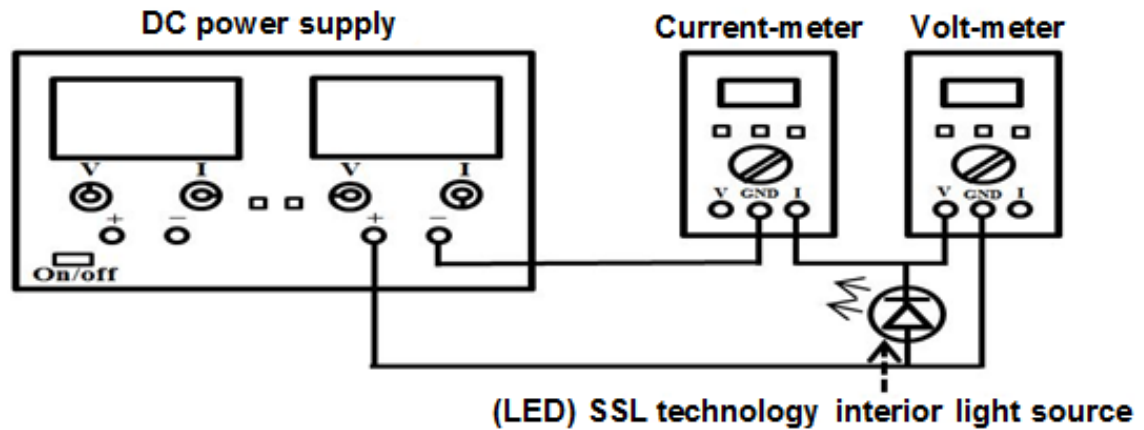


Figure 42 Set-up used to determine the power-efficiency of SSL technologies based on LEDs

A multimeter (Top Tronic T235H) was utilised to measure and verify the voltage and current supplied to the Light source being tested. Table 18 shows manufacture and measured power rating of evaluated light sources.

Table 18 Manufacturers and measured power rating

Part number	Manufacturers rating		Measured rating		
	Voltage (V)	Power (W)	Voltage (V)	Current (A)	Power (W)
MR16**(PAR16)	12	3	12	0.19	2.28
MR16W4P4W	12	4	12	0.34	4.08
MR16 60SMD	11-14	4	12	0.24	2.88
MR16 W6W	12	6	12	0.42	5.04
MR16/GU10/E27	12	3	12	0.27	3.24
G4-10 SMD	12	1.8	12	0.16	1.92

3.5 Power-efficiency evaluation of DC-DC converters

Literature studied in Chapter 2 highlighted that DC-DC converters are normally employed for load matching in off-grid photovoltaic systems. It was also established in Chapter 2 that one of the principal loads to an off-grid e-learning centre is computers (laptops). Three DC-DC converters were selected for evaluation because their manufactured output rating matched the evaluated laptop charger parameters. Two of each type of the selected DC-DC converter (labelled A and B) were evaluated to verify the manufacturers' electrical rating. Table 19 lists the manufacturers' electrical parameters of the evaluated DC-DC converter.

Table 19 DC-DC converter manufacturers' electrical parameters

Manufacturer and Part Number	Input (DC) parameters		Output (DC) parameters		η (%)	Cost (ZAR)
	Voltage (V)	Current (A)	Voltage (V)	Current (A)		
Mean Well SD-50A-24	9.2-18	7	24	0-2.1	74	309.08
Motormate IPC-2010	10-16	NAD	27.6	10	90	1523.0
Kerio Technologies DD70	11-15	30	24	5	90	615.00

Where : NAD \equiv Not Available on Datasheet

Literature reviewed in Chapter 2 also showed that the one of the essential prerequisites for DC-DC converters is high efficiency. Figure 43 shows a set-up used to evaluate electrical parameters of DC-DC converters. The block diagram

set-up in Figure 43 was used to evaluate the input voltage range, output voltage cut-off point and determine efficiency of each DC-DC converter.

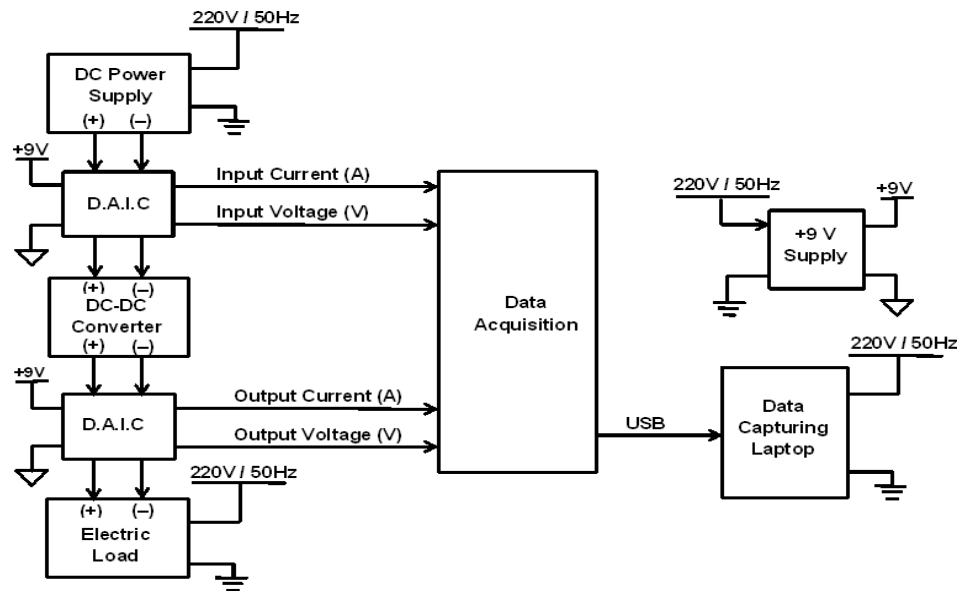


Figure 43 Set-up block diagram used to evaluate DC-DC converters

Figure 44 shows the actual laboratory set-up used to evaluate DC-DC converters (wired as the block diagram in Figure 43).

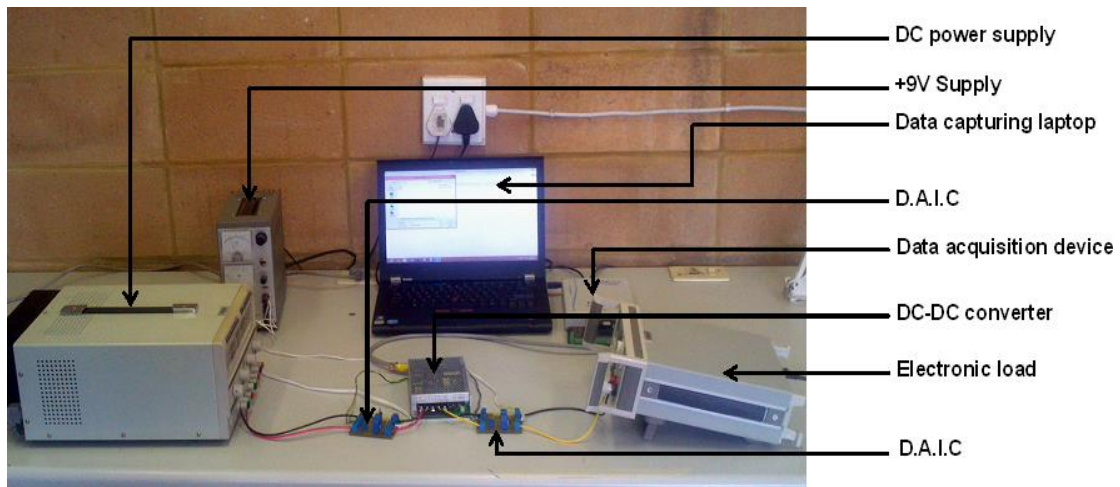


Figure 44 Laboratory set-up used to evaluate DC-DC converters

Two DC power supplies (ATTEN instruments, TPR 3005 - 3C) were utilised to supply the evaluated DC-DC converters. The two DC power supplies were connected in parallel. This was done to attain the required input current of the evaluated DC-DC converters. Input and output parameters (voltage and current) of the DC-DC converters were measured using a D.A.I.C. A data acquisition device (Pico Log ADC-24 data logger) was used to record measured parameters. Real time data capturing was done using an additional laptop (data capturing laptop). Pico Log data acquisition software was used on the data capturing laptop to record, display and export measured data.

Input voltage range of each DC-DC converter was determined by varying the input voltage (manually) from 0V to a voltage at which the observed DC-DC converter maximum output voltage is cut-off. Figure 45 shows the measured input voltage range of a Kerio Technologies DC-DC converter (DD70).

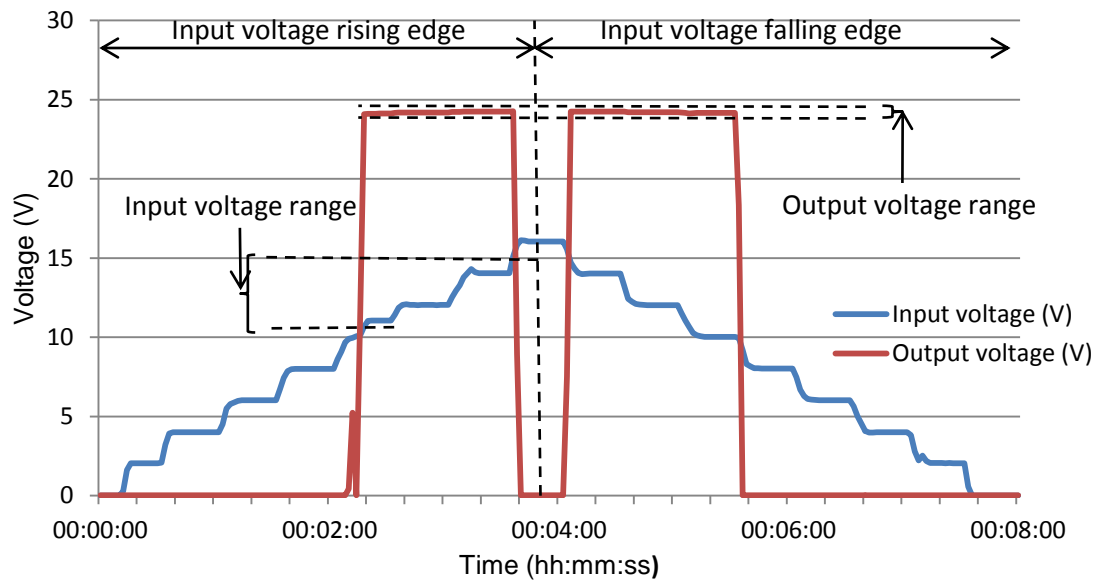


Figure 45 Measured input voltage range of a Kerio Technologies DC-DC converter (DD70)

An electronic load was used to simulate current load conditions to evaluate the DC-DC converters. The load current was selected at 0.5A, 1A, 1.5A and 2A to be equivalent to the minimum current requirement of the evaluated laptops.

Table 20 summarises the measured input voltage range for all evaluated DC-DC converters.

Table 20 Measured input voltage range for all evaluated DC-DC converters

Manufacturer and Part Number		Input voltage range (V)		Output voltage range (V)	
		Rising Edge	Falling Edge	Rising Edge	Falling Edge
Mean Well SD-50A-24	A	8.63-NLS	NLS-4.93	24.09 -NLS	NLS-20.83
	B	8.39-NLS	NLS-4.89	24.28-NLS	NLS-20.88
Motormate IPC-1210	A	8.48-16.11	16.20-4.76	27.38-27.7	27.7-16.67
	B	8.75-15.93	15.51-4.9	25.98-27.67	27.67-13.42
Kerio Technologies DD70	A	10.12-15.12	14.71-9.97	24.09-24.25	24.25-24.13
	B	10.65-15.36	14.92-10.01	24.16-24.33	24.31-24.19

Where : NLS \equiv No cutoff limit set

Efficiency of each DC-DC converter was determined from measured voltage and current at varying load currents of 0.5A, 1A, 1.5A and 2A. It was established in literature reviewed in Chapter 2 that efficiency is the ratio of the measured output power to the measured input power.

The input and output parameters (voltage and current) were measured at the various set load currents (0.5A, 1A, 1.5A and 2A). The input voltage was varied manually from 0V to the manufacturers' specified maximum input voltage. Input and output power of each DC-DC converter was determined for the measured

input and output parameters (voltage and current). Figure 46 shows the measured input and output voltage from a Motormate DC-DC converter (IPC-1210) at 2A load current.

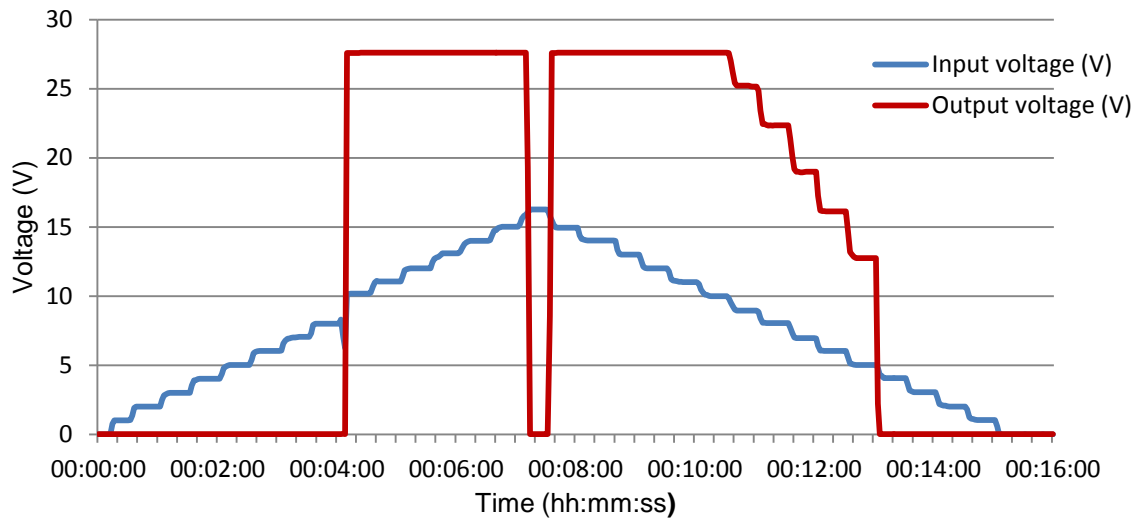


Figure 46 Measured input and output voltage (Motormate (IPC-1210) DC-DC converter)

Figure 47 illustrates the measured input and output current from a Motormate DC-DC converter (IPC-1210) at 2A load current.

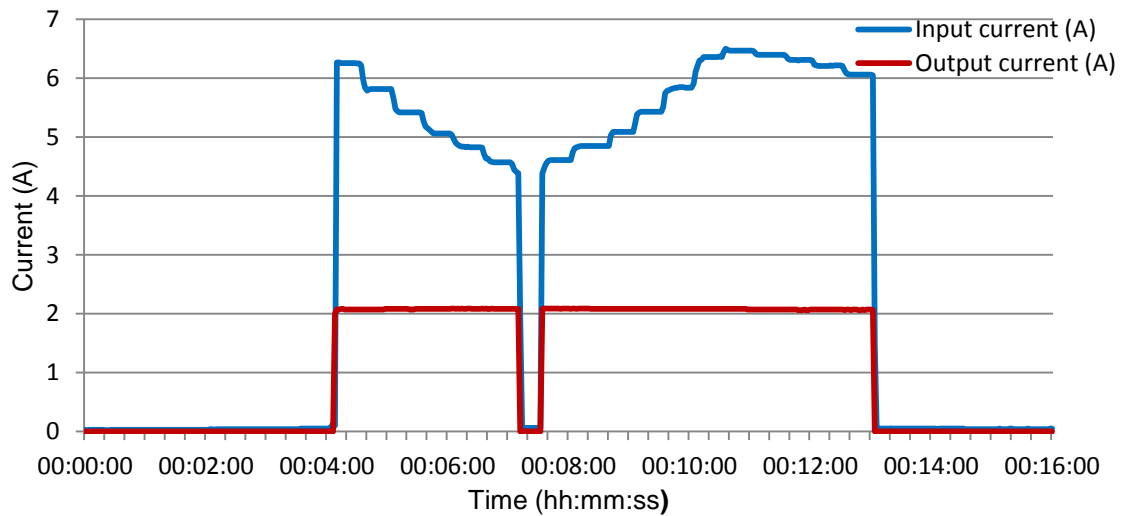


Figure 47 Measured input and output current (Motormate (IPC-1210) DC-DC converter)

Figure 48 illustrates the determined input and output power for a Motormate DC-DC converter (IPC-1210) at 2A load current.

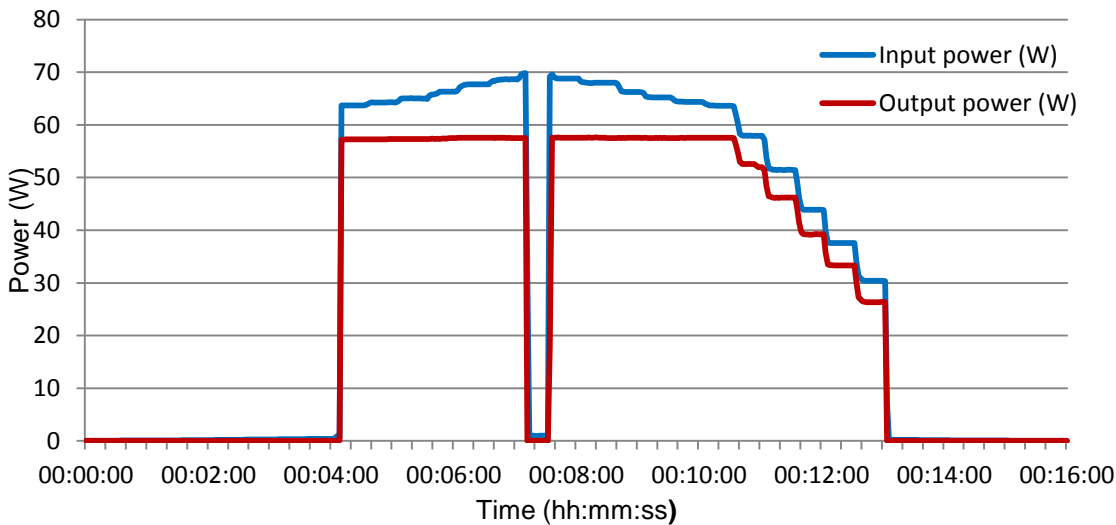


Figure 48 Input and output power (Motormate (IPC-1210) DC-DC converter)

Figure 49 illustrates the determined power-efficiency from computed input and output power for a Motormate DC-DC converter (IPC-1210) at 2A load current.

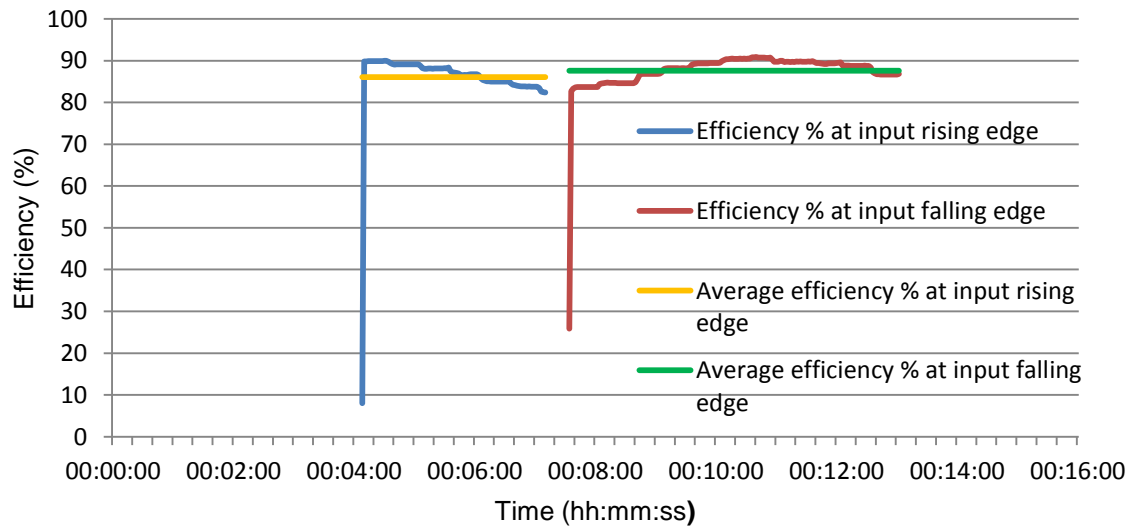


Figure 49 Power-efficiency (Motormate IPC-1210 DC-DC converter)

Table 21 outlines the average efficiency for all evaluated DC-DC converters from measured input and output parameters (voltage and current).

Table 21 Average efficiency for all evaluated DC-DC converters

Manufacturer and Part Number		Average efficiency (%)		
		Input rising edge	Input falling edge	Total input range
Mean Well SD-50A-24	A	80.513	86.028	83.832
	B	81.863	72.434	76.619
Motormate IPC-1210	A	86.745	86.963	86.875
	B	86.099	87.593	87.058
Kerio Technologies DD70	A	74.768	75.155	74.980
	B	78.695	77.828	78.244

3.6 Power-efficiency evaluation of charge controllers

In Chapter 2 it was shown that charge controllers are required in a PV system to maintain the operational lifespan of connected system batteries. Charge controllers maintain the operational lifespan of batteries by regulating their charging and discharging voltage.

Three charge controllers were selected for evaluation. The charge controllers were selected, based on their system voltage (load voltage) range which is equivalent to the load matching DC-DC converter input voltage range. Table 22 lists the electrical parameters as specified by the manufacturer for each charge controller. Two of each type of the selected charge controllers (labelled A and B) were evaluated to verify the products' electrical consistency.

Table 22 Charge controller manufacturers' electrical parameters

Manufacturer and Part Number	RCV (V)	LRV (V)	HVD (V)	LVD (V)	Cost (ZAR)
Microcare 12/24 10AMP MPPT	NAD	NAD	14.8	10	1366.00
Phocos CX20-1.1	13.7	12.8	14.8	11.0-12.2	1486.80
Provista ISC 1000	NAD	NAD	14.4	11	440.00

Where : *NAD* \equiv *Not Available on Datasheet*

Figure 50 shows the set-up block diagram utilised to evaluate electrical parameters (voltage and current) of charge controllers. The set-up was used to determine the photovoltaic panel voltage at which following charge controller parameters: RCV, LRV, HVD and LVD as specified in Chapter 2 occur. A DC power supply (ATTEN instrument, TPR 3005 – 3C) was used to simulate the PV panel input to the charge controller.

The output voltage of the PV panel simulator was varied manually from 0V to 18V (based on V_{mp} of evaluated PV panels). A diode (D1) was used (forward-biased) to allow current flow in one direction (from PV panel simulator to the charge controller).

Two digital multi-meters (Top Tronic TBM525) were used to measure the input current and voltage of the charge controllers. An electronic load was set as a resistive load and used as a load for the charge controllers. Two digital multi-meters (Top Tronic TBM525) were used to measure the load current and voltage. A Top Tronic (TBM201) digital multi-meter was used to measure load voltage of the charge controllers.

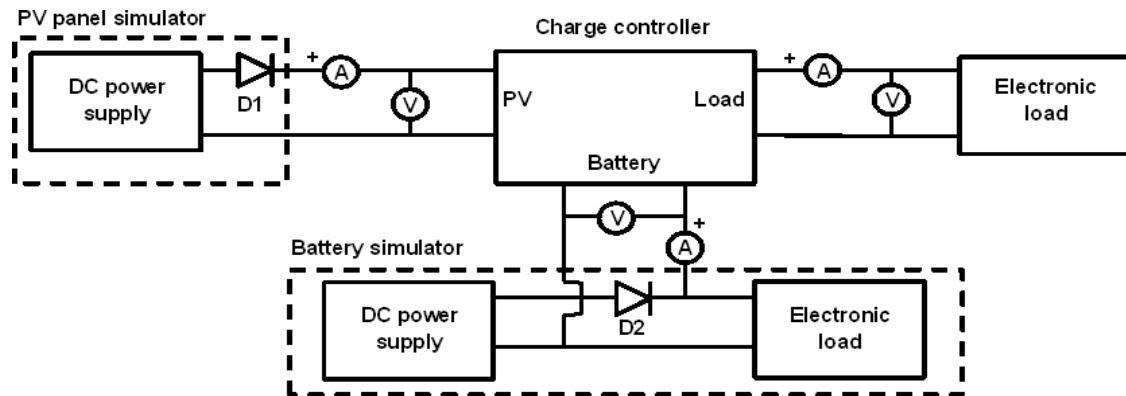


Figure 50 Set-up block diagram used to evaluate charge controllers

Figure 51 shows the actual lab set-up used to evaluate charge controllers (wired as the block diagram in Figure 50).

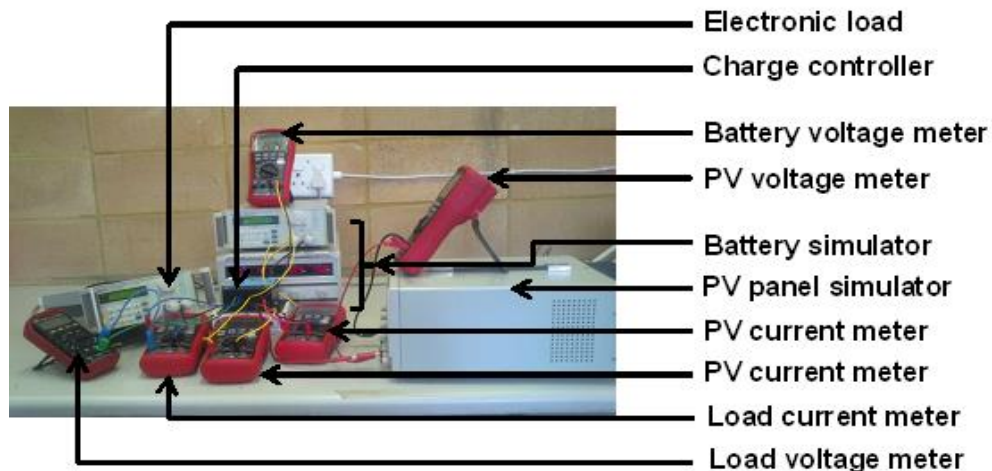


Figure 51 Laboratory set-up used to evaluate charge controllers

A dc power supply connected via a forward biased diode (D2) to an electronic load was utilised to simulate a battery. The dc power supply was used to simulate battery voltage level. D2 was used to prevent current flowing into the dc power supply. The electronic load (set as a resistive load) was used to simulate a battery's internal resistance. The internal resistance of a battery is

inversely proportional to the SOC of a battery and also increases when a battery reaches the end of its operational lifespan (Astley 2009:50) Two digital multi-meters (Top Tronic TBM525) were used to measure the battery current and voltage of the charger controller. The polarity of the ampere meter measuring the charge controller's battery indicates battery charging (when positive) and discharging (when negative).

To determine the photovoltaic panel voltage at which RCV, LRC, LVD and HVD of each charge controller occur, the battery simulator was set at the 'disconnect load, start charging' state of 11V as established in Chapter 2, Table 8. The PV panel simulator was initially switched off. The PV panel voltage was increased manually to 18V. Measured voltage and current values were recorded for every 1V increment of the PV voltage. Figure 52 shows the measured photovoltaic panel voltage and current to establish RCV, LRC, LVD and HVD of each charge controller for a microcare 12/24 10AMP MPPT charge controller.

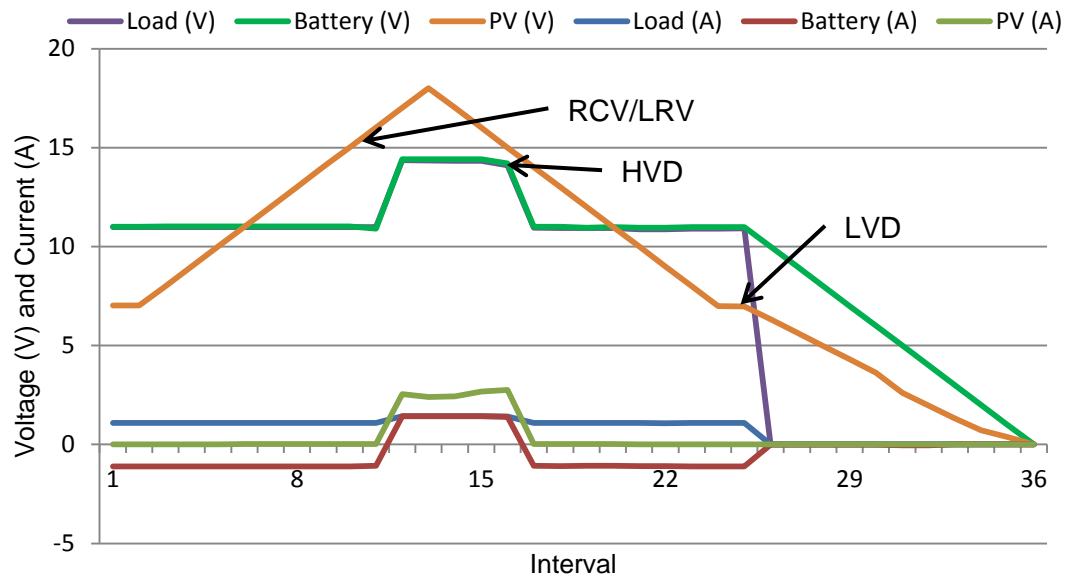


Figure 52 Microcare 12/24 10AMP MPPT charge controller measured voltage and current

Table 23 shows the measured photovoltaic panel voltage to establish RCV, LRV, LVD and HVD of each charge controller.

Table 23 Photovoltaic panel voltage to establish RCV, LRV, LVD and HVD of each charge controller

Manufacturer and Part Number		Photovoltaic panel voltage			
		RCV (V)	LRV (V)	HVD (V)	LVD (V)
Microcare 12/24 10AMP MPPT	A	16	16	15	7
	B	16	16	15	7
Phocos CX20-1.1	A	13	13	16	11
	B	13	13	16	11
Provista ISC 1000	A	12	*	12	*
	B	12	*	12	*

Where : * \equiv Not Reached with Low Battery Voltage

The power-efficiency of each charge controller (photovoltaic panel to load) was determined using measured load and photovoltaic parameters (voltage and current) from Table 23 when the simulated battery was being charged. Table 24 shows the determined efficiency of evaluated charge controllers.

Table 24 Efficiency of evaluated charge controllers

Manufacturer and Part Number		Efficiency (%)
Microcare 12/24 10AMP MPPT	A	50.12
	B	50.08
Phocos CX20-1.1	A	47.12
	B	47.49
Provista ISC 1000	A	Load not switched on
	B	Load not switched on

3.7 Summary

This chapter utilised practical set-ups to evaluate the PV system equipment. It also illustrated the result for verification of manufacturers' electrical specification in order to establish reliability.

Chapter 4 presents discussion leading from this chapter to establish the most cost-effective equipment mix to build a pilot e-learning centre.

Chapter 4 Research data analysis

4.1 Introduction

This chapter presents discussions based on data analysis of results obtained in Chapter 3. This data analysis of results attained in Chapter 3 was done to determine the most efficient and cost-effective equipment.

A pilot e-learning centre set-up using a determined cost-effective equipment mix is outlined in this chapter. The results of the pilot e-learning centre are also presented in this chapter.

4.2 Data analysis to determine the most power-efficient photovoltaic panels

Statistical hypothesis testing and confidence interval approximation was utilized to determine the most cost-effective PV panel from the evaluated PV panels results (Watts per Rand) in Chapter 3.

The P-value approach was utilised in hypothesis testing. The P-value approach expresses data comparison at a selected significance level (α) of 5% ($\alpha = 0.05$). According to Montgomery and Runger (2010) the P-value is the minimum level significance which would establish whether the null hypothesis (H_0) can be accepted or rejected using equation (12).

$$P - \text{value}(z - \text{test}) \quad \dots(12)$$

$$z - \text{test} = \frac{(\bar{X} - \mu_0)}{(\sigma / \sqrt{n})} \quad \dots(13)$$

Where: $\bar{X} \equiv$ data mean
 $\mu_0 \equiv$ null hypothesis
 $\sigma \equiv$ population standard deviation
 $n \equiv$ sample size

The P-value was established using the z-test in MS EXCEL Data Analysis Tool pack for all three panels recorded data in Figures 29, 30 and 31 on page 52. Table 25 shows the results of the hypothesis testing (P-value).

Table 25 Hypothesis (P-value) testing results for evaluated PV panels

	H₀_PV1	H₀_PV2	H₀_PV3
PV1		1	0.9649959
PV2	1.2665×10^{-127}		9.4323×10^{-110}
PV3	0.0505577	1	

According to Montgomery and Runger (2010) conditions for accepting or rejecting a null hypothesis (P-value testing) are shown in Table 26.

Table 26 Conditions for accepting or rejecting a null hypothesis

H₀ acceptance or rejection conditions	
Accept H0	P-value < α
Reject H0	P-value > α

The results in Table 25, point out that PV2 is the most cost-effective PV panel. Result verification was achieved by comparing the average power measured for each panel over the duration of the experiment as shown in figure 53.

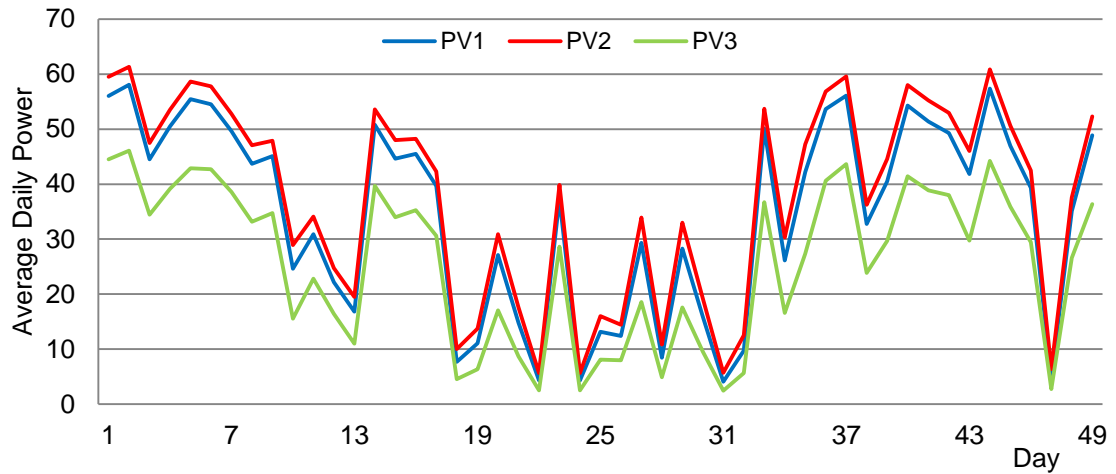


Figure 53 Photovoltaic panel daily average power

From Figure 53 it is also clear that PV2 has the highest percentage power output when compared to PV1 and PV3. Therefore PV2 is the most power-efficient and cost-effective PV panel when compared to PV1 and PV3. The output power of all three panels was observed to be less than the STC manufacturer rating. The total average power measured over the test cycle of 49 days is shown in Table 27.

Table 27 Photovoltaic panel total average power

	Manufacturer STC power specification (W) [A]	Total Average measured power (W) [B]	Normalised average measured power (%) $\left[\frac{100 \times B}{A}\right]$
PV1	75	34.49	45.99
PV2	75	37.64	50.19
PV3	55	25.47	46.31

All three panels operate between 25.47% and 37.64% of the STC rating. This is in line with literature reviewed in Chapter 2 that the actual output of PV panels is less than the STC manufacturer rating.

4.3 Data analysis to determine the most power-efficient ICT equipment (laptops)

In Chapter 3 the power consumption of ICT equipment (laptops) was determined. Initial laptop power consumption evaluation was done without battery packs connected. The P-value approach was utilized in hypothesis testing on the data collected during the duration of the experiment at a selected significance level (α) of 5% ($\alpha = 0.05$). H_0 test on the recorded data (in Figure 33) was done to determine which laptop consumed more power when compared to the other evaluated laptops. Equations 8 and 9 were used to determine the P-value. Table 28 illustrates the obtained H_0 test results.

Table 28 Hypothesis (P-value) testing results for power consumption of evaluated laptops

	H_0 (Lenovo)	H_0 (Toshiba)	H_0 (Acer)
Lenovo		1	1
Toshiba	0		0
Acer	0	1	

Conditions for accepting or rejecting a H_0 (P-value testing) are shown in Table 23. The results in Table 28 indicate that a Toshiba laptop consumed the highest power followed by the Acer laptop while the Lenovo laptop consumed the least power of the three laptops.

Results verification was done by comparing the average power consumed by each laptop over the duration of the experiment as shown in Figure 33. It can be deduced from Figure 33 that the Lenovo laptop consumes the lowest power when compared to the Acer and Toshiba laptops.

The second laptop power consumption test was done with the laptop battery packs connected. This evaluation was undertaken to determine the laptop

battery's charge, discharge parameters and laptop's power management. Table 29 summarises the results obtained in Figures 34 and 35.

Table 29 Laptop peak charge current, charge and discharge time summarised

	Peak charge power (W)	Charge time (hh:mm)	Discharge time (hh:mm)
Lenovo	30.37	2:40	4:10
Toshiba	50.75	2:05	4:40
Acer	37.69	3:15	3:40

The results in Table 29 highlight that the Toshiba laptop had the highest peak power consumption to charge its battery pack and the highest discharge time when compared to the other laptops.

Contrary to the Toshiba laptop, the Lenovo laptop had the lowest peak charge current. The Lenovo laptop had a 37.143% peak charge power-saving in comparison to the Toshiba laptop. Although the Toshiba laptop had the longest battery discharge time it was also the most expensive of the three evaluated laptops. The Lenovo laptop had a 9.832% less purchase cost and 7% lower discharge time when compared to the Toshiba laptop.

Therefore from the analysis of both evaluation tests results it was concluded that the Lenovo laptop was the most cost-effective and energy efficient laptop.

4.4 Data analysis to determine the most power-efficient light sources

LED-based SSL technology interior light sources were evaluated in Chapter 3 to determine and compare their illuminance efficiency in lux per watt (lx/W). The evaluation was based on the inverse square principle of light. Gordon (2010) quantifies the inverse square principle of light as illuminance inversely

proportional to the square of the distance of the light source and directly proportional to the light intensity of the luminaire. The average surface illuminance efficiency (lx/W) of each evaluated luminaire is shown in Figure 54. The illuminance efficiency was determined from measured illuminance in Table 15 (page 61) and measured power rating in Table 18 (page 64).

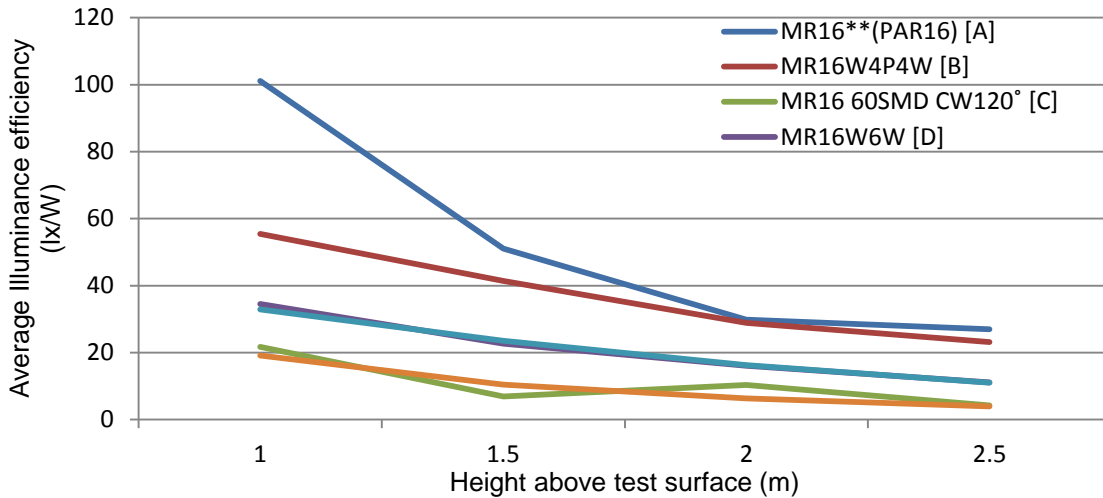


Figure 54 Average Illuminance efficiency (lx/W)

It can be deduced from Figure 54 that MR16**(PAR16) is the most efficient LED-based SSL technology interior light source. In Chapter 2 the recommended luminary cut-off angle in a room where a VDU is used continuously was established. From Table 17 it can also be deduced that MR16**(PAR16) has the lowest determined viewing. This makes the MR16**(PAR16) the best choice for illuminating rooms where VDU continuous use occurs.

Reviewed literature in Chapter 2 pointed out that an illuminance of 500 lx should be maintained in rooms where all work stations utilise a visual display unit (VDU). A practical set-up in Figure 55 was used to determine the required number of MR16**(PAR16) LED-based SSL technology interior light sources to maintain an illuminance of 500 lx.

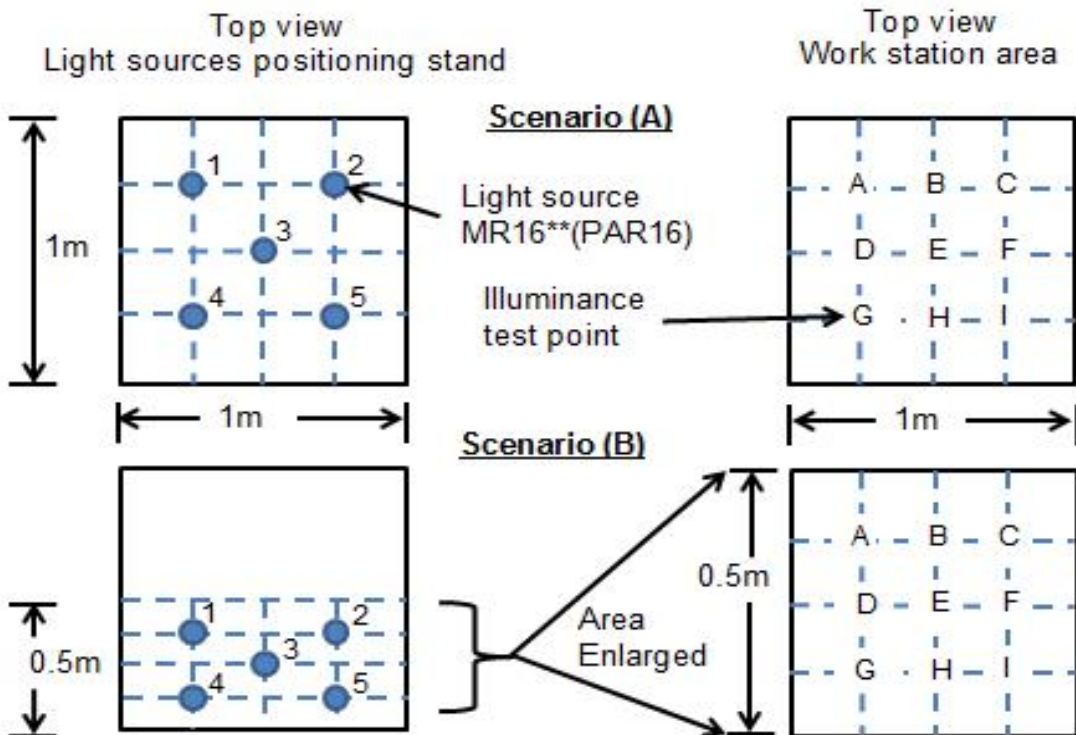
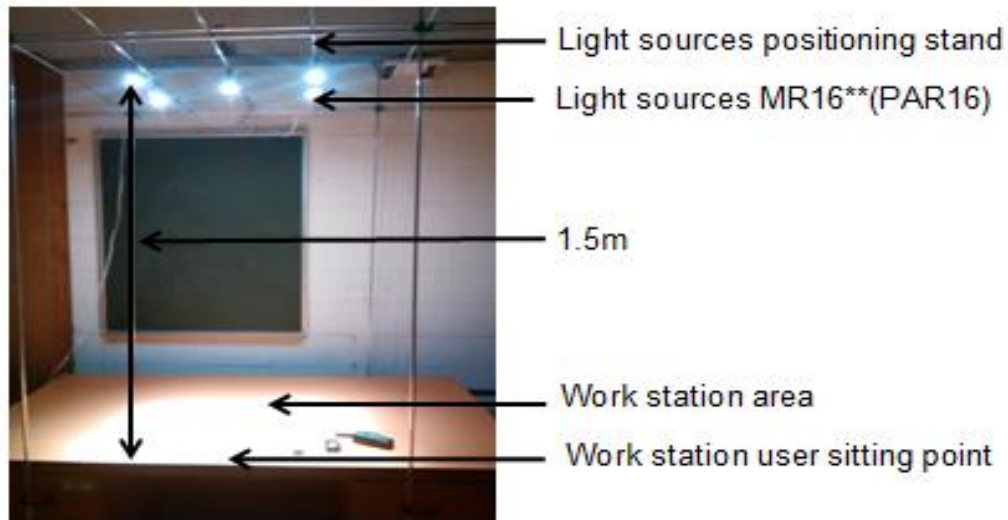


Figure 55 Set-up used to determine the required number of MR16(PAR16) LED**

The MR16**(PAR16) LED-based SSL technology interior light sources were placed 1.5m above the 1m² VDU work station. According to University of Melbourne (2011:11) a sitting work station should be 0.68m – 0.72m above the

floor. The height of the light sources of 1.5m was selected so that the sum of the height of the light sources and sitting work station, from the floor was less than the minimum ceiling height (2.4m) of a habitable room (South African National Standards 2010:5).

Two scenarios (A and B) were considered for positioning the light sources above the work station. Scenario (A) was used to determine the number of MR16**(PAR16) LEDs required to maintain a minimum illuminance of 500lx, only next to the user of the work station (0.5m² of work station). Scenario (B) was employed to determine the number of MR16**(PAR16) LED required to maintain a minimum illuminance of 500lx on the whole work station area (1m² total work area).

Light intensity was measured at the indicated test points (A-I) on the work station surface as shown in Figure 55 (top view work station area). All light intensity measurements were done at night. This was so as to eliminate the influence of sunlight on the reading. A Tenmars LED light meter (TM – 209M) was used to measure light intensity in lux.

Initially light intensity was measured with five MR16**(PAR16) LEDs connected (for both scenarios) in position as shown in Figure 55 scenario (A) and (B). The number of MR16**(PAR16) LEDs evaluated was reduced by one at a time until the illuminance average measured surface (work station area) was less than the required minimum illuminance of 500 lx.

Light intensity for four MR16**(PAR16) LEDs was determined by disconnecting the MR16**(PAR16) LED at position 3 (in Figure 55, top view light positioning stand) for both scenarios. Light intensity for three MR16**(PAR16) LEDs was determined by disconnecting the MR16**(PAR16) LEDs at position 1 and 2 (in

Figure 55, top view light positioning stand) for both scenarios. Table 30 shows the average measured light intensity at the work station area using scenario (A).

Table 30 Scenario (A) measured light intensity for multiple MR16(PAR16) LEDs to maintain illuminance of 500 lx**

Number of lights used	Light intensity (lx) at work station surface test point									Av. work station illuminance (lx)
	A	B	C	D	E	F	G	H	I	
5	694	521	673	567	882	549	680	567	682	646
4	659	478	597	317	296	319	655	423	526	474.4

Table 31 tabulates the average measured light intensity at the work station area using scenario (B).

Table 31 Scenario (B) measured light intensity for multiple MR16(PAR16) LEDs to maintain illuminance of 500 lx**

Number of lights used	Light intensity (lx) at work station surface test point									Av. work station illuminance (lx)
	A	B	C	D	E	F	G	H	I	
5	710	609	806	861	953	836	792	737	857	795.6
4	634	441	629	691	395	696	636	471	623	579
3	168	195	91	294	512	263	678	763	664	403.1

It was deduced from Tables 30 and 31 that five MR16**(PAR16) LED-based SSL technology interior light sources are required to maintain a minimum illuminance of 500lx using light positioning in scenario A.

4.5 Data analysis to determine the most power-efficient DC-DC converters

In Chapter 3 the power-efficiency of DC-DC converters was evaluated. Six DC-DC converters (two of each type) were evaluated. The percentage variation in power-efficiency of DC-DC converters from the same manufacturer are shown in Table 32. The percentage variation in power-efficiency was determined from established power-efficiency for each DC-DC converter.

Table 32 Variation in power-efficiency of DC-DC converters from the same manufacturer

Manufacturer and Part Number	Efficiency percentage variation		
	Input rising edge	Input falling edge	Total input range
Mean Well SD-50A-24	1.35	13.594	7.213
Motormate IPC-1210	0.646	0.63	0.183
Kerio Technologies DD70	3.927	2.673	3.264

Table 32 showed that the Motormate IPC-1210 DC-DC converters had the lowest percentage variation in power-efficiency. This shows reliability of maintaining the determined efficiency with a variation of 0.183% for the Motormate IPC-1210 DC-DC converter.

Results in Table 32 also showed that the Motormate IPC-1210 DC-DC converter is the most power-efficient DC-DC converter. The Motormate IPC-1210 DC-DC converter is thus the most power-efficient and most cost-effective DC-DC converter from amongst the evaluated DC-DC converters.

4.6 Charge controller power-efficiency data analysis

In the previous chapter the power-efficiency and the electrical consistency of three types of charge controllers were evaluated. Electrical consistency was established by measuring the photovoltaic panel voltage at which RCV, LRV, HVD and LVD occurred.

It was observed from Table 23 (page 75) that the Microcare 12/24 10AMP MPPT charge controller had the lowest LVD (photovoltaic panel voltage). The low LVD (photovoltaic panel voltage) at the start charging battery voltage state increases the battery's charge time and load operation period.

Table 24 also showed that the Microcare 12/24 10AMP MPPT charge controller is the most power-efficient charge controller with the lowest purchase cost. It was therefore concluded that the Microcare 12/24 10AMP MPPT charge controller is the most cost-effective charge controller.

4.7 Pilot e-learning centre

The most cost effective equipment mix for utilisation in a photovoltaic system was determined in the previous sections of this chapter. In Chapter 2 photovoltaic system types were classified in Figure 9 (page 20).

In this section a pilot e-learning centre was designed and built using the established cost-effective equipment mix. A stand-alone photovoltaic system design (classified in Chapter 2) was used for the pilot e-learning centre. The stand-alone photovoltaic system design was used to gain the following system advantage: zero inverter power losses because no AC load was utilised and has maximum battery storage if the system is used during the day.

A pilot e-learning centre set-up with system measuring devices is shown in Figure 56. The pilot e-learning centre was constructed for one VDU user interface.

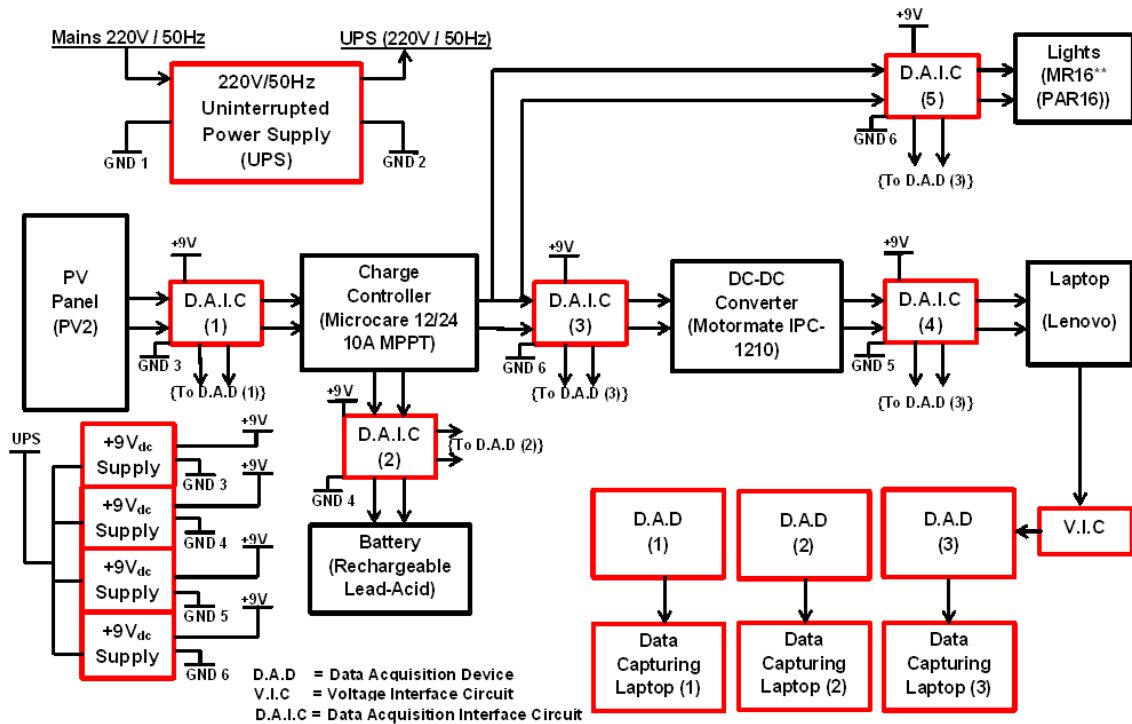


Figure 56 Pilot e-learning centre set-up with system measuring devices marked in red

The system measuring devices consisted of the following devices (marked in red in Figure 56): three data acquisition devices (D.A.D), a V.I.C, five D.A.I.Cs, an uninterrupted power supply, four 9V_{DC} power supplies and three data capturing laptops. Three D.A.Ds and laptops were used to maintain ground isolation of the measured terminals of the charge controller.

The stand-alone photovoltaic system consists of the following devices (marked in black in Figure 56): a photovoltaic panel (PV2), a charge controller (Microcare 12/24 10AMP MPPT), a DC-DC converter (Motormate IPC-1210), LED-based

SSL technology interior light sources (MR16**(PAR16)), a laptop (Lenovo) and a rechargeable lead acid battery.

Literature reviewed in Chapter 2 showed that lead acid batteries are the most favourable energy storage devices for utilisation in photovoltaic systems. Table 33 summarises the battery's voltages and DOD levels for a 12V lead acid battery as reviewed in literature in Chapter 2.

Table 33 Summary of a battery's voltages and DOD levels for a 12V lead acid battery

Battery voltage (V)	DOD level (%)	Description
12.7	0	Battery fully charged (Table 8)
12	Manufacturer rating	Manufacturer rating
11.43	90	Optimizes the battery's discharge time and number of useful charge-discharge cycles (Figure 19 and Table 10)
10.5	Cut-off voltage	Recommended cut-off voltage (Table 9). Six cells multiplied by $1.75V_{\text{cut-off}}$ voltage for each cell
10.16	80	Deep battery discharge

Literature reviewed in Chapter 2 highlighted that in SA the teacher's official school day is limited to seven hours (OECD 2008:173). The required battery back-up for seven hours (one day) was calculated using the teacher's official school day duration (seven hours). To calculate the required battery back-up for seven hours (one day) using equation 6 (page 40), the total load current was

determined. The total load current was determined from the measured laptop current and lights current in Chapter 3.

$$I_{Total} = I_{laptop} + I_{lights} \quad \dots(14)$$

$$I_{Total} = 1.52A + [0.19A \times 5 \text{ (No. of LED lights)}]$$

$$I_{Total} = 2.47A$$

The number of batteries required for optimum energy storage was calculated using equation 2 (page 35), 6 and 7 (page 40). Equation 2 was used to determine required battery capacity:

$$C = (I_{Total})(T) \quad \dots(15)$$

$$C = 2.47A \times 7$$

(teacher official working hours is 7 hours)

$$C = 17.29Ah$$

The total load energy was determined using equation 7 (page 40):

$$E_{L(laptop)} = P_L \times H_D \times D_W \div 7 \quad \dots(16)$$

$$E_{L(laptop)} = (1.52A \times 19.98V) \times 7 \times 1 \div 7$$

$$E_{L(laptop)} = 30.37Wh$$

$$E_{L(lights)} = P_L \times H_D \times D_W \div 7 \quad \dots(17)$$

$$E_{L(lights)} = (0.19A \times 12V \times 5) \times 7 \times 1 \div 7$$

$$E_{L(lights)} = 11.4Wh$$

$$E_{L(Total)} = E_{L(laptop)} + E_{L(lights)} \quad \dots(18)$$

$$E_{L(Total)} = 30.37 + 11.4$$

$$E_{L(Total)} = 41.77Wh$$

Equation 6 (page 40) was used to determine the number of batteries required to achieve seven hours (one day) energy back-up:

$$Number\ of\ batteries = \frac{N_c \times E_L}{DOD \times C} \quad \dots(19)$$

$$Number\ of\ batteries = \frac{5 \times 41.77}{0.9 \times (17.29Ah \times 12V)}$$

$$Number\ of\ batteries = 1.118$$

$$\therefore Required\ battery\ capacity = 1.118 \times 17.29Ah$$

$$\therefore Required\ battery\ capacity = 19.33Ah$$

$$Market\ available\ battery\ capacity = 20Ah$$

Calculations indicate that the required battery back-up for seven hours (one day) can be achieved using a 20Ah (market available battery capacity).

According to Solar Energy International (2004:62) local weather conditions and microclimates must be taken into consideration when sizing battery back-up for a stand-alone photovoltaic system. In the Vaal Triangle region Swart et al. (2011) account that weather conditions are characterized by thunderstorms and intense air pollution. Thunderstorms causing overcast weather conditions can last for days in the Vaal Triangle region (Dyson 2009:627).

The required battery back-up time of five days during days without sunlight was deduced in Chapter 2 from the teacher's official school days in SA which are five

days a week. The battery back-up required for five days without sunlight was calculated using equation 6 and 7.

The total load energy was determined using equation 7:

$$E_{L(laptop)} = P_L \times H_D \times D_W \div 7 \quad \dots(20)$$

$$E_{L(laptop)} = (1.52A \times 19.98V) \times 7 \times 5 \div 7$$

$$E_{L(laptop)} = 151.848Wh$$

$$E_{L(lights)} = P_L \times H_D \times D_W \div 7 \quad \dots(21)$$

$$E_{L(lights)} = (0.19A \times 12V \times 5) \times 7 \times 5 \div 7$$

$$E_{L(lights)} = 57Wh$$

$$E_{L(Total)} = E_{L(laptop)} + E_{L(lights)} \quad \dots(22)$$

$$E_{L(Total)} = 151.848 + 57$$

$$E_{L(Total)} = 208.848Wh$$

Equation 6 was used to determine the number of batteries required for five days of energy back-up running seven hours each day:

$$Number\ of\ batteries = \frac{N_c \times E_L}{DOD \times C} \quad \dots(23)$$

$$Number\ of\ batteries = \frac{5 \times 208.848}{0.9 \times (17.29Ah \times 12V)}$$

$$Number\ of\ batteries = 5.5921$$

$$\therefore Required\ battery\ capacity = 5.5921 \times 17.29Ah$$

$$\therefore Required\ battery\ capacity = 96.687Ah$$

$$Market\ available\ battery\ capacity = 100Ah$$

This calculation indicated that the required battery back-up for 5 days can be achieved using a 100Ah instead of 5.5921 batteries with capacity of 17.29Ah. This eliminates the need for charge balancing. According to battery charge equalisation or battery charge balancing prevents multi-connected batteries life cycle degradation.

The pilot e-learning centre in Figure 56 was used to determine the number of photovoltaic panels (PV2) required for maintaining the battery (100Ah) at its fully charged level. The prerequisite for the established number of photovoltaic panels (PV2) is to utilize the available daily sunlight hours per day to maintain the battery charged. The photovoltaic panel's (PV2) orientation and tilt angle was retained at 26 degrees due north as established in Chapter 2. Initially one photovoltaic panel was connected to the pilot e-learning centre set-up in Figure 56.

Continuous data capturing was done from the pilot e-learning centre for various operational periods for a minimum of seven hours. The operational period of the pilot e-learning centre was evaluated for either day or night utilisation. The pilot e-learning centre ran at full load during all the operational period. Full load conditions for the pilot e-learning centre constituted the following:

- Five MR16**(PAR16) LED light sources switched on.
- Lenovo laptop battery charged status at zero per cent at the start the beginning of the operational period of the e-learning centre.

Figure 57 shows the initial operational period of the pilot e-learning centre set to 24 hours to evaluate the 100 Ah battery's charge status. One photovoltaic panel (PV2) was connected to the pilot e-learning centre with a 100Ah lead acid battery storage.

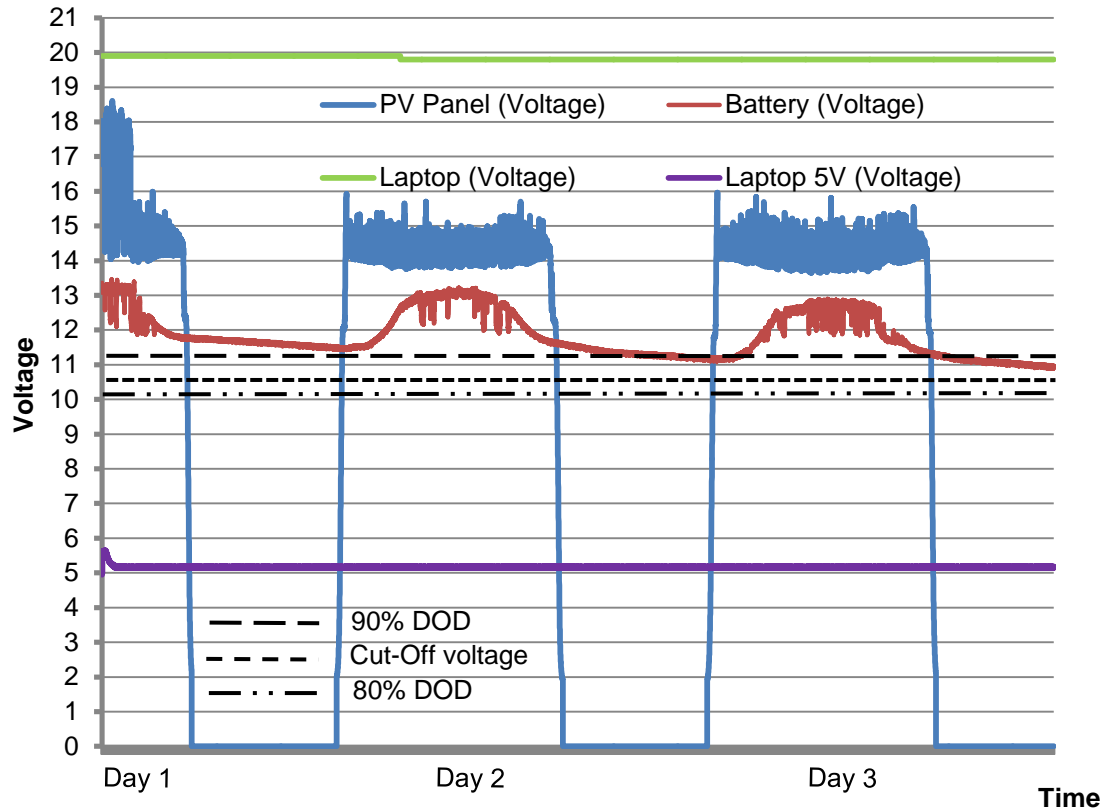


Figure 57 Pilot e-learning centre set to 24 hour operational periods with a 100Ah battery

Figure 57 illustrates the measured battery voltage, photovoltaic panel (PV2) voltage, laptop charge voltage and the laptop +5V USB line (laptop battery pack run time). Laptop user interface was simulated using a recorded macro (Annexure B).

It was deduced from Figure 57 that the battery charge state was not maintained at a fully-charged level after charging. The battery voltage decreased at a rate of 0.5V after charging for every consecutive night. It was also inferred from Figure 51 by using data interpolation that the battery voltage at a decrease rate of 0.5V, the cut-off voltage (shown in Figure 57) will be reached at the start of day 4. The decrease in battery voltage was caused either by the low battery charge time or by the insufficient number of photovoltaic panels (PV2).

The operational period of the pilot e-learning centre was reduced to evaluate its impact on the battery's charge status. The operational period of the pilot e-learning centre was reduced from 24 hours to 17 hours (3pm – 8am). The operational period was selected from 3pm – 8am, this was done because the photovoltaic panel's peak power production is attained during late morning and early afternoon (Balfour, Shaw & Nash 2011:88).

Figure 58 shows the operational period of the pilot e-learning centre set to 17 hours (3pm – 8am) using one photovoltaic panel (PV2) as well as the battery DOD levels as summarised in Table 33. Figure 58 also illustrates the measured battery voltage, photovoltaic panel (PV2) voltage, laptop charge voltage and the laptop +5V (laptop battery pack run time).

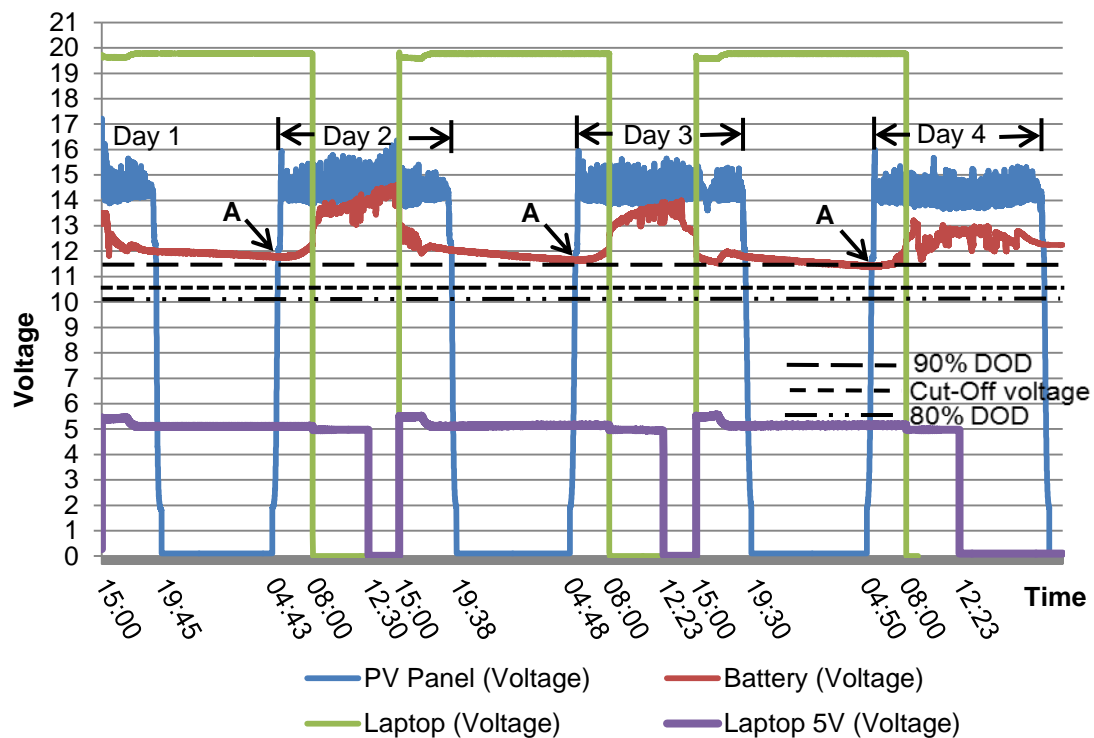


Figure 58 Pilot e-learning centre set to 17 hour operational periods with a 100Ah battery

The laptop battery pack's run time (until the battery pack is fully discharged) was determined using the measured laptop USB port voltage utilising the V.I.C interface as shown in Figure 56.

It was inferred from Figure 58 that the battery charge status was not maintained at a fully charged level after charging using the available sunlight hours. The reduction of the operational period of the pilot e-learning centre from 24 hours to 17 hours decreased the battery discharge rate from 0.5V to 0.17V – 0.21V. The battery's discharge difference (battery's 0% DOD level (12.7V) less the measured battery voltage at the start of each charge cycle) is indicated by "A" in Figure 58.

It was also deduced from Figure 58 by using data interpolation of the battery voltage at a decrease rate of 0.21V that the battery's cut-off voltage will be reached during the start of day 10. The results from a reduced operational period of the pilot e-learning centre indicated an improved battery discharge rate. The result also indicated that the available sunlight hours were not sufficient for the system to fully charge the battery.

The operational period of the pilot e-learning centre was further reduced from 17 hours to 7 hours and two photovoltaic panels (PV2) were used. The operational period was selected from 8am – 3pm this was done to gain full load conditions while the battery was charging at solar noon. Solar noon is when solar irradiance is at its highest during the day and the fully-charged status of a battery can be maintained in a photovoltaic stand-alone system (Ziuku & Meyer 2010). Figure 59 shows the operational period of the pilot e-learning centre set to 7 hours (8am – 3pm) using two photovoltaic panels (PV2).

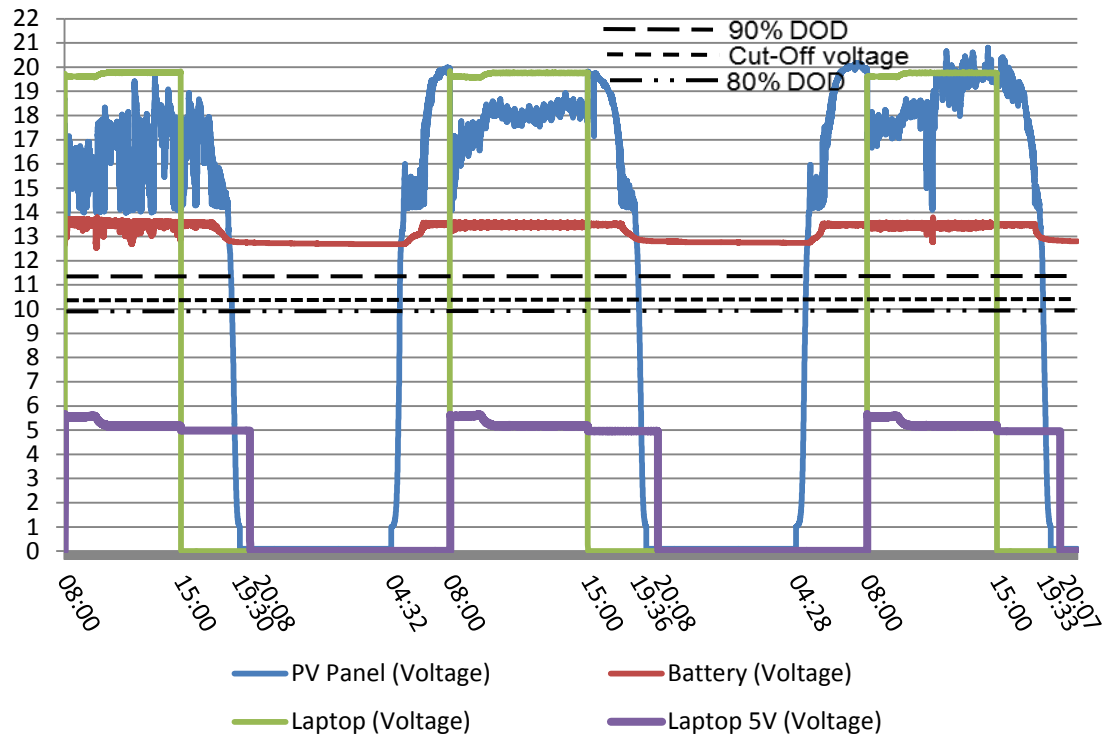


Figure 59 Pilot e-learning centre set to 7 hour operational periods with a 100Ah battery using two photovoltaic panels (PV2)

It was deduced from Figure 59 that the battery charge status was maintained at fully charged (0.078% DOD – 12.69V) after charging using the available sunlight hours utilising two photovoltaic panels.

One photovoltaic panel was used on the pilot e-learning centre to evaluate its impact on the battery's charge status. The operational period of the pilot e-learning centre was maintained at 7 hours. The operational period was selected from 9am – 4pm this was done to gain full load conditions while the battery is charging at solar noon. Figure 60 shows the operational period of the pilot e-learning centre set to 7 hours (9am – 4pm) using one photovoltaic panel (PV2).

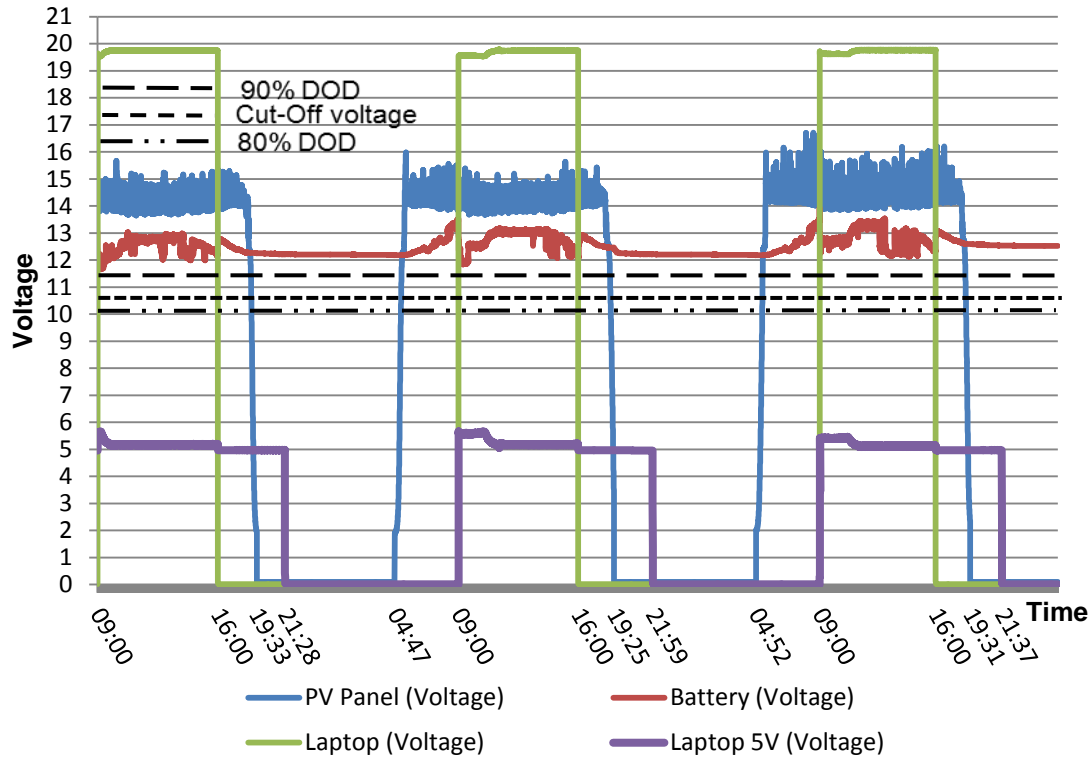


Figure 60 Pilot e-learning centre set to 7 hour operational periods with a 100Ah battery using one photovoltaic panel (PV2)

It was deduced from Figure 60 that the battery charge status was maintained at a fully charged (4.016% DOD – 12.19V) level after charging using the available sunlight hours. It can also be deduced from Figure 60 that the reduced battery charged status of 4.016% DOD when compared to Figure 59 can be attributed to partly cloudy weather condition during the evaluation days.

It was concluded that one photovoltaic panel (PV2) can be employed to recharge the battery (100Ah) fully for a pilot e-learning centre operational period of 7 hours. It was also concluded that for a minimum of one day battery back up a 20Ah battery would be charged fully using one photovoltaic panel. The operation period of the e-learning centre should be selected to coincide with solar noon to utilize the available maximum solar irradiance. It was deduced

that the ratio of back-up battery capacity (Ah) to number of days (seven hours per day) without sunlight is 20:1.

4.8 Pilot e-learning centre sizing for full scale implementation

A pilot e-learning centre was designed and built utilising the established cost-effective equipment mix. A stand-alone photovoltaic system outline was used as the design of a pilot e-learning centre with one VDU user interface. The pilot e-learning centre consisted of the following devices: a photovoltaic panel (PV2), a charge controller (Microcare 12/24 10AMP MPPT), a DC-DC converter (Motormate IPC-1210), LED-based SSL technology interior light sources (MR16**(PAR16)), a laptop (Lenovo) and a rechargeable lead acid battery.

It was established that one photovoltaic panel can be utilised to fully recharge the pilot e-learning centre's battery using the available sunlight hours. The pilot e-learning centre was utilised for a period of 7 hours while the battery was being recharged. Table 34 illustrates the equipment list (including quantity used) assembled to construct a pilot e-learning centre.

Table 34 Pilot e-learning centre's equipment list (including quantity used)

Device	Manufacturer Part No.	Quantity
Photovoltaic panel	CHN75-72P	1
Charge controller	Microcare 12/24 10A MPPT	1
DC-DC converter	Motormate IPC 1210	1
Battery storage	Lead acid	20Ah (one day back up)
Lights	MR16**(PAR16)	5
Laptop	Lenovo	1

Electrical connections between devices listed in Table 34 were made using polyvinyl chloride (PVC) insulated copper cables based on the reviewed NEC standard in Table 6. The maximum allowed cable length between devices was determined using the measured current (equipment current determined in Chapter 3) to maintain a cable voltage drop less than 5%. Table 35 shows the measured current of equipment listed in Table 34.

Table 35 Measured current of equipment listed equipment in Table 34

Device	Measured current (A)
Photovoltaic panel (CHN75-72P)	
Photovoltaic panel to charge controller	4.26*
Charge controller (Microcare 12/24 10A MPPT)	
Charge controller to DC-DC converter	2.07
Charge controller to lights [MR16**(PAR16)]	0.95
Charge controller to Battery [charge current]	10*
DC-DC converter (Motormate IPC 1210)	
DC-DC converter to laptop [Lenovo]	1.52

Where : * \equiv Manufacturer maximum STC current parameters

The manufacturer maximum STC current parameters for the photovoltaic panel (PV2) and charge controller (battery charge current) were used in Table 35. The maximum STC current parameter was used as it is independent of solar radiation variations. The measured photovoltaic panel current (at installation site) is directly proportional to solar radiation variations (Bostan, Gheorghe, Dulgheru, Sobor, Bostan & Sochirean 2012:133). The peak current output of a photovoltaic panel is measured at STC (Solanki 2009:340). In a stand-alone photovoltaic system the battery charge current is regulated by the charge controller from the photovoltaic panel current (Skouby & Idongesit 2014:206).

Table 36 lists the cable specifications for wiring the pilot e-learning centre to maintain a cable voltage drop less than 5%.

Table 36 Cable specifications for wiring the pilot e-learning centre

Cable type	AWG size	Length used in pilot e-learning centre (m)	Maximum allowed length (m)
Photovoltaic panel to charge controller			
Copper	6	10.2	27
Charge controller to DC-DC converter			
Copper	6	1.2	40
Charge controller to lights			
Copper	6	3.6	162
Charge controller to Battery			
Copper	6	2	16
DC-DC converter to laptop [Lenovo]			
Copper	6	1	81

Equation 24 shows the pilot e-learning centre's wiring cable length scaling algorithm derived from Table 36.

$$f(CL) = f(pv - cc) + f(cc - dc) + f(cc - LED) + .. \quad \dots(24)$$

$$... + f(cc - batt) + f(dc - laptop)$$

$$f(pv - cc) \leq 27 \quad \dots(25)$$

$$f(cc - dc) \leq 40 \quad \dots(26)$$

$$f(cc - LED) \leq 162 \quad \dots(27)$$

$$f(cc - batt) \leq 16 \quad \dots(28)$$

$$f(cc - Laptop) \leq 81 \quad \dots(29)$$

Where

$$\begin{aligned}
 f(CL) &\equiv \text{Total length of wiring cable (copper ,AWG 6)} \\
 f(pv - cc) &\equiv \text{Cable length (Photovoltaic pane} \\
 f(pv - cc) &\equiv \text{Cable length (Photovoltaic panel to charge controller)} \\
 f(cc - dc) &\equiv \text{Cable length (Charge controller to dc - dc converter)} \\
 f(cc - LED) &\equiv \text{Cable length (Charge controller to lights)} \\
 f(cc - batt) &\equiv \text{Cable length (Charge controller to Battery)} \\
 f(dc - laptop) &\equiv \text{Cable length (dc - dc converter to laptop)}
 \end{aligned}$$

Equation 30 shows the pilot e-learning centre's device quantity scaling (quantity) algorithm derived from Table 34 and equation 21.

$$\begin{aligned}
 f(Q) = f(pv) + f(cc) + f(dc) + [f(batt) \times NBD] + .. \\
 ..5f(LED) + f(LT) + f(CL)
 \end{aligned} \quad \dots(30)$$

Where

$$\begin{aligned}
 f(Q) &\equiv \text{Quantity of e - learning centre's VDU} \\
 f(pv) &\equiv \text{Quantity of photovoltaic panels (CHN75 - 72P)} \\
 f(cc) &\equiv \text{Quantity of charge controllers (Microcare } \frac{12}{24} \text{ 10A MPPT)} \\
 f(dc) &\equiv \text{Quantity of dc - dc converters} \\
 f(batt) &\equiv \text{Quantity of 20Ah batteries (Lead acid)} \\
 f(LED) &\equiv \text{Quantity of LED - based SSL technology interior} \\
 &\quad \text{light sources (MR16 ** (PAR16))} \\
 f(LT) &\equiv \text{Quantity of laptops (Lenovo)} \\
 f(CL) &\equiv \text{Total length of wiring cable (Copper, AWG 6)}
 \end{aligned}$$

Equation 30 can be used to size an e-learning centre based on the recommended teacher – learner ratio in SA which is 1:40.

4.9 Summary

In this chapter the cost-effective equipment mix was established. A pilot e-learning centre was designed and built using the determined cost-effective equipment mix. Data analysis of the pilot e-learning centre was undertaken to optimize its energy storage using the available sunlight hours. Recommendation for the full scale implementation of the pilot e-learning centre was presented.

Chapter 5 presents conclusions and recommendations for future research based on this study.

Chapter 5 Conclusion and recommendations

5.1 Introduction

This chapter presents conclusions and future research recommendations based on this study.

5.2 Conclusions

A pilot e-learning centre was designed and built utilising the established cost-effective equipment mix. A stand-alone photovoltaic system design was used for the pilot e-learning centre. The stand-alone photovoltaic system consisted of the following devices: a photovoltaic panel (PV2), a charge controller (Microcare 12/24 10AMP MPPT), a DC-DC converter (Motormate IPC-1210), LED-based SSL technology interior light sources (MR16**(PAR16)), a laptop (Lenovo) and a rechargeable lead acid battery.

Owing to the susceptibility of the Vaal Triangle region to thunderstorms causing overcast conditions for days, battery back-up time of 5 days was deduced for the Vaal Triangle region. The ratio of back up battery capacity (Ah) to number of days (seven hours per day) without sunlight was determined to be 20:1.

It was established that one photovoltaic panel can be employed to fully recharge a battery of a pilot e-learning centre with an operational period of 7 hours using the available sunlight hours per day.

Table 37 lists the conclusions reached to meet the objectives of this study to design and develop an off-grid e-learning centre for rural communities.

Table 37 Conclusions reached to meet the objectives of this study

Study objective	Conclusion to meet objective
Determine an appropriately available renewable energy resource for powering a rural e-learning centre	➤ Solar energy (Ample available alternative energy resource in SA)
Determine the most cost-effective equipment mix of power utilisation, power management/storage and ICT equipment	<ul style="list-style-type: none"> ➤ Poly crystalline photovoltaic panel (RET type used) ➤ Stand-alone photovoltaic system design ➤ See Table 34 for the established cost-effective and power-efficient equipment mix
Design and build a pilot e-learning centre using the most cost-effective equipment mix.	<ul style="list-style-type: none"> ➤ Stand-alone photovoltaic system design used (Maximum battery storage advantage when used during the day) ➤ The pilot e-learning centre was constructed for one VDU user interface.
Provide guidelines for the full scale implementation of an off grid e-learning centre for rural communities	➤ Equation 30 shows the pilot e-learning centre's full scale sizing (quantity) algorithm

5.3 Future research recommendations based on this study

Future research recommended based on this study is reducing the electric load of an e-learning centre by installing it in intelligent buildings. Load reduction can be attained using more sunlight blinds control and individual lighting control.

This can lead to a reduction of the number of lighting sources required to maintain the required illuminance level yielding reduced system cost.

Prospective research can also investigate the cost-effective integration of laptop battery pack storage capacity to stand-alone photovoltaic energy storage capacity. This prospective research will have an objective to reduce back up energy storage costs of e-learning centres using a stand-alone photovoltaic system.

Reduced system costs of an off-grid e-learning centre for rural communities powered by a renewable energy resource can increase access to basic education and reduce the global digital divide.

References

ADOBE READER. 2013. Client system requirement: Hosted and licensed by deployment. [Online]. Available at:<<http://www.adobe.com/products/adobeconnect/tech-specs.html>>. Accessed: 04 November 2013.

ALVARENGA, C.A., COSTA, D. & LOBO, A.R. 1996. Renewable sources for decentralized energy supply. *Renewable Energy*, 9(1–4):1152-1155.

APPLASAMY, V. 2011. Cost evaluation of a stand-alone residential photovoltaic power system in Malaysia. In *Business, Engineering and Industrial Applications (ISBEIA), 2011 IEEE Symposium on*. 25-28 Sept. 2011. pp. 214-218.

ARROW NORTH AMERICAN COMPONENTS. 2014. LED viewing angle. [Online]. Available at:<<https://www.arrownac.com/solutions-applications/lighting/whatisanled.html>>. Accessed: 05 June 2014.

ASTLEY, R. 2009. *Classic British car electrical systems: Your guide to understanding, repairing and improving the electrical components a*. Veloce Publishing.

ATHANASE, N., JIANG, C., LI, H. & CHEN, Z. 2008. Organizational e-learning strategies for technical and vocational education and training (TVET) in Sub-Sahara Africa. In *Computer Science and Software Engineering, 2008 International Conference on*. 12-14 Dec. 2008. pp. 267-270.

BABAZADEH, H., WENZHONG, G. & DUNCAN, K. 2012. A new control scheme in a battery energy storage system for wind turbine generators. In *Power and Energy Society General Meeting, 2012 IEEE*. 22-26 July 2012. pp. 1-7.

BALFOUR, J.R. 2011. *Advanced photovoltaic system design*. Jones & Bartlett Learning.

BALFOUR, J.R., SHAW, M. & NASH, N.B. 2011. *Review guide for the NABCEP entry-level exam*. Jones & Bartlett Learning, LLC.

- BAÑOS, R., MANZANO-AGUGLIARO, F., MONTOYA, F.G., GIL, C., ALCAYDE, A. & GÓMEZ, J. 2011. Optimization methods applied to renewable and sustainable energy: A review. *Renewable and Sustainable Energy Reviews*, 15(4):1753-1766.
- BANSAL, S., SAINI, L.M. & JOSHI, D. 2012. Design of a DC-DC converter for photovoltaic solar system. In *Power Electronics (IICPE), 2012 IEEE 5th India International Conference on*. 6-8 Dec. 2012. pp. 1-5.
- BARD, A.J., INZELT, G. & SCHOLZ, F. 2012. *Electrochemical dictionary*. Springer.
- BATTERY UNIVERSITY. 2003. What's the best battery. [Online]. Available at:<http://batteryuniversity.com/learn/article/whats_the_best_battery>. Accessed: 18 November 2013.
- BLAKERS, A.W. 1998. Substrates for thin crystalline silicon solar cells. *Solar Energy Materials and Solar Cells*, 51(3-4):385-392.
- BÖER, K.W. 2011. Cadmium sulfide enhances solar cell efficiency. *Energy Conversion and Management*, 52(1):426-430.
- BOSTAN, I., GHEORGHE, A.V., DULGHERU, V., SOBOR, I., BOSTAN, V. & SOCHIREAN, A. 2012. *Resilient energy systems: Renewables: Wind, solar, hydro*. Springer.
- BOWER, W. & WHITAKER, C. 2002. Certification of photovoltaic inverters: the initial step toward PV system certification. In *Photovoltaic Specialists Conference, 2002. Conference Record of the Twenty-Ninth IEEE*. 19-24 May 2002. pp. 1406-1409.
- BOYCE, P.R. 2003. *Human factors in lighting*. 2nd ed. New York: Taylor & Francis.
- BRANKER, K., PATHAK, M.J.M. & PEARCE, J.M. 2011. A review of solar photovoltaic levelized cost of electricity. *Renewable and Sustainable Energy Reviews*, 15(9):4470-4482.
- BUGAJE, I.M. 2006. Renewable energy for sustainable development in Africa: A review. *Renewable and Sustainable Energy Reviews*, 10(6):603-612.

BURGER, B. & RÜTHER, R. 2006. Inverter sizing of grid-connected photovoltaic systems in the light of local solar resource distribution characteristics and temperature. *Solar Energy*, 80(1):32-45.

CAMPOCCIA, A., FAVUZZA, S., SANSEVERINO, E.R. & ZIZZO, G. 2010. Reliability analysis of a stand-alone PV system for the supply of a remote electric load. In *Power Electronics Electrical Drives Automation and Motion (SPEEDAM), 2010 International Symposium on*. 14-16 June 2010. pp. 158-163.

CHAPMAN, R.N. 1990. The synthesis of solar radiation data for sizing stand-alone photovoltaic systems. In *Photovoltaic Specialists Conference, 1990., Conference Record of the Twenty First IEEE*. 21-25 May 1990. pp. 965-970.

CHE-CHI, W., SHAO-YU, C. & JIH-CHIEN, C. 2013. Predicting remaining discharge time of a Lithium-ion battery by using residual capacity and workload. In *Consumer Electronics (ISCE), 2013 IEEE 17th International Symposium on*. 3-6 June 2013. pp. 179-180.

CHEL, A., TIWARI, G.N. & CHANDRA, A. 2009. Simplified method of sizing and life cycle cost assessment of building integrated photovoltaic system. *Energy and Buildings*, 41(11):1172-1180.

CHEN, S., LI, P., BRADY, D. & LEHMAN, B. 2013. Determining the optimum grid-connected photovoltaic inverter size. *Solar Energy*, 87(0):96-116.

CHENG, C.L., SANCHEZ JIMENEZ, C.S. & LEE, M.-C. 2009. Research of BIPV optimal tilted angle, use of latitude concept for south orientated plans. *Renewable Energy*, 34(6):1644-1650.

COATON, J.R. & MARSDEN, A.M. 1997. *Lamps and lighting*. London: Arnold.

CROMPTON, T.P.J. 2000. *Battery reference book*. Elsevier Science.

CROMPTON, T.R. 2000. *Battery reference book*. Newnes.

- DARMAWI, SIPAHUTAR, R., BERNAS, S.M. & IMANUDDIN, M.S. 2013. Renewable energy and hydropower utilization tendency worldwide. *Renewable and Sustainable Energy Reviews*, 17(0):213-215.
- DASAPPA, S. 2011. Potential of biomass energy for electricity generation in sub-Saharan Africa. *Energy for Sustainable Development*, 15(3):203-213.
- DEEPTI, D.J. & RAMANARAYANAN, V. 2006. State of charge of lead acid battery. In *Power Electronics, 2006. IICPE 2006. India International Conference on*. 19-21 Dec. 2006. pp. 89-93.
- DELL, R.M., RAND, D.A.J. & CHEMISTRY, R.S.O. 2001. *Understanding batteries*. Royal Society of Chemistry.
- DENGYUAN, S., JINGFENG, X., ZHIYAN, H., GAOFEI, L., HONGFANG, W., HAIJIAO, A., BO, Y., GREKO, B., BORDEN, K., SAUER, K., ROESSLER, T., JIANHUA, C., HAITAO, W., BULTMAN, J., VLOOSWIJK, A.H.G. & VENEMA, P.R. 2012. Progress in n-type Si solar cell and module technology for high efficiency and low cost. In *Photovoltaic Specialists Conference (PVSC), 2012 38th IEEE*. 3-8 June 2012. pp. 003004-003008.
- DONG, L., YUNFANG, Z., XIAO, F., FUTE, Z., TAO, S. & BAOQUAN, S. 2013. An 11%-power-conversion-efficiency organic;Inorganic hybrid solar cell achieved by facile organic passivation. *Electron Device Letters, IEEE*, 34(3):345-347.
- DYSON, L.L. 2009. Heavy daily-rainfall characteristics over the Gauteng Province. *Water SA*, 35:627-638.
- EDUCATION DYNAMICS. 2012. Hardware and software you'll need for e-learning. [Online]. Available at:<<http://www.elearners.com/online-education-resources/online-learning/hardware-and-software-youll-need-for-elearning/>>. Accessed: 04 November 2013.
- EIICHI, E. & KUOKAWA, K. 1994. Sizing procedure for photovoltaic systems. In *Photovoltaic Energy Conversion, 1994, Conference Record of the Twenty Fourth IEEE Photovoltaic Specialists Conference - 1994, 1994 IEEE First World Conference on*. 5-9 Dec 1994. pp. 1196-1199

EL CHAAR, L., LAMONT, L.A. & EL ZEIN, N. 2011. Review of photovoltaic technologies. *Renewable and Sustainable Energy Reviews*, 15(5):2165-2175.

ELMA, O. & SELAMOGULLARI, U.B. 2011. The effect of inverter efficiency on stand-alone residential PV system sizing. In *Electrical and Electronics Engineering (ELECO), 2011 7th International Conference on*. 1-4 Dec. 2011. pp. I-317 - I-319.

ELMASRY, G. & SUN, D.-W. 2010. CHAPTER 1 - Principles of Hyperspectral Imaging Technology. In Sun, D.-W., ed. *Hyperspectral imaging for food quality analysis and control*. San Diego: Academic Press. pp. 3-43.

ERICKSON, J.D. & CHAPMAN, D. 1995. Photovoltaic technology: Markets, economics, and rural development. *World Development*, 23(7):1129-1141.

ERICKSON, R.W. 2001. DC–DC Power converters. *Wiley encyclopedia of electrical and electronics engineering*. John Wiley & Sons, Inc.

EU ENERGY STAR. 2012a. Desktop vs laptop. [Online]. Available at:<http://www.eu-energystar.org/en/en_022.shtml>. Accessed: 04 November 2013.

EU ENERGY STAR. 2012b. Energy star 5.0 qualified desktop computers. [Online]. Available at:<<http://www.eu-energystar.org/en/database/?cmd=sort;sort1=category>>. Accessed: 04 November 2013.

FISCHER, D. 1986. Interior lighting. *Electric Power Applications, IEE Proceedings B*, 133(2):115-139.

FOSTER, R., GHASSEME, M. & COTA, A. 2010. *Solar energy renewable energy and the environment*. United States of America: Taylor and Francis Group.

FOSTER, R., GHASSEMI, M. & COTA, A. 2009. *Solar energy: Renewable energy and the environment*. Taylor & Francis.

- FREY, G.W. & LINKE, D.M. 2002. Hydropower as a renewable and sustainable energy resource meeting global energy challenges in a reasonable way. *Energy Policy*, 30(14):1261-1265.
- FUCHS, C. & HORAK, E. 2008. Africa and the digital divide. *Telematics and Informatics*, 25(2):99-116.
- GEBREMICHAEL, M.D. & JACKSON, J.W. 2006. Bridging the gap in Sub-Saharan Africa: A holistic look at information poverty and the region's digital divide. *Government Information Quarterly*, 23(2):267-280.
- GHARAKHANI SIRAKI, A. & PILLAY, P. 2012. Study of optimum tilt angles for solar panels in different latitudes for urban applications. *Solar Energy*, 86(6):1920-1928.
- GOETZBERGER, A. & HEBLING, C. 2000. Photovoltaic materials, past, present, future. *Solar Energy Materials and Solar Cells*, 62(1-2):1-19.
- GORDON, G. 2010. *Interior lighting for designers*. Wiley.
- GUHA, S. 1998. Amorphous silicon alloy photovoltaic technology and applications. *Renewable Energy*, 15(1-4):189-194.
- GUHA, S. & YANG, J. 2006. Progress in amorphous and nanocrystalline silicon solar cells. *Journal of Non-Crystalline Solids*, 352(9-20):1917-1921.
- HAIFENG, G., LIQIN, N. & ASGARPOOR, S. 2008. Reliability-based stand-alone photovoltaic system sizing design - A case study. In *Probabilistic Methods Applied to Power Systems, 2008. PMAPS '08. Proceedings of the 10th International Conference on*. 25-29 May 2008. pp. 1-8.
- HALONEN, L., TETRI, E. & BHUSAL, P. 2010. *Annex 45: Guidebook on energy efficient electric lighting for buildings*. Finland: Alto University.
- HAMAKAWA, Y. 1994. Recent advances in solar photovoltaic technology and its new role for environmental issue. *Renewable Energy*, 5(1-4):34-43.

HANKINS, M. 2010. *Stand-alone solar electric systems: The Earthscan Expert handbook for planning, design and installation*. Earthscan.

HEACOCK, D. & FREEMAN, D. 1995. Capacity monitoring in advanced battery chemistries. *In Battery Conference on Applications and Advances, 1995., Proceedings of the Tenth Annual*. 10-13 Jan 1995. pp. 185-191.

HELD, G. 2008. *Introduction to light emitting diode technology and applications*. Taylor & Francis.

HENDRIK, F. & SERFONTEIN, B. 2004. A workable e-learning strategy for distance education in South Africa. *In Advanced Learning Technologies, 2004. Proceedings. IEEE International Conference on*. 30 Aug.-1 Sept. 2004. pp. 943-947.

HONTORIA, L., AGUILERA, J. & ZUFIRIA, P. 2003. A tool for obtaining the LOLP curves for sizing off-grid photovoltaic systems based in neural networks. *In Photovoltaic Energy Conversion, 2003. Proceedings of 3rd World Conference on*. 18-18 May 2003. pp. 2423-2426.

IBRAHIM, H., ILINCA, A. & PERRON, J. 2008. Energy storage systems—Characteristics and comparisons. *Renewable and Sustainable Energy Reviews*, 12(5):1221-1250.

IBWAVE. 2013. Online certification system requirements. [Online]. Available at:<<http://www.ibwave.com/LearningHub/iBwaveCertification/SystemRequirements.aspx>>. Accessed: 04 November 2013.

IEEE. 1998. IEEE Guide for terrestrial photovoltaic power system safety.

IEEE STD 1013. 2007. IEEE Recommended practice for sizing lead-acid batteries for stand-alone photovoltaic (PV) systems. *IEEE Std 1013-2007 (Revision of IEEE Std 1013-2000)*:1-55.

INTERNAL ENERGY AGENCY. 2006. Light's labour's lost (policies for energy-efficient lighting). Available: <http://www.iea.org/publications/freepublications/publication/light2006.pdf> [Accessed 24 February 2014].

INTERNATIONAL, S.E. 2004. *Photovoltaics: Design and installation manual*. New Society Publishers, Limited.

JAFARKAZEMI, F. & SAADABADI, S.A. 2013. Optimum tilt angle and orientation of solar surfaces in Abu Dhabi, UAE. *Renewable Energy*, 56(0):44-49.

JAKHRANI, A.Q., OTHMAN, A.-K., RIGIT, A.R.H., SAMO, S.R. & KAMBOH, S.A. 2012. A novel analytical model for optimal sizing of standalone photovoltaic systems. *Energy*, 46(1):675-682.

JIANHUA, Z. & YINGJIAN, J. 2008. A factor analysis on the differences of group learning between classroom-based and web-based learning environments. *In Education Technology and Training, 2008. and 2008 International Workshop on Geoscience and Remote Sensing. ETT and GRS 2008. International Workshop on*. 21-22 Dec. 2008. pp. 56-59.

JIANWU, Z., WEI, Q. & LIYAN, Q. 2012. A single-switch isolated DC-DC converter for photovoltaic systems. *In Energy Conversion Congress and Exposition (ECCE), 2012 IEEE*. 15-20 Sept. 2012. pp. 3446-3452.

JOHN, W. 2001. Photovoltaic power systems and the National Electrical Code: Suggested practice. *SAND*, (0674):1-177.

JONG-PIL, L., BYUNG-DUK, M., DONG-WOOK, Y., TAE-JIN, K. & JI-YOON, Y. 2007. A new topology for PV DC/DC converter with high efficiency under wide load range. *In Power Electronics and Applications, 2007 European Conference on*. 2-5 Sept. 2007. pp. 1-6.

KALOGIROU, S.A. 2009. Solar economic analysis. *Solar Energy Engineering*. Boston: Academic Press. pp. 665-701.

KAREKEZI, S. & RANJA, T. 1997. *Renewable energy technologies in Africa*. London: Zed Books Ltd.

KAUNDA, C.S. 2013. Energy situation, potential and application status of small-scale hydropower systems in Malawi. *Renewable and Sustainable Energy Reviews*, 26(0):1-19.

KAUNDINYA, D.P., BALACHANDRA, P. & RAVINDRANATH, N.H. 2009. Grid-connected versus stand-alone energy systems for decentralized power - A review of literature. *Renewable and Sustainable Energy Reviews*, 13(8):2041-2050.

KAYE, R.J. 1994. A new approach to optimal sizing of components in stand-alone photovoltaic power systems. In *Photovoltaic Energy Conversion, 1994., Conference Record of the Twenty Fourth. IEEE Photovoltaic Specialists Conference - 1994, 1994 IEEE First World Conference on*. 5-9 Dec 1994. pp. 1192-1195.

KAZMERSKI, L.L. 1997. Photovoltaics: A review of cell and module technologies. *Renewable and Sustainable Energy Reviews*, 1(1-2):71-170.

KEATS, D.W. & BEEBE, M.A. 2004. Addressing digital divide issues in a partially online masters programme in Africa: the NetTel@Africa experience. In *Advanced Learning Technologies, 2004. Proceedings. IEEE International Conference on*. 30 Aug.-1 Sept. 2004. pp. 953-957.

KELLER, L. & AFFOLTER, P. 1995. Optimizing the panel area of a photovoltaic system in relation to the static inverter - Practical results. *Solar Energy*, 55(1):1-7.

KIMEMIA, D. & ANNEGARN, H. 2011. An urban biomass energy economy in Johannesburg, South Africa. *Energy for Sustainable Development*, 15(4):382-387.

KOEPEL, G. & KORPAS, M. 2006. Using storage devices for compensating uncertainties caused by non-dispatchable generators. In *Probabilistic Methods Applied to Power Systems, 2006. PMAPS 2006. International Conference on*. 11-15 June 2006. pp. 1-8.

KONER, P.K., DUTTA, V. & CHOPRA, K.L. 2000. A comparative life cycle energy cost analysis of photovoltaic and fuel generator for load shedding application. *Solar Energy Materials and Solar Cells*, 60(4):309-322.

KOPONEN, T., TEDRE, M. & VESISENAHU, M. 2011. An analysis of the state and prospects of e-learning in developing countries. In *IST-Africa Conference Proceedings, 2011*. 11-13 May 2011. pp. 1-9.

- KUNZ, T., GAZUZ, V., HESSMANN, M.T., GAWEHNS, N., BURKERT, I. & BRABEC, C.J. 2011. Laser structuring of crystalline silicon thin-film solar cells on opaque foreign substrates. *Solar Energy Materials and Solar Cells*, 95(8):2454-2458.
- LIANG, Z.C., CHEN, D.M., LIANG, X.Q., YANG, Z.J., SHEN, H. & SHI, J. 2010. Crystalline Si solar cells based on solar grade silicon materials. *Renewable Energy*, 35(10):2297-2300.
- LIMING, H. 2009. Financing rural renewable energy: A comparison between China and India. *Renewable and Sustainable Energy Reviews*, 13(5):1096-1103.
- MANZANO-AGUGLIARO, F., ALCAYDE, A., MONTOYA, F.G., ZAPATA-SIERRA, A. & GIL, C. 2013. Scientific production of renewable energies worldwide: An overview. *Renewable and Sustainable Energy Reviews*, 18(0):134-143.
- MARKVART, T. 1988. Principles of the radiation damage in solar cells. *In Solar Cells for Space Applications, IEE Colloquium on*. 15 Nov 1988. pp. 3/1-3/4.
- MARKVART, T. 2000. *Solar electricity*. 2nd ed. England: John Wiley and Sons.
- MARWALI, M.K.C., MARICAR, N.M. & SHRESTHA, S.K. 2000. Battery capacity tests evaluation for stand-alone photovoltaic systems. *In Power Engineering Society Winter Meeting, 2000. IEEE*. 2000. pp. 540-545.
- MAZDA, F.F. 1981. *Discrete electronic components*. Cambridge University Press.
- MCCANN, J., MICHELLE, R. CATCHPOLE, K., J. WEBER, K. & W. BLAKERS, A. 2001. A review of thin-film crystalline silicon for solar cell applications. Part 1: Native substrates. *Solar Energy Materials and Solar Cells*, 68(2):135-171.
- MCCARNEY, S., OLSON, K. & WEISS, J. 1987. *Photovoltaics (A manual of design and installation for practitioners)* . Carbondale: Solar Energy International.
- MESSINGER, R.A. & VENTRE, J. 2005. *Photovoltaic system engineering*. Florida: Taylor & Francis.

MICROSOFT WINDOWS. 2013. Stay protected, do more. [Online]. Available at:<<http://windows.microsoft.com/en-ZA/windows/end-support-help>>. Accessed: 04 November 2013.

MONTGOMERY, D.C. & RUNGER, G.C. 2010. *Applied statistics and probability for engineers*. John Wiley & Sons.

MOSCINSKA, K. & RUTKOWSKI, J. 2011. Barriers to introduction of e-learning: A case study. *In Global Engineering Education Conference (EDUCON), 2011 IEEE*. 4-6 April 2011. pp. 460-465.

MUNZER, K.A., HOLDERMANN, K.T., SCHLOSSER, R.E. & STERK, S. 1999. Thin monocrystalline silicon solar cells. *Electron Devices, IEEE Transactions on*, 46(10):2055-2061.

MUNZHEDZI, R. & SEBITOSI, A.B. 2009. Redrawing the solar map of South Africa for photovoltaic applications. *Renewable Energy*, 34(1):165-169.

NEUMANN, G.J. 2013. Deep-black optical paint. [Online]. Available at:<<http://www.gerdneumann.net/english/instrument-building-parts-teile-fuer-den-fernrohrbau/totmatte-schwarze-optikfarbe-deep-black-optical-paint.html>>. Accessed: 17 September 2014.

NGUYEN, K.Q. 2007. Alternatives to grid extension for rural electrification: Decentralized renewable energy technologies in Vietnam. *Energy Policy*, 35(4):2579-2589.

NIKHIL, P.G. & SUBHAKAR, D. 2012. An improved algorithm for photovoltaic system sizing. *Energy Procedia*, 14(0):1134-1142.

NIKHIL, P.G. & SUBHAKAR, D. 2013. Sizing and Parametric Analysis of a Stand-Alone Photovoltaic Power Plant. *Photovoltaics, IEEE Journal of*, 3(2):776-784.

NORTHERN ARIZONA WIND AND SUN COMPANY. 2012. Wire loss tables for solar electric systems. [Online]. Available at:<<http://www.solar-electric.com/wire-loss-tables.html>>. Accessed: 14 November 2013.

NOTTON, G., MUSELLI, M. & POGGI, P. 1998. Costing of a stand-alone photovoltaic system. *Energy*, 23(4):289-308.

NWOKEDIUKO, A.A. 2012. Advancing e-learning in African native communities: The language factor. In *Education and e-Learning Innovations (ICEELI)*, 2012 International Conference on. 1-3 July 2012. pp. 1-4.

NYARKO, M. & VENTURA, N. 2010. E-Learning: Virtual classrooms as an added learning platform. In *Computational Technologies in Electrical and Electronics Engineering (SIBIRCON)*, 2010 IEEE Region 8 International Conference on. 11-15 July 2010. pp. 426-431.

OECD. 2008. *Reviews of national policies for education: South Africa 2008*. OECD Publishing.

OYEDEMI, T.D. 2012. Digital inequalities and implications for social inequalities: A study of Internet penetration amongst university students in South Africa. *Telematics and Informatics*, 29(3):302-313.

PAPADOPOULOU, E. 2011. *Photovoltaic industrial systems: An environmental approach*. Springer.

PARIDA, B., INIYAN, S. & GOIC, R. 2011. A review of solar photovoltaic technologies. *Renewable and Sustainable Energy Reviews*, 15(3):1625-1636.

PASCOE, P.E. & ANBUKY, A.H. 2000. VRLA battery capacity estimation using soft computing analysis of the coup de fouet region. In *Telecommunications Energy Conference, 2000. INTELEC. Twenty-second International*. 2000. pp. 589-596.

PASCOE, P.E. & ANBUKY, A.H. 2004. A unified discharge voltage characteristic for VRLA battery capacity and reserve time estimation. *Energy Conversion and Management*, 45(2):277-302.

PEGELS, A. 2010. Renewable energy in South Africa: Potentials, barriers and options for support. *Energy Policy*, 38(9):4945-4954.

- PHUANGPORNPIITAK, N. & KUMAR, S. 2007. PV hybrid systems for rural electrification in Thailand. *Renewable and Sustainable Energy Reviews*, 11(7):1530-1543.
- PODE, R. & DIOUF, B. 2011. *Solar lighting*. Springer.
- POSADILLO, R. & LÓPEZ LUQUE, R. 2008. Approaches for developing a sizing method for stand-alone PV systems with variable demand. *Renewable Energy*, 33(5):1037-1048.
- PRITCHARD, D.C. 1995. *Lighting*. London: Longman Scientific & Technical.
- QUASCHNING, V. 2005. *Understanding renewable energy systems*. Earthscan.
- RADUE, C., VAN DYK, E.E. & MACABEBE, E.Q. 2009. Analysis of performance and device parameters of CIGS PV modules deployed outdoors. *Thin Solid Films*, 517(7):2383-2385.
- RAHMAN, S. & DE CASTRO, A. 1995. Environmental impacts of electricity generation: A global perspective. *Energy Conversion, IEEE Transactions on*, 10(2):307-314.
- RAO, S.S. 2005. Bridging digital divide: Efforts in India. *Telematics and Informatics*, 22(4):361-375.
- RATCLIFF, E., ZACHER, B., STEIRER, X., GANTZ, J., MACDONALD, G., MACECH, M., TADYTIN, D., OU, K. & ARMSTRONG, N.R. 2011. The interface science of interlayer materials and contacts in organic solar cells. In *Photovoltaic Specialists Conference (PVSC), 2011 37th IEEE*. 19-24 June 2011. pp. 003472-003476.
- RAZYKOV, T.M., FERKIDES, C.S., MOREL, D., STEFANAKOS, E., ULLAL, H.S. & UPADHYAYA, H.M. 2011. Solar photovoltaic electricity: Current status and future prospects. *Solar Energy*, 85(8):1580-1608.
- RENEWABLE ENERGY POLICY NETWORK FOR THE 21ST CENTURY (REN21). 2013. *Renewable 2013 global status report*. Paris.

REPUBLIC OF SOUTH AFRICA. Department of Minerals and Energy. 2002. White paper on the promotion of renewable energy and clean energy development. Part one - promotion of renewable energy. Pretoria: Government Printing Works.

REPUBLIC OF SOUTH AFRICA. Department of Development, Environment, Conservation and Tourism. 2012. Renewable energy strategy for the North West. Pretoria: Government Printing Works.

RIZZO, R., PIEGARI, L., TRICOLI, P., MUNTEANU, C. & TOPA, V. 2009. Sizing of photovoltaic sources and storage devices for stand-alone power plants. *In PowerTech, 2009 IEEE Bucharest*. June 28 2009-July 2 2009. pp. 1-6.

SALANKI, C.S. 2013. *Solar photovoltaic technology and systems (a manual for technicians, trainers and engineers)*. Delhi: PHI private learning.

SANGWINE, S.J. 1994. *Electronic components & technology, 2nd ed.*: Taylor & Francis.

SAP. 2011. E-learning products. [Online]. Available at:<<http://training.sap.com/pdf/e-learning-technical-requirements.pdf>>. Accessed: 04 November 2013.

SCHOEMAN, R.M., SWART, A.J. & PIENAAR, C. 2013. Negating temperature on photovoltaic panels. *In AFRICON, 2013*. 9-12 Sept. 2013. pp. 1-5.

SHARMA, V.K., COLANGELO, A. & SPAGNA, G. 1995. Photovoltaic technology: Basic concepts, sizing of a stand alone photovoltaic system for domestic applications and preliminary economic analysis. *Energy Conversion and Management*, 36(3):161-174.

SHEN, W. 2008. Design of standalone photovoltaic system at minimum cost in Malaysia. *In Industrial Electronics and Applications, 2008. ICIEA 2008. 3rd IEEE Conference on*. 3-5 June 2008. pp. 702-707.

SIN GIAP, Y., CHONG ENG, T. & THANGAVELOO, R. 2011. Green Power architecture considerations for rural computing. *In Communications (MICC), 2011 IEEE 10th Malaysia International Conference on*. 2-5 Oct. 2011. pp. 18-22.

- SITSHINGA, M.M. 2012. Provision of alternative energy: A case study in the Eastern Cape rural communities. *In Domestic Use of Energy Conference (DUE), 2012 Proceedings of the 20th.* 3-4 April 2012. pp. 117-122.
- SKOUBY, K.E. & IDONGESIT, W. 2014. *The African mobile story*. River Publishers.
- SKUNPONG, R. & PLANGKLANG, B. 2011. A practical method for quickly PV sizing. *Procedia Engineering*, 8(0):120-127.
- SOLANKI, C.S. 2009. *Solar photovoltaics: Fundamentals technologies and applications*. Prentice-Hall of India Pvt. Limited.
- SOLANKI, C.S., BILYALOV, R.R., BEAUCARNE, G. & POORTMANS, J. 2003. Thin monocrystalline silicon films for solar cells. *In Photovoltaic Energy Conversion, 2003. Proceedings of 3rd World Conference on.* 18-18 May 2003. pp. 1320-1323.
- SONNENENERGIE, D.G.F. 2008. *Planning and installing photovoltaic systems: A guide for installers, architects and engineers*. Earthscan.
- SOUTH AFRICAN NATIONAL STANDARDS. 2005. SANS 10114-1:Interior lighting. Pretoria: South African Bureau of Standards.
- SOUTH AFRICAN NATIONAL STANDARDS. 2010. The application of the National Building Regulations. Pretoria: South African Bureau of Standards.
- SPAKOWSKI, A.E. 1967. Some problems of the thin-film cadmium-sulfide solar cell. *Electron Devices, IEEE Transactions on*, 14(1):18-21.
- SRIRAM, N. & SHAHIDEHPOUR, M. 2005. Renewable biomass energy. *In Power Engineering Society General Meeting, 2005. IEEE.* 12-16 June 2005. pp. 612-617.
- SUMBWANYAMBE, M., NEL, A. & CLARKE, W. 2011. Challenges and proposed solutions towards telecentre sustainability: A Southern Africa case study. *In IST-Africa Conference Proceedings, 2011.* 11-13 May 2011. pp. 1-8.

SWART, A.J., SCHOEMAN, R.M. & PIENAAR, H.C. 2011. Assessing the effect of variable atmospheric conditions on the performance of photovoltaic panels: A case study from the Vaal Triangle. In *Energy Efficiency Convention (SAEEEC), 2011 Southern African*. 16-17 Nov. 2011. pp. 1-6.

TAELE, B.M., MOKHUTŠOANE, L. & HAPAZARI, I. 2012. An overview of small hydropower development in Lesotho: Challenges and prospects. *Renewable Energy*, 44(0):448-452.

TAYLOR, R.H. 1983. *Alternative energy sources for the centralised generation of electricity*. Great Britain: Adam Hilger.

TEXAS INSTRUMENTS. 2011. Characteristics of rechargeable batteries. [Online]. Available at:<<http://www.ti.com/general/docs/lit/getliterature.tsp?literatureNumber=suva533&fileType=pdf>>. Accessed: 18 November 2013.

THUMANN, A. & FRANZ, H. 2009. *Efficient electrical systems design handbook*. Fairmont Press.

TYAGI, V.V., RAHIM, N.A.A., RAHIM, N.A. & SELVARAJ, J.A.L. 2013. Progress in solar PV technology: Research and achievement. *Renewable and Sustainable Energy Reviews*, 20(0):443-461.

UNIVERSITY OF MELBOURNE. 2011. Design standards. [Online]. Available at:<http://www.pcs.unimelb.edu.au/standards_and_policies/docs/design_standards/PCS_Design_Standards_Final_Nov_2011.pdf>. Accessed: 10 October 2014.

VAN SWAAIJ, R.A.C.M.M., SMETS, A.H.M. & ZEMAN, M. 2012. Thin-film silicon technology for highly-efficient solar cells. In *Bipolar/BiCMOS Circuits and Technology Meeting (BCTM), 2012 IEEE*. Sept. 30 2012-Oct. 3 2012. pp. 1-7.

WHITAKER, J.C. 2005. *The electronics handbook, 2nd ed.*: Taylor & Francis.

WILLIAMS, A. 1993. Role of fossil fuels in electricity generation and their environmental impact. *Science, Measurement and Technology, IEE Proceedings A*, 140(1):8-12.

- WINDER, S. 2011. *Power supplies for LED driving*. Elsevier Science.
- WINKLER, H. 2005. Renewable energy policy in South Africa: Policy options for renewable electricity. *Energy Policy*, 33(1):27-38.
- WRIGHT, M. & UDDIN, A. 2012. Organic — inorganic hybrid solar cells: A comparative review. *Solar Energy Materials and Solar Cells*, 107(0):87-111.
- WU, L., TIAN, W. & JIANG, X. 2005. Silicon-based solar cell system with a hybrid PV module. *Solar Energy Materials and Solar Cells*, 87(1–4):637-645.
- XING, C., SIMIN, W., ZHANG, L., SHENGZHI, Z., ZHICHENG, L., HAO, J. & SHENG, L. 2012. An investigation on structure and materials of laminated organic solar cell packaging. *In Electronic Components and Technology Conference (ECTC), 2012 IEEE 62nd*. May 29 2012-June 1 2012. pp. 2129-2134.
- YADAV, A.K. & CHANDEL, S.S. 2013. Tilt angle optimization to maximize incident solar radiation: A review. *Renewable and Sustainable Energy Reviews*, 23(0):503-513.
- YÜKSEL, I. 2010. Hydropower for sustainable water and energy development. *Renewable and Sustainable Energy Reviews*, 14(1):462-469.
- YUVENTI, J. 2012. A method for evaluating the influence of wiring on the performance of components in a photovoltaic system design. *Solar Energy*, 86(10):2996-3003.
- ZAHEDI, A. 2011. Maximizing solar PV energy penetration using energy storage technology. *Renewable and Sustainable Energy Reviews*, 15(1):866-870.
- ZHOKHAVETS, U., ERB, T., GOBSCH, G., AL-IBRAHIM, M. & AMBACHER, O. 2006. Relation between absorption and crystallinity of poly(3-hexylthiophene)/fullerene films for plastic solar cells. *Chemical Physics Letters*, 418(4–6):347-350.
- ZIUKU, S. & MEYER, E.L. 2010. Electrical performance results of an energy efficient building with an integrated photovoltaic system. *Journal of Energy in Southern Africa*, 21(3).

ZOBAA, A.F. & BANSAL, R.C. 2011. *Handbook of renewable energy technology*. Singapore: World Scientific Publishing Co. Pte. Ltd.

ZUMTOBEL. 2013. *The lighting handbook*. Dornbirn: Zumtobel Lighting.

Annexure A Photovoltaic panels manufacturer parameters

PV1



Chinaland Solar Energy Co., Ltd.

合肥中南光电有限公司

Address: Feidong New City Economic Development Zone, Hefei, 231600,

Anhui Province, PR China Tel/Fax: +86 551 7758555

Web: www.chnland.com E-mail: chn2011@chnland.com

Model :	
Monocrystalline silicon solar panel	CHN75-36M
Specification:	
Cell	Monocrystalline silicon solar cells 125*100mm
Cell Efficiency	17.34%
No. of cells and connections	36(6*6)
Dimension of module (mm)	660*808*30mm
Weight	6.2kg
Limits	
Operating temperature	-40 to+85
Maximum system voltage	715 V DC °C
Temperature and Coefficients	
Nominal Operation Cell Temperature	48 ±2
Current temperature coefficient (%/k)	0.06±0. °C 01
Voltage temperature coefficient (mV/k)	-(78±10)
Power temperature coefficient (%/k)	-(0.5±0.05)
Output	
Type of output terninal	Junction box
Cable	LAPP (4.0mm²) C
Asymetrical lengths	900mm(-) and 900mm(+)
Connection	CHN Plug Type IV
Characteristics	
Model	CHN75-36M
Open circuit voltage (Voc)	21.17V
Optimum operating voltage (Vmp)	17.16V
Short circuit Current (Isc)	4.67A
Optimum operating current (Imp)	4.37A
Maximum power at STC (Pm)	75Wp

PV2



Chinaland Solar Energy Co., Ltd.

合肥中南光电有限公司

Address: Feidong New City Economic Development Zone, Hefei, 231600,

Anhui Province, PR China Tel/Fax: +86 551 7759376/7758555

Web: www.chnland.com E-mail: sabrinahan@chnland.com

Model :	
Polycrystalline silicon solar panel	CHN75-72P
Specification:	
Cell	Polycrystalline silicon solar cells 156*52mm
Solar cell efficiency	13.00%
No. of cells and connections	72(4*18)
Dimension of module (mm)	1020*670*30
Limits	
Operating temperature	-40 to+85℃
Maximum system voltage	715 V DC
Temperature and Coefficients	
Nominal Operation Cell Temperature	48℃±2℃
Current temperature coefficient (%/k)	0.06±0.01
Voltage temperature coefficient (mV/k)	-(155±10)
Power temperature coefficient (%/k)	-(0.5±0.05)
Characteristics	
Model	CHN75-72P
Solar panel efficiency	10.97%
Tolerance	±5%
Open circuit voltage (Voc)	22.1V
Optimum operating voltage (Vmp)	17.6V
Short circuit Current (Isc)	4.78A
Optimum operating current (Imp)	4.26A
Maximum power at STC (Pm)	75Wp

Note: Test condition are STC Irradiance 1000W/m2 with AM 1.5 spectrum, cell temperature 25℃, Test method according to IEC 904-1, Tolerance Efficiency 5% rel.

PV3

SETSOLAR M500P

TYPICAL PERFORMANCE CHARACTERISTICS				
Typical power (Wp)	45	50		55
Tolerance (%)	± 5%			
Voltage at max.power (V)	18.0	18.2		18.4
Current at max.power (A)	2.60	2.67		2.98
Open circuit voltage (Voc)	22.0	22.2		22.4
Short circuit current (Isc)	2.70	2.80		3.11

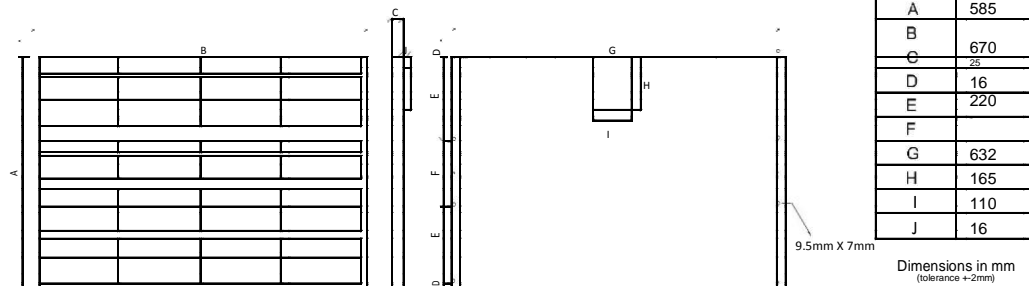
Standard test conditions: 1000W/m², AM1.5G and 25 degree C

TEMPERATURE COEFFICIENTS				
Voltage	-79.20mV / degree C			
Current	+1.50mA / degree C			
Power	-0.46% / degree C			
NOCT (degrees)	45			

CELLS				
Type	Monocrystalline			
Dimensions	156mm x 58mm			
Layout	36 cells (4rows x 9cells)			

GENERAL INFORMATION				
Maximum System voltage	600V			
Diodes	2 x 10A bypass			
Type of connection	Junction box			
Frame	25mm black powder-coated aluminium			
Weight (kg)	12			
Packaging	4 modules per carton box			

WARRANTY				
Product	5 years			
Power output	Terrestrial: 20 years / 80% yield Marine: 10 years / 90% yield			










** SETSOLAR reserves the right to modify all data without notice, due to continuous product development.



Annexure B

Jitbit macro program

Command		
OPEN FILE	C:\Users\CentreofAlternativeE\Desktop\Postgraduate guideline...	
WAIT FOR WINDOW	Postgraduate guidelines.pdf - Adobe Reader	appear
MOVE WINDOW	Postgraduate guidelines.pdf - Adobe Reader	0 : 731 : 670 : 728
REPEAT	13	
DELAY	2000	
MOUSE	Wheel	Wheel: -150
END REPEAT		
OPEN FILE	C:\Program Files (x86)\Google\Chrome\Application\chrome.exe	
WAIT FOR WINDOW	Vaal University of Technology - Google Chrome	appear
IF WINDOW EXISTS	New Tab - Google Chrome	
REPEAT	50	
IF WINDOW EXISTS	New Tab - Google Chrome	
DELAY	1000	
CLOSE WINDOW	New Tab - Google Chrome	
ELSE		
DELAY	1000	
EXIT LOOP		
END IF		
END REPEAT		
ELSE		
END IF		
IF WINDOW EXISTS	Vaal University of Technology - Google Chrome	
SWITCH TO WINDOW	Vaal University of Technology - Google Chrome	
MOVE WINDOW	Vaal University of Technology - Google Chrome	0 : 0 : 734 : 728
DELAY	5000	
MOVE WINDOW	Vaal University of Technology - Google Chrome	404 : 0 : 734 : 324
END IF		
IF WINDOW EXISTS	http://www.vut.ac.za/ is not available - Google Chrome	
MOVE WINDOW	http://www.vut.ac.za/ is not available - Google Chrome	384 : 0 : 734 : 341
END IF		
MOVE WINDOW	Postgraduate guidelines.pdf - Adobe Reader	0 : 731 : 670 : 728
DELAY	500	
OPEN FILE	C:\Users\CentreofAlternativeE\Desktop\Learn Computer Basics...	
WAIT FOR WINDOW	Windows Media Player	appear
MOVE WINDOW	Windows Media Player	397 : 726 : 644 : 334
DELAY	1000	
MOVE WINDOW	Postgraduate guidelines.pdf - Adobe Reader	0 : 731 : 670 : 401
DELAY	1000	
OPEN FILE	C:\Users\CentreofAlternativeE\Documents\System power cons...	
WAIT FOR WINDOW	00 00 0000_00 00 00.docx - Microsoft Word	appear
MOVE WINDOW	00 00 0000_00 00 00 - Microsoft Word	1 : 0 : 746 : 407
TYPE TEXT	Electricity has a major influence on a nation's development and it...	
DELAY	5000	
KEYBOARD	KeyPress	"F12"
DELAY	5000	
TYPE DATE	MM dd yyyy_ HH mm ss	
DELAY	5000	
KEYBOARD	KeyPress	"Enter"
DELAY	5000	
OPEN FILE	C:\Users\CentreofAlternativeE\Documents\System power cons...	
WAIT FOR WINDOW	Microsoft Excel - 00 00 0000_00 00 00.xlsx	appear
MOVE WINDOW	Microsoft Excel - 00 00 0000_00 00 00	0 : 688 : 678 : 411
TYPE TEXT	TimePV1_PowerPV2_PowerPV3_PowerPV1_AvPV2_AvPV3_A...	
DELAY	5000	
KEYBOARD	KeyPress	"F12"
DELAY	5000	
TYPE DATE	MM dd yyyy_ HH mm ss	
DELAY	5000	
KEYBOARD	KeyPress	"Enter"
DELAY	5000	
SWITCH TO WINDOW	Windows Media Player	
MOVE WINDOW	Windows Media Player	397 : 726 : 644 : 334
DELAY	60000	
CLOSE WINDOW	Windows Media Player	
SWITCH TO WINDOW	Postgraduate guidelines.pdf - Adobe Reader	
MOVE WINDOW	Postgraduate guidelines.pdf - Adobe Reader	0 : 731 : 670 : 401
DELAY	2000	
CLOSE WINDOW	Postgraduate guidelines.pdf - Adobe Reader	
SWITCH TO WINDOW	Microsoft Word	
MOVE WINDOW	Microsoft Word	0 : 731 : 670 : 401

 DELAY	2000	
 CLOSE WINDOW	Postgraduate guidelines.pdf - Adobe Reader	
 SWITCH TO WINDOW	Microsoft Word	
 MOVE WINDOW	Microsoft Word	0 : 731 : 670 : 401
 DELAY	2000	
 CLOSE WINDOW	Microsoft Word	
 SWITCH TO WINDOW	Microsoft Excel	
 MOVE WINDOW	Microsoft Excel	0 : 731 : 670 : 401
 DELAY	2000	
 CLOSE WINDOW	Microsoft Excel	
 IF FILE EXISTS	C:\Program Files (x86)\Google\Chrome\Application\chrome.exe	
 CLOSE WINDOW	Vaal University of Technology - Google Chrome	
 CLOSE WINDOW	http://www.vut.ac.za/ is not available - Google Chrome	
 END IF		
 DELAY	2000	
 KEYBOARD	KeyPress	"F5"

Annexure C Charge controller (Microcare 12/24 10A MPPT)

MICRO CARE[®]

SOLAR COMPONENTS

MPPT Regulators, Pure Sine Wave Bi-Directional inverters, Grid Tied Inverters, and Grid Tied Limiters are designed, developed, and manufactured by MICROCARE in Port Elizabeth, South Africa

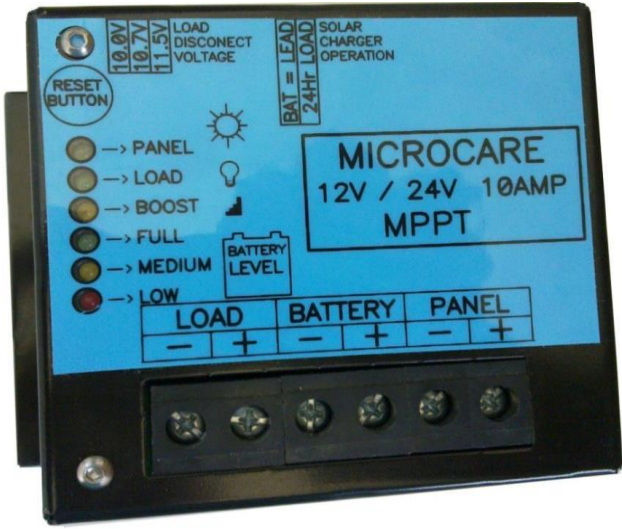
Microcare 10 amp LED MPPT Regulator with Load Shed

The MICROCARE MPPT REGULATOR is designed to interface between the SOLAR PANEL, the BATTERIES and the LOAD. The TRACKER will always find the optimum power point of the solar panel system to ensure that maximum power is extracted from the solar panel and put into the batteries. Using this system up to 30% more power can be extracted from the solar panel than using shunt or series pass regulators.

The MICROCARE MPPT REGULATOR is also able to charge batteries of a lower voltage than the solar panel. By means of LEDs it will show the status of the system. It also incorporates various charge modes which will automatically increase the charge level to the batteries when first starting up or if the battery voltage falls below the minimum volts.

The MICROCARE MPPT REGULATOR will read the nominal battery voltage. This unit is designed to run on a 12/24 volt battery set. It will then read the solar panel voltage and automatically find the optimum power point. The charging, battery values and boost modes are then automatically adjusted.

Via links the load voltage disconnect can be selected, whether the battery is lead acid or sealed, and whether the unit operates as a normal load shedder or as a day/night switch.



The image shows a black rectangular Microcare MPPT regulator. The top face is blue with white text and symbols. It features a 'RESET BUTTON' in the top left corner. Below it are five LEDs labeled 'PANEL', 'LOAD', 'BOOST', 'FULL', and 'MEDIUM', with a 'LOW' label at the bottom. To the right of these LEDs is a 'BATTERY LEVEL' indicator with a battery icon. Further right is a 'LOAD DISCONNECT VOLTAGE' section with three switches labeled '10.0V', '10.7V', and '11.5V'. To the right of these is a 'BAT = LEAD' switch and a 'SOLAR CHARGER OPERATION' section with a '24Hr' switch. The central text reads 'MICROCARE 12V / 24V 10AMP MPPT'. At the bottom, there are three sets of terminals labeled 'LOAD', 'BATTERY', and 'PANEL', each with '-' and '+' terminals.

1st Floor Neave Industrial Park, 7 Bennett Road, Korsten, Port Elizabeth – P O Box 7227, Newton Park, 6055 – Email: info@microcare.co.za
Tel: 041 453 5761 Fax: 041 453 5763 – VAT Registered: 4480110222 – www.microcare.co.za

Features:

- Automatically measures the battery voltage and then sets up the charge parameters (12v-24v)
- Operates the Solar Panels at the maximum efficiency
- Charges batteries by setting up the best power point of the solar panels
- Can improve power extracted from the solar panels by 30% over normal shunt/series pass regulators
- LED Display
- Maximum Current 20 Amps.
- 10 amp Load controller.
- Temperature controlled Cooling Fan
- Selectable low voltage disconnect.
- 24 hour load or Street Light mode

Specifications:

Output Current Rating	10 amps
Nominal Battery Voltage	Multi-Voltage 12-24vdc (Automatic selection of voltage)
PV Input Voltage	Absolute Maximum 50VDC
Charge Algorithm	2-stage Boost/Float
Boost Voltage	Charges to 14.8v for minimum of 3 hours (12v system) 29.6v (24v system)
Float Voltage	13.8v per battery (12v system) 27.6v (24v system)
Power Conversion	DC/DC Switch Mode
Output Efficiency	>95% Typical @ 14 Volt 7.5 Amps Output
Voltage Step down Capability	Can charge a lower voltage battery from a higher voltage PV array.
Status display	6 LED Display <ul style="list-style-type: none"> • Panel • Load • Boost • Full • Medium • Low
Features	<ol style="list-style-type: none"> 1. MPPT Charge Controller 2. 10 amp Load Shed 3. 24 hour load shed or Street Light Controller 4. Programmable; Dusk to Dawn, ½ hour 1hour or 1.5 hour delays. 5. Selectable battery low cutout. 10.0v, 10.7v, 11.5v for 12 volt system 6. Selectable battery low cutout. 20.0v, 21.4v, 23.0v for 24 volt system.
Power Consumption	Less than 1watt
Environmental Rating	0 – 40°C
Protection System	<ul style="list-style-type: none"> • Lighting Protection • Reverse polarity Panel/Battery • Internal Fuse
Cable Entry	Connector (Max Cable size 16mm)
Dimensions	0.5kg 110mm (L) x 110mm (W) x 70mm (H)
PV Panel Range	12v - Max 120 watt PV Panel 24v - Max 240 watt PV Panels

All Microcare Products have a 3 year carry in warranty

Annexure D DC-DC converter (Motormate IPC 1210)



DC-DC Isolated Power Converter

A stable and clean power source for your motor-home

Technical Specifications 12V / 24V models

MODELS	IPC-1205	IPC-1210	IPC-1215	IPC-1220	IPC-2110	IPC-2120	IPC-2130	IPC-2140
INPUT AND OUTPUT								
Continuous Output Current	5A	10A	15A	20A	10A	20A	30A	40A
Input Voltage	12VDC (10 ~ 16VDC operative)				24VDC (20 ~ 32VDC operative)			
Output Voltage	27.6VDC				13.8VDC			
Line Regulation	40mV				20mV			
Efficiency	90% at full load				90% at full load			
Ripple & Noise	50mV rms				30mV rms			
Load regulation	20mV from no load to full load				30mV from no load to full load			
PROTECTIONS								
Ignition Protected	Yes				Yes			
Short Circuit Protected	Yes				Yes			
Overload Protected	Yes				Yes			
Overheat Protected	Yes				Yes			
FEATURES								
Allow parallel operation	Yes, allow parallel connection				Yes, allow parallel connection			
Suitable for battery charging	Yes, suitable for battery boost charging				Yes, suitable for battery boost charging			
Galvanic isolated	Yes, input and output is fully isolated				Yes, input and output is fully isolated			
PHYSICAL								
Input connection	Cable with terminal rings				Cable with terminal rings			
Output connection	Terminal block				Terminal block			
Display	Green - Standby Mode, Green - Power On, Yellow - Input Low, Red - Output Overload							
Cooling	Natural	Thermally control cooling fan			Natural	Thermally control cooling fan		
Operation temperature	-20°C to 50°C							
Case	Anodized aluminum case with mounting cover				Anodized aluminum case with mounting cover			
Weight (kg)	0.75	1.2	1.6	1.9	0.75	1.2	1.6	1.9
Size (cm) L x W x H	10 x 11.5 x 7	16 x 11.5 x 7	21 x 11.5 x 7	24 x 11.5 x 7	10 x 11.5 x 7	16 x 11.5 x 7	21 x 11.5 x 7	24 x 11.5 x 7

* Specifications subject to change without prior notice.

Technical Specifications 36V / 48V models

MODELS	IPC-3110	IPC-3120	IPC-3130	IPC-3140	IPC-4110	IPC-4120	IPC-4130	IPC-4140
INPUT AND OUTPUT								
Continuous Output Current	10A	20A	30A	40A	10A	20A	30A	40A
Input Voltage	36VDC (30 ~ 48VDC operative)				48VDC (40 ~ 60VDC operative)			
Output Voltage	13.8VDC				13.8VDC			
Line Regulation	20mV				20mV			
Efficiency	90% at full load				90% at full load			
Ripple & Noise	30mV rms				30mV rms			
Load regulation	20mV from no load to full load				30mV from no load to full load			
PROTECTIONS								
Ignition Protected	Yes				Yes			
Short Circuit Protected	Yes				Yes			
Overload Protected	Yes				Yes			
Overheat Protected	Yes				Yes			
FEATURES								
Allow parallel operation	Yes, allow parallel connection				Yes, allow parallel connection			
Suitable for battery charging	Yes, suitable for battery boost charging				Yes, suitable for battery boost charging			
Galvanic isolated	Yes, input and output is fully isolated				Yes, input and output is fully isolated			
PHYSICAL								
Input connection	Cable with terminal rings				Cable with terminal rings			
Output connection	Terminal block				Terminal block			
Display	Green - Standby Mode, Green - Power On, Yellow - Input Low, Red - Output Overload							
Cooling	Natural	Thermally control cooling fan			Natural	Thermally control cooling fan		
Operation temperature	-20°C to 50°C							
Case	Anodized aluminum case with mounting cover				Anodized aluminum case with mounting cover			
Weight (kg)	0.75	1.2	1.6	1.9	0.75	1.2	1.6	1.9
Size (cm) L x W x H	10 x 11.5 x 7	16 x 11.5 x 7	21 x 11.5 x 7	24 x 11.5 x 7	10 x 11.5 x 7	16 x 11.5 x 7	21 x 11.5 x 7	24 x 11.5 x 7

* Specifications subject to change without prior notice.

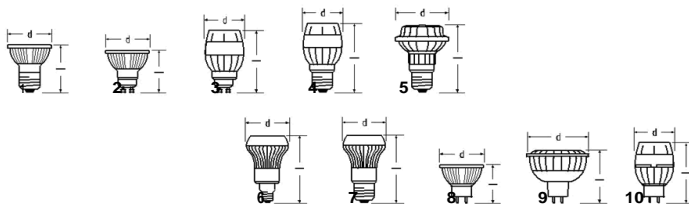



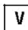
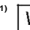
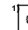
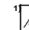


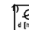
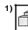
Annexure E Lights [MR16**(PAR16)]

LED LAMPS – PARATHOM® PAR 16, PAR 20, R50 AND MR16



PARATHOM® PAR 16, PAR 20, R50 and MR16



Product reference Product number   ¹⁾      ¹⁾  

PARATHOM® PAR 16

PAR16 20 D	4008321965721	E27	220-240	4.5	600	35	6500	68	50	10	1
PAR16 20 WW	4008321965769	E27	220-240	4.5	450	35	3000	68	50	10	1
PAR16 20 D	4008321965806	GU10	220-240	4.5	600	35	6500	80	50	10	2
PAR16 20 WW	4008321965844	GU10	220-240	4.5	450	35	3000	80	50	10	2
PAR16 35 WW	4008321963963	GU10	220-240	8	600	35	3000	85	50	10	3
PAR16 35 WW	4008321964007	E27	220-240	8	600	35	3000	93	50	10	4
PAR16 35 D	4008321964045	GU10	220-240	8	> 600	35	6500	85	50	10	3
PAR16 35 D	4008321964083	E27	220-240	8	> 600	35	6500	93	50	10	4
PAR16 50 WW	4008321964120	GU10	220-240	10	950	35	3000	85	50	10	3
PAR16 50 WW	4008321964168	E27	220-240	10	950	35	3000	93	50	10	4
PAR16 50 D	4008321964205	GU10	220-240	10	> 950	35	6500	85	50	10	3
PAR16 50 D	4008321964243	E27	220-240	10	> 950	35	6500	93	50	10	4

PARATHOM® PAR 20

PAR20 35 WW	4008321963703	E27	220-240	to be determined	25	to be determined	10	5
PAR20 50 WW	4008321963741	E27	220-240	to be determined	25	to be determined	10	5

PARATHOM® R50

R50 25 D	4008321965400	E14	100-240	3	140	30	6500	86	50	10	6
R50 25 WW	4008321965448	E14	100-240	3	100	30	3000	86	50	10	6
R50 25 D	4008321965486	E27	100-240	3	140	30	6500	83	50	10	7
R50 25 WW	4008321965523	E27	100-240	3	100	30	3000	83	50	10	7
R50 40 D	4008321965561	E14	100-240	6	240	30	6500	86	50	10	6
R50 40 WW	4008321965608	E14	100-240	6	170	30	3000	86	50	10	6
R50 40 D	4008321965646	E27	100-240	6	240	30	6500	83	50	10	7
R50 40 WW	4008321965684	E27	100-240	6	170	30	3000	83	50	10	7

PARATHOM® MR16

MR16 20 WW	4008321521927	GU5.3	12	4.5	450	36	3000	48	50	10	8
MR16 20 WW Advanced	4008321963802	GU5.3	12	5.5	500	36	3000	49	50	10	9
MR16 20 D Advanced	4008321963840	GU5.3	12	5.5	> 500	36	6500	49	50	10	9
MR16 35 WW Advanced	4008321963888	GU5.3	12	10	950	36	3000	77	50	10	10
MR16 35 D Advanced	4008321963925	GU5.3	12	10	> 950	36	6500	77	50	10	10

¹⁾ All the technical parameters apply to the entire lamp. In view of the complex manufacturing process for light-emitting diodes, the typical values given above for the technical LED parameters are merely statistical values that do not necessarily correspond to the actual technical parameters of an individual product; individual products may vary from the typical values.

RT 12200 (12V20Ah)

RT 12200 is a general purpose battery with 5 years floating design life , meet with IEC, JIS standard .With heavy duty grid, thickness plates, special additives, RT series battery have long and reliable standby service life.

RITAR®

Cells Per Unit	6
Voltage Per Unit	12
Capacity	20Ah @20hr-rate to 1.75V per cell @25°C
Weight	Approx. 5.90 Kg
Max. Discharge Current	200 A (5 sec)
Internal Resistance	Approx. 14 mΩ
Operating Temperature Range	Discharge: -20°C~60°C Charge: 0°C~50°C Storage: -20°C~60°C
Normal Operating Temperature Range	25°C ± 5°C
Float charging Voltage	13.7 to 13.9 VDC/unit Average at 25°C
Recommended Maximum Charging Current Limit	6 A
Equalization and Cycle Service	14.6 to 14.8 VDC/unit Average at 25°C
Self Discharge	RITAR batteries can be stored for more than 6 months at 25°C. Self-discharge ratio less than 3% per month at 25°C. Please charge batteries before using.
Terminal	Faston F3/F13
Constrainer Material	A.B.S. (UL94-HB) , Flammability resistance of UL94-V2 can be available upon request.



MH28539



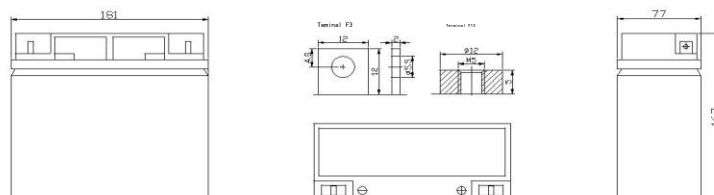
G4M20206-0910-E-16



ISO9001:2000 Certificate

Unit: mm

Dimension: 181(L)×77 (W)×167(H)



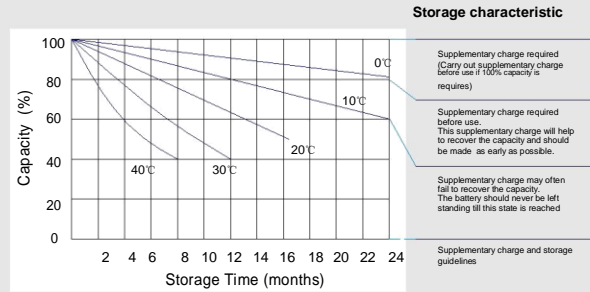
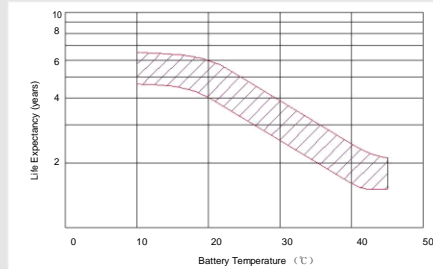
Current (A)	5MIN	10MIN	15MIN	30MIN	1HR	2HR	3HR	4HR	5HR	8HR	10HR	20HR
9.60V	79.000	52.8 00	40.600	23.4 60	13.880	7.2348	5.1200	4.2000	3.4 814	2.3092	1.99 92	1.1220
1 0.0V	76.146	50.7 44	39.298	23.1 00	13.800	7.1826	5.1000	4.1800	3.4 608	2.3000	1.97 88	1.0812
1 0.2V	72.030	49.1 76	38.396	22.9 20	13.700	7.1652	5.0800	4.1600	3.4 402	2.2908	1.95 84	1.0608
1 0.5V	65.072	46.0 21	36.397	22.4 00	13.500	7.0783	5.0600	4.1400	3.4 196	2.2816	1.93 80	1.0200
1 0.8V	58.114	42.8 85	34.378	21.8 60	13.300	6.9565	5.0200	4.1200	3.3 990	2.2724	1.89 72	0.9792
1 1.1V	51.215	39.7 29	32.379	21.3 20	13.120	6.8522	4.9800	4.1000	3.3 784	2.2632	1.87 68	0.9588

	Power	Discharge	Capacity (mAh)									
F.V/Time	5MIN	10MIN	15MIN	30MIN	1HR	2HR	3HR	4HR	5HR	8HR	10HR	20HR
9.60V	86.4.00	561.60	456.36	281.52	166.44	8.6.713	61.320	50.160	49.069	27.764	23.6.34	13.211
1.00V	84.1.50	561.00	449.81	276.96	165.96	8.6.191	61.200	50.040	48.698	27.541	23.3.92	12.726
0.20V	82.4.67	544.17	439.49	275.16	165.60	8.5.983	61.080	50.040	48.575	27.505	23.1.49	12.484
1.0.5V	74.5.23	521.73	416.60	268.56	162.84	8.4.626	60.720	49.680	48.451	27.430	22.9.07	11.999
0.8V	66.5.68	488.07	393.60	262.20	160.08	8.3.478	60.240	49.320	48.328	27.318	22.5.43	11.635
1.1.1V	58.6.25	454.41	370.71	255.84	157.32	8.2.226	59.760	48.960	48.204	27.318	22.1.80	11.272

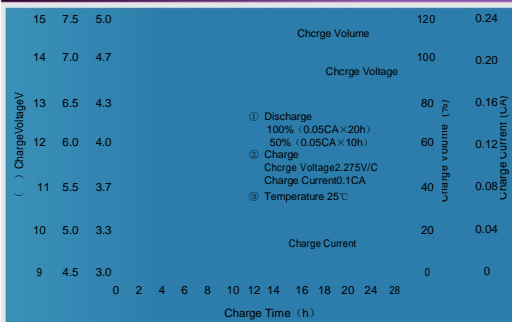
All mentioned values are average values.

RT 12200

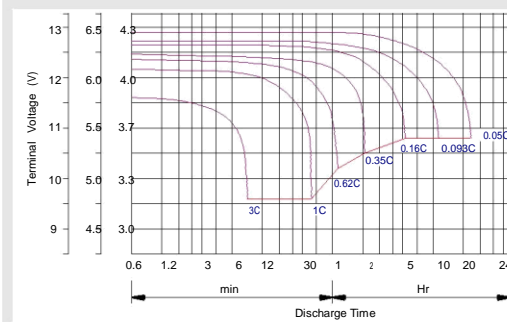
12V20Ah



Charge characteristic Curve for standby use



Discharge characteristic Curve



Capacity Factors With Different Temperature

Battery Type		-20°C	-10°C	0°C	5°C	10°C	20°C	25°C	30°C	40°C	45°C
GEL Battery	6V&12V	50%	70%	83%	85%	90%	98%	100%	102%	104%	105%
	2V	60%	75%	85%	88%	92%	99%	100%	103%	105%	106%
AGM Battery	6V&12V	46%	66%	76%	83%	90%	98%	100%	103%	107%	109%
	2V	55%	70%	80%	85%	92%	99%	100%	104%	108%	110%

Discharge Current VS. Discharge Voltage

Final Discharge Voltage V/cell	1.75V	1.70V	1.60V
Discharge Current (A)	(A) ≤ 0.2C	0.2C < (A) < 1.0C	(A) ≥ 1.0C

Charge the batteries at least once every six months, if they are stored at 25°C.

Charging Method:

Constant Voltage	-0.2Cx2h+2.4~2.45V/Cellx24h, Max. Current 0.3CA
Constant Current	-0.2Cx2h+0.1CAx12h
Fast	-0.2Cx2h+0.3CAx4.0h

Maintenance & Cautions

Float Service:

- ※ Every month, recommend inspection every battery voltage.
- ※ Every three months, recommend equalization charge for one time.

Equalization charge method:

Discharge: 100% rate capacity discharge.

Charge: Max. current 0.3CA, constant voltage 2.4-2.45V/Cell charge 24h.

- ※ Effect of temperature on float charge voltage: -3mV/°C/Cell.
- ※ Length of service life will be directly affected by the number of discharge cycles, depth of discharge, ambient temperature and charging voltage.

SHENZHEN RITAR POWER CO.,LTD.

URL:www.ritarpower.com

Annexure G Lead acid battery (100Ah)



RA12-100AD (12V100Ah)

RA12-100AD is AGM Deep cycle battery with 10 years floating design life, specially designed for frequent cyclic discharge usage. By using strong grid and specific paste plate, it makes battery have 30% more cyclic life time than standby series. It is applicable for solar energy system, golf cart, electric wheelchair, etc..



Specification

Cells Per Unit	6
Voltage Per Unit	12
Capacity	100Ah@ 10hr-rate to 1.80V per cell @25°C
Weight	Approx. 29.0 Kg
Max. Discharge Current	1000 A (5 sec)
Internal Resistance	Approx. 5 mΩ
Operating Temperature Range	Discharge: -20°C~60°C Charge: 0°C~50°C Storage: -20°C~60°C
Normal Operating Temperature Range	25°C±5°C
Float charging Voltage	13.6 to 13.8 VDC/unit Average at 25°C
Recommended Maximum Charging Current Limit	30 A
Equalization and Cycle Service	14.6 to 14.8 VDC/unit Average at 25°C
Self Discharge	RITAR Valve Regulated Lead Acid (VRLA) batteries can be stored for more than 6 months at 25°C. Self-discharge ratio less than 3% per month at 25°C. Please charge batteries before using.
Terminal	Terminal F5/F12
Container Material	A.B.S. (UL94-HB) , Flammability resistance of UL94-V1 can be available upon request.



MH28539



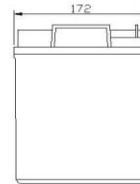
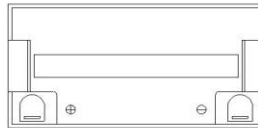
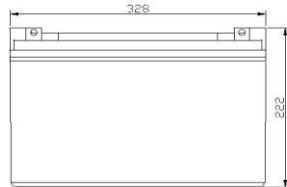
GHM20206-0910-E-16



ISO9001:2000 Certificate

Dimensions

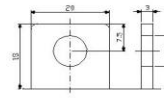
Unit: mm Dimension: 328(L)×172(W)×222(H)



Terminal F12



Terminal F5



Constant Current Discharge Characteristics: A (25°C)

F.V/Time	5MIN	10MIN	15MIN	30MIN	1HR	2HR	3HR	4HR	5HR	8HR	10HR	20HR
9.60V	320.7	226.9	181.4	112.7	65.00	38.89	26.88	22.03	18.03	12.42	10.50	5.777
10.0V	311.4	215.8	177.7	110.8	64.70	38.60	26.78	21.93	17.93	12.32	10.40	5.672
10.2V	302.2	208.2	174.9	109.8	64.10	38.31	26.57	21.83	17.82	12.22	10.30	5.567
10.5V	271.3	192.1	166.5	107.1	63.50	38.02	26.47	21.62	17.61	12.12	10.20	5.462
10.8V	244.9	175.2	153.5	102.4	62.00	37.33	25.75	21.11	17.29	11.92	10.10	5.357
11.1V	209.1	156.6	137.7	95.91	58.90	35.68	24.62	20.09	16.55	11.41	9.796	5.041

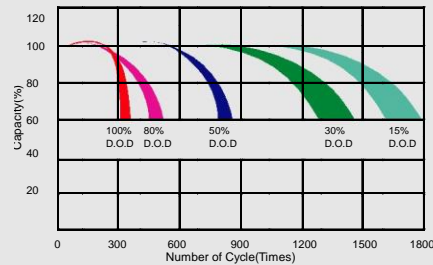
Constant Power Discharge Characteristics: A (25°C)

F.V/Time	5MIN	10MIN	15MIN	30MIN	1HR	2HR	3HR	4HR	5HR	8HR	10HR	20HR
9.6 V	3317	2416	1996	1284	751.1	458.4	319.9	262.6	215.1	148.3	125.5	69.26
10.0V	3251	2342	1964	1269	749.3	456.0	320.0	262.3	214.6	147.6	124.7	68.06
10.2V	3214	2280	1941	1260	743.5	453.3	318.6	261.7	213.9	146.6	123.6	66.80
10.5V	2926	2123	1852	1230	736.8	450.0	317.4	259.3	211.3	145.4	122.4	65.54
10.8V	2665	1957	1712	1179	723.2	444.2	308.7	253.4	207.5	143.0	121.2	64.28
11.1V	2341	1770	1541	1108	692.3	427.7	295.4	241.1	198.6	136.9	117.6	60.50

All mentioned values are average values.

RA12-100AD

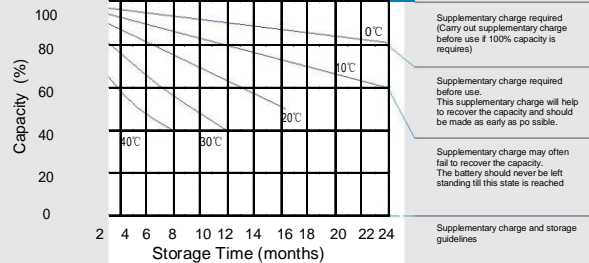
Life characteristics of cyclic use



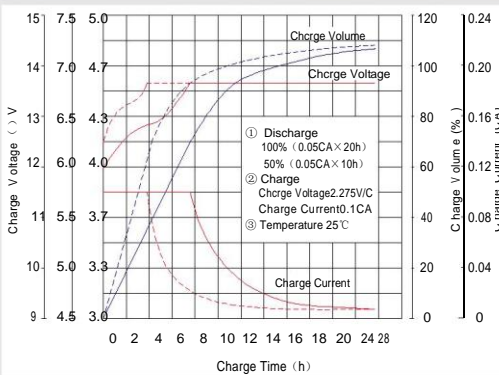
12V100Ah



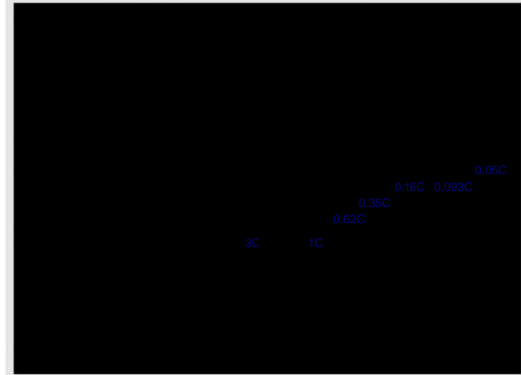
Storage characteristic



Charge characteristic curve for cyclic use



Discharge characteristic curve



Capacity Factors With Different Temperature

Battery Type		-20℃	-10℃	0℃	5℃	10℃	20℃	25℃	30℃	40℃	45℃
GEL Battery	6V&12V	50%	70%	83%	85%	90%	98%	100%	102%	104%	105%
	2V	60%	75%	85%	88%	92%	99%	100%	103%	105%	106%
AGM Battery	6V&12V	46%	66%	76%	83%	90%	98%	100%	103%	107%	109%
	2V	55%	70%	80%	85%	92%	99%	100%	104%	108%	110%

Discharge Current VS. Discharge Voltage

Final Discharge Voltage V/cell	1.75V	1.70V	1.60V
Discharge Current (A)	(A) ≤ 0.2C	0.2C < (A) < 1.0C	(A) ≥ 1.0C

Charge the batteries at least once every six months, if they are stored at 25°C.

Charging Method:

Constant Voltage	-0.2Cx2h+2.4~2.45V/Cellx24h,Max. Current 0.3CA
Constant Current	-0.2Cx2h+0.1CAx12h
Fast	-0.2Cx2h+0.3CAx4.0h

Maintenance & Cautions

Cycle service

- ※ Avoid battery over discharge, especially battery series connection use.
- ※ Charged with recommend voltage, ensure battery can be full recharged. In general, recharge capacity should be 1.1-1.15 times discharge capacity.
- ※ Effect of temperature on cycle charge voltage: -4mV/°C/Cell.
- ※ There are a number of factors that will affect the length of cyclic service. The most significant are depth of discharge, ambient temperature, discharge rate, and the manner in which the battery is recharged. Generally speaking, the most important factors is depth of discharge.

SHEN ZHEN RITAR POWER CO.,LTD.

URL:www.ritarpower.com

Address: Rm405,Tower C, Huahan Building,Langshan Rd16, Nanshan District, ShenZhen, 518057, China
Tel:+86-755-33981668 Fax:86-755-8347-5180

2011- Version 1

Annexure H Laptops purchase invoice

ELANDEO TEN t/a



Physical Address:

117 PIET RETIEF BLVD
SE1
VANDERBIJLPARK

Postal Address:

P O Box 1249
Vanderbijlpark
1900

Contact Details:

Phone: 016 932 3728
Fax: 086 560 9183
E-Mail: antoinette@mediaunlimited.co.za

Company	V U T
Phone	
Fax	
E-Mail	
Contact Person	VUSI

Quotation Number	Prepared By:	DATE
	ANTOINETTE	2014/05/20

Part No	Description	Unit Price	Qty	Line Total
NX.MGREA.014	ACER ASPIRE E1-510-28202G50MNKK	4 035,00	1 R	4 035,00
59403878,00	LENOVO G500 1005M 4/500	4 035,00	1 R	4 035,00
	TOSHIBA C50 1037U 4/1TB W8	4 475,00	1 R	4 475,00
			R	-
			R	-
			R	-
			R	-
			R	-
			R	-

PRICES ARE EXCLUDING VAT

Elandeo Ten cc T/A Media Unlimited

Reg No: 97/07071/07 VAT No: 4110166560

Subtotal R 12 545,00

VAT 14% R 1 756,30

Total R 14 301,30

Thank you for your business!

Annexure I Turnitin originality report



Turnitin Originality Report

Design and Development of an Off Grid E-learning Centre for Rural Communities by Vusi Selaule

From Submissions (TCE)

Similarity Index	Similarity by Source
5%	Internet Sources: 4% Publications: 4% Student Papers: N/A

Processed on 02-Feb-2015 23:02

SAST

ID: 413955569

sources:

Word Count: 24062

1

1% match (Internet from 20-Jun-2014)

<http://vut.netd.ac.za/bitstream/handle/10352/112/Thesis%20-%20M%20Tech.%20Ruaan%20Schoeman.pdf?sequence=1>

2

< 1% match (publications)

[El Chaar, L. "Review of photovoltaic technologies". Renewable and Sustainable Energy Reviews. 2011:06](#)

3

< 1% match (Internet from 21-Oct-2013)

http://www.tdx.cat/bitstream/handle/10803/83493/PhD_mfons.pdf.txt?sequence=2

4

< 1% match (Internet from 24-May-2009)

[http://www.moh.govt.nz/moh.nsf/0/E967EF8FEC435353CC256F62000C96FD/\\$File/trackingtheobesityepidemic-1.pdf](http://www.moh.govt.nz/moh.nsf/0/E967EF8FEC435353CC256F62000C96FD/$File/trackingtheobesityepidemic-1.pdf)

5

< 1% match (Internet from 14-Oct-2013)

<http://www.coursehero.com/file/2225316/HartCSpring2008/>

6

< 1% match (Internet from 21-Dec-2007)

<http://mct.de/download/philips/lpc213x.pdf>

7

< 1% match (publications)

[Yoon, Jongho. "Power Output Characteristics of Transparent a-Si BiPV Window Module". Solar Cells - Thin-Film Technologies. 2011.](#)

8

< 1% match (publications)

[Nelson, Vaughn. "Economics". Energy and the Environment. 2009.](#)

Annexure J NRF nexus title search



Vaal University of Technology

NEXUS SEARCH

To whom it may concern

This letter serves to inform, that a literature search has been performed on behalf of Mr V.E. Selaule
(20145250) on the topic:

“Design and development of an off grid e-learning centre for rural communities”

A NRF search has been carried out by K du Bruyn (Employed in the Gold Fields Library)

on 28/10/2013.

According to my knowledge, there is currently no duplication of this research title on the NRF database.

Regards

K du Bruyn

Telephone: 016 950 9651

e-mail: kariendb@vut.ac.za

A handwritten signature in black ink, appearing to be 'K du Bruyn', written over a horizontal line.